THE EFFECTS OF LIFELONG GLUTATHIONE DEFICIENCY ON FUNCTIONAL DECLINE AND REDOX SIGNALING

DISSERTATION

Presented to the Graduate Council of the Graduate School of Biomedical Sciences

University of North Texas Health Science Center at Fort Worth

In Partial Fulfillment of the Requirements

For the Degree of

DOCTOR OF PHILOSOPHY

By

J. Thomas Mock, B.A., M.S.

Fort Worth, Texas

July 2018

ACKNOWLEDGEMENTS

I would like to thank my committee members, Dr. Michael Forster, Dr. Michael Salvatore, Dr. Shaohua Yang, and Dr. Gulab Zode for their help in preparing this document and overseeing my research project. I would also like to thank and highlight my mentor, Dr. Nathalie Sumien for helping me grow as a scientist and as an individual. Above all, I would like to thank my wife Maria for her endless support, patience, and love. My labmates, Jess, Haydee, Akram, Kiran, Delaney, Ritu and Phillip helped so much with my project and with my growth as a graduate student. I would also like to thank my parents, my late grandfather, and my in-laws for their support and love over many, many years. Lastly, I would like to thank my friends and siblings for helping keep me sane, Ali Winters for her help and friendship, and to Cheryl Bryant for putting up with my antics.

THE EFFECTS OF LIFELONG GLUTATHIONE DEFICIENCY ON

FUNCTIONAL DECLINE AND REDOX SIGNALING

J. Thomas Mock, B.A., M.S.

APPROVED:

_____

Nathalie Sumien, Ph.D, Major Professor

_____

Michael Forster, Ph.D., Committee Member

_____

Michael Salvatore, Ph.D., Committee Member

_____

Shaohua Yang, Ph.D., Committee Member

_____

Gulab Zode, Ph.D., University Member

_____

Michael Forster, Ph.D., Department Chair

_____

Johnny He, Ph.D., Interim Dean
Graduate School of Biomedical Sciences

TABLE OF CONTENTS

CHAPTER 1

INTRODUCTION

1.1 Aging and functional decline

Aging is a universal process leading to deficits in the functions required for living and ultimately resulting in death. These deficits are highlighted by progressive declines in cognition, muscular strength, and motor function [1], as well as increased risk for chronic diseases and mortality clinically defined as “frailty” [2]. Older individuals may spend decades in this “frail” period with decreased quality of life, functional limitations, or even disability [3]. Advances in healthcare have led to longer average lifespans, and the global population of people aged 60 or older is projected to increase 56% by 2030 and over 100% by 2050 [4]. The population aged 60 or older within just the United States is projected to increase from approximately 43 million to 83 million by 2050, and this large influx of elderly persons will lead to substantial financial healthcare costs as well as individual health concerns [5]. Furthermore, by 2050 individuals aged 80 or older across the globe will more than triple from current numbers [6]. While globally great advances are being made in extending the average lifespan, there is not always a compression of morbidity or decreases in frailty which equates to a shortened “healthspan” or period of healthy

living. As such, aged individuals have a much higher incidence and risk for age-related diseases such as sarcopenia, cardiovascular disease, hypertension, cancer, osteoarthritis, osteoporosis, fall risk, decreased activities of daily living, dementia, and Alzheimer's disease [6]. Additionally, recent research has shown that while lifespans have been extended, it is coupled with an increased ratio of living with disease and functional decline to healthy living [7]. Thus the extension of lifespan in the absence of increased healthspan, defined as the years of healthy living (without any disease), rings hollow as the quality of life of elderly individuals is still decreased. Furthermore, age-related deficits in motor function, cognitive function, and sensory function lead to decreased quality of life, higher risk for mortality, and increased health care costs. With such a large increase in the number of aged individuals looming over the next 30 years, understanding the mechanisms of aging is of utmost importance in helping discover ways to delay age-related decline, thereby shrinking the period of morbidity and decreased function. Various theories of the central cause of aging have been proposed, and while the central mechanisms underlying the aging process leading to age-related functional declines remain unclear, research on aging has indicated several potential pathways of interest [8]. In the following section, I will discuss some of theories that have received wide support and are the focus of my dissertation work.

1.2 Theories of Aging

1.2.1 Free Radical Theory of Aging

The Free Radical Theory of Aging (FRTA) was first proposed by Dr. Denham Harman in 1956 after the discovery of free radicals, namely oxygen-based free radicals such as the hydroxyl

radical ($OH^{\cdot}$) in biological samples by Commoner in 1954 [9, 10]. The free radicals that were observed are simply molecules with an odd number of electrons [11]. This characteristic results in free radicals being highly reactive, and when produced in sufficient quantity can readily react with biomolecules resulting in oxidative damage to DNA, proteins, carbohydrates, and lipids. Dr. Harman proposed that these free radicals were produced as enzymatic by-products in tissues, and they would lead to oxidative damage, cellular degeneration, and result in the observed aging process. Free radicals are produced naturally as a result of aerobic metabolism in mitochondria [12], in defense against pathogens [13], and as a signal molecule in response to cytokines or other signals [14]. The FRTA gained additional support in 1969 after the discovery of superoxide dismutase (SOD), an enzyme whose function is to detoxify superoxide anion ($O_2^{\cdot -}$) molecules [15]. This clearly indicated that not only was $O_2^{\cdot -}$ potentially toxic, but that mammals had a specific pathway dedicated to removing these toxic molecules. These data paved the way for decades of research into both the FRTA and the study of free radical damage in many disease states.

1.2.2 Oxidative stress theory of aging

In 1985 Dr. Helmut Sies defined the term "oxidative stress" as "a disturbance in the pro-oxidant : antioxidant balance in favor of the former" [16]. This highlighted the concept that if oxidative stress were to underlie disease or the aging process that oxidants must overwhelm the balance over antioxidant enzymes or substrates. The possibility and ultimately, probability of damage from excessive oxidative stress is the common denominator of various theories of aging related to oxidative stress [17-19]. Namely, an overabundance of reactive oxygen species overwhelms the endogenous antioxidant defenses and leads to irreversible accumulation of

macromolecular oxidative damage. However, all cells that undergo aerobic respiration receive a basal level of oxidative stress. The major endogenous sources of oxidative stress include mitochondrial production through the electron transport chain (ETC) [20], antibacterial defense via phagocytes and the oxidative burst [21], and peroxisomes as they degrade macromolecules such as fatty acids and proteins [22]. While there are physiological levels produced from these sources, overproduction of oxidative stress across the lifespan was suggested to lead to accumulation of oxidative damage and drive the aging process.

Most organisms have some type of antioxidant system in place that protects against high levels of oxidative stress. Mitochondrial electron leakage and oxidase enzymes are the two major sources of intracellular $O_2^{\cdot -}$, a highly reactive reactive oxygen species [23]. Superoxide dismutate (SOD) dismutates $O_2^{\cdot -}$ into hydrogen peroxide (H_2O_2) which can then either be converted to H_2O by various enzymes such as catalase (CAT) or glutathione peroxidase (GPx), or alternatively be converted into the hydroxyl radicals ($OH^{\cdot}$) after reacting with metal cations such as Fe^{2+} [23]. These various reactive species can cause damage to proteins, lipids, and DNA, leading to disruption of cellular function and eventually cell death [24]. As such, protection against oxidative stress was observed to increase lifespan in nematodes [25], in flies [26], and mice [27], highlighting a potential key role of limiting oxidative stress as a mechanism to slow the aging process. Increased oxidative stress has been observed with aging in humans, and as such researchers moved forward with the framework of 1) oxidative stress occurs in virtually all organisms, 2) oxidative stress increases with age, and 3) resistance to oxidative stress extends lifespan in some model organisms. The next portion of research would focus on oxidative damage as the potential causal factor underlying oxidative stress in aging.

1.2.3 Oxidative damage theory

The accumulation of oxidative damage over time was proposed to lead to the aging phenotype from a loss in functional capacity at both the cellular and systemic levels, ultimately leading to decreased resilience and death [28]. Further research has shown that there are indeed measurable age-related increases in these free radicals, which lead to increased oxidative stress and oxidative damage [28]. Age-related increases in oxidative stress and damage appeared to affect function as well as overall lifespan. Several studies have reported connections between oxidative damage or stress and deficits in cognitive function in both rodents [29, 30] and humans [31]. Furthermore, oxidative damage in the brain was also correlated with motor impairment in aged rodents [29]. Importantly, oxidative damage was observed within the brain for both cognitive and motor impairments, suggesting that these functional deficits had a central deficit component.

However, the abundance of oxidative stress research has led to conflicting results, with many studies showing that ameliorating oxidative stress has limited effects on overall lifespan in higher organisms or under optimal conditions. Limiting oxidative stress via overexpression of SOD or CAT, individually or in combination failed to extend lifespan in transgenic mice (Perez et al, 2008). Overexpression of SOD can enhance resistance to oxidative stress, decrease endogenous oxidative damage, and alleviate age-related decline in mitochondrial metabolism, however these benefits appear insufficient to extend lifespan in mice (Jang et al, 2009). Alternatively, under normal physiological conditions overexpression of SOD impaired neural and motor function as seen in decreased nerve regeneration after nerve injury [32], accelerated motor-neuron degeneration similarly to amyotrophic lateral sclerosis models [33], and induced deficits in hippocampal neurons and mitochondrial function [34, 35]. Additionally, only 1 of 6

systemic antioxidant enzyme knockout mouse strains had a decreased life span [36]. Thus, it does not seem to be as simple as limiting oxidative stress or boosting antioxidant enzymes leads to decreased oxidative damage and the delay of functional loss or the aging process.

Although the global alteration of antioxidant enzymes has not proven fruitful in modulation of lifespan, targeted overexpression to the mitochondria appears to be more beneficial than systemic changes in antioxidant enzymes, as it can extend mouse lifespan [37]and overexpression of mitochondrial SOD extends the lifespan of drosophila [38]. Interestingly, overexpression of SOD in *C. Elegans* increases H_2O_2 production but paradoxically extended lifespan, and this lifespan extension was not reversed with the overexpression of catalase. Overall, enzymatic overexpression in this case led to increased ROS production, and higher levels of protein oxidation. This mild increase in oxidative stress appeared to lead to an extension of lifespan [39]. Although oxidative stress is classically thought of in terms of its damaging effects, more recent research has highlighted the importance of oxidative stress in terms of its signaling effects. This can be defined as redox signaling, and is not equivalent to oxidative damage. Given the importance of the mitochondria in energy production and metabolism, further research has focused on examining the role of oxidative stress and redox state in modulating metabolic signaling and function.

1.3 Redox biology

The field advanced again in the late 1980's as $O_2^{\cdot -}$ and H_2O_2were found to be biologically useful signals eliciting cellular signaling cascades in normal physiology [40]. These data provided evidence of the duality of ROS in that although oxidative stress can lead to oxidative

damage, moderate ROS is also potentially necessary for normal physiological function. The necessity of some ROS as a signal is apparent where a blockade of redox signaling via antioxidant supplementation prevents some benefits from exercise and other interventions that induce mild oxidative stress [41, 42]. This required research to account for both increases and decreases of ROS as a redox signal capable of leading to positive or negative outcomes.

The framework of the dual nature of redox modulation is reflected in multiple theories, namely hormesis and adaptive homeostasis, and more recently oxidative eustress and distress. Importantly, hormesis indicates a positive response to some damaging stimulus, while adaptive homeostasis does not require damage and instead is defined as a response within the adaptive range. Adaptive homeostasis places an emphasis on a temporary signal outside the normal homeostatic range leading to induction of a stress response or other signaling cascade, and resulting in some type of adaptation [25]. This signal cannot go vastly outside the range of homeostasis or else it would lead to a negative effect and/or damage response. Similarly, the dichotomy of redox stress was defined as oxidative eustress and oxidative distress, where the beneficial redox signaling turns into a negative across a spectrum of redox stress [43] .

Building off previous research emphasizing the necessity of ROS as a useful biological signal, overexpression of SOD in nematode lead to enhanced lifespan. However, this lifespan increase was not due to decreased oxidative stress and damage, but rather associated with a moderate but significant increase in H_2O_2 via superoxide anion shifting over into H_2O_2. Interestingly catalase overexpression alone led to H_2O_2 deficiency and cell rupture/mortality, negatively affecting lifespan [21] and suggesting the necessity of some basal level of redox stress as a form of redox signaling. Alternatively, overexpression of both SOD and catalase maintained the extended lifespan, but did not significantly decrease protein carbonyl levels suggesting that

the extended lifespan cannot be explained by simply limiting oxidative damage. These results highlight the spectrum of oxidative stress: from normal physiological signal leading to positive adaptation to substantial redox stress leading to damage or aberrant signaling [19].

While blocking redox signaling via exogenous antioxidants in otherwise healthy organisms can prevent some positive adaptations, the overexpression of specific antioxidant enzymes can positively affect lifespan. In drosophila, overexpression of glutamate cysteine ligase (GCL) or glucose-6 phosphate dehydrogenase (G6PD), two key enzymes in glutathione synthesis or glutathione regeneration and influencer of red, have been shown to extend lifespan, even in long-lived strains [44, 45]. Additionally, even transient decreases in glutathione (GSH) levels can induce long-term cognitive deficits in mice [46] and lower levels of GSH are associated with increased disease progression in patients with Alzheimer's disease or mild cognitive impairment [47]. Whether through de novo synthesis or enzymatic regeneration, GSH appears to play a major role in age-related redox stress adaptations.

1.4 Glutathione

Age-related increases in oxidative stress coupled with decreased antioxidant defense [48] can cause macromolecular oxidative damage, and this information led to the development of various iterations of the Oxidative Stress Hypothesis of Aging [49]. In humans and in rodents, studies have provided evidence of increased reactive oxygen species (ROS) and oxidative damage in the aging brain [50, 51], and that damage accumulation varied in different regions of the brain [52]. Furthermore, protein oxidative damage in the cerebral cortex and in the cerebellum of old mice was found to vary directly with the severity of their cognitive (water maze acquisition) and motor (bridge walking) impairments, respectively [29]. However, this

hypothesis has failed to withstand the past 60 years of research as controversy has emerged, as over and under-expression of many different antioxidant enzymes in animal models had minimal effects on lifespan [53]. Although oxidative stress and oxidative damage occur with aging, they are not thought to be the central mechanism underlying aging processes, but rather a potential indicator of an underlying issue in redox regulation [54-56]. Classically, experiments have focused on individual measures of reactive oxygen or reactive nitrogen species along with oxidative damage markers, while more recent experiments have used shifts in the redox state of glutathione (GSH:GSSG; reduced glutathione:oxidized glutathione) as a more sensitive indicator of cellular redox state [57], and have indicated a progressive, age-dependent pro-oxidizing shifts in several brain regions that began as early as 6 months of age [58]. Importantly, this pro-oxidizing shift is sufficient to produce redox-dependent cellular signaling dysfunction [59]. Redox status, as measured via GSH can be predictive of cognitive decline in otherwise healthy older individuals [60] which suggests GSH is an important biomarker, as well as an important molecule in overall health. Thus, there is a likely role of oxidative stress within aging, but oxidative damage of macromolecules alone does not appear sufficient to explain the aging process.

Given the limitations of the oxidative stress hypothesis of aging, the central cause of aging is still under investigation and has led to the updated Redox Stress Theory of Aging [57, 61]. This theory postulates that overabundant reactive oxygen species (ROS) can cause oxidative damage and a pro-oxidizing shift in reduction-oxidation (redox) state, while moderate levels of ROS are a biologically useful signal [57]. Aging is theorized to occur due to a progressive shift of redox state from a reductive to more oxidative environment, leading to dysregulation of redox signaling [62]. Although several redox couples are responsible for the overall redox state,

glutathione (GSH) in the reduced or oxidized form is the predominant redox couple, and as such modulation of redox state can be achieved by altering levels of GSH. Additionally, GSH levels are affected by aging, where typically GSH is decreased as well as the GSH:GSSG ratio, indicating a pro-oxidant shift in aging [63]. GSH, as a tripeptide thiol, can directly scavenge free radicals, is also the main determinant of redox state, and is involved in cell signaling and cell regulation [64]. Therefore GSH levels may be a more sensitive indicator of redox state of the cell measures of ROS/RNS, and have functions beyond antioxidant defense.

GSH:GSSG is the dominant redox couple within biological tissues, representing the largest pool of reduction potential, estimated to be between -150 and -260 mV. [65]. It is metabolically linked to the other major redox couples nicotinamide adenine dinucleotide phosphate (NADPH:NADP) and nicotinamide adenine dinucleotide (NADH:NAD+), through a series of electron transfers via enzymatic reactions. NADPH:NADP directly regenerates GSH:GSSG through glutathione-peroxidase (GPx) enzymes, while NADH:NAD+ is indirectly connected to GSH:GSSG levels via an alternative pathway of NADPH:NADP regeneration by the nicotinamide nucleotide transhydrogenase (NNT) enzyme. All three of these redox couples combine to supply the majority of the reducing power of biological tissues [66]. However, of the three redox couples GSH:GSSG supplies the largest share of the overall reductive power as they are present at levels 2-4 orders of magnitude higher than the NADPH:NADP and NADH:NAD+ couples [65]. GSH synthesis is rate-limited by glutamate cysteine ligase (GCL), a heterodimer consisting of a catalytic (GCLC) subunit and a modifier (GCLM) subunit [64]. Elimination of the GCLC subunit is embryonic lethal, while genetic knockout of the GCL modifier subunit ($GCLM^{-/-}$) in mice leads to a 70-90% decrease in GSH levels across various tissues, including the liver, brain, kidney, and lung [67] (Figure 1).

Although there is a distinct lack of data on chronic GSH deficiency through models such as GCLM$^{-/-}$, acute GSH deficiency leads to lasting impaired motor function and balance in young rodents, worsens motor neuron decline in disease models, impairs cognitive function, and disrupts redox signaling in young and old rodents [68-71]. Interestingly, either acutely deficient GSH via buthionine sulfoxamine (BSO) administration or GSH overproduction via overexpression of GCL lead to degeneration of dopaminergic neurons in rats implicating redox signaling dysfunction, rather than increased oxidative damage or stress, in these studies [72]. Furthermore, GSH naturally decreases across the lifespan and has been associated with cognitive decline in both humans and mice [73, 74]. As such, for our paradigm, GCLM$^{-/-}$ mice have chronically decreased levels of GSH, are more susceptible to additional endogenous or exogenous oxidative insults [75], but more importantly have a much more pro-oxidative redox environment likely leading to a dysregulated redox state [67]. Understandably, GCLM$^{-/-}$ mice already have oxidative damage in cerebellar neurons at 4 months [76], and we expected that chronic GSH deficiency across the lifespan will lead to a worsening of oxidative damage and continued dysregulation of redox state. This should lead to an early aging phenotype if redox state is in fact a determinant factor in aging. An alternative model of chronic neuronal GSH depletion, is the excitatory amino acid carrier–1 knockout (EAAC1$^{-/-}$) mouse. In this model, chronic GSH depletion led to increased oxidative stress and damage, along with brain atrophy and substantial impairment of hippocampal-dependent memory [77] by 11 months. Cultured neurons from EAAC1-/- mice were also greatly sensitized to oxidative insults, and wild-type neurons pre-treated with BSO displayed a similar sensitized phenotype. Interestingly, while biochemical phenotypes were present at ~2 months, behavioral deficits were not observed until 11 months. Importantly, GSH in mice peaks at maturation then is stable up to ~26 months, and

decreased dramatically by 31 months in male C57BL/6 mice [73]. As such, even in animals with drastically impaired redox balance, age is still a factor in determining the response.

Moderate levels of oxidative stress can induce cell signaling cascades through GSH cycling, and although it is primarily thought of in regards to its antioxidant function it is also an important modulator of redox signaling [78]. Experimentation with genetic models of redox dysregulation ($GCLM^{-/-}$) dramatically increased the sensitivity of mice to *in vivo* oxidative insult with 90% mortality, while a lower dose of exogenous oxidative stressors had no mortality but caused hemolysis and decreased kidney function *in vivo*. In vitro erythrocytes from these mice were highly sensitized to oxidative insults as well. GSH levels in erythrocytes were 10% of wild-type mice [79]. Primary cerebellar granule cells from $GCLM^{-/-}$ mice are highly sensitized to oxidative stress leading to increased cell death and increased apoptosis with caspase 3 activation. GSSG levels were increased with oxidative stress insults in both $GCLM^{+/+}$ and $GCLM^{-/-}$ cells, but to a greater extent in $GCLM^{-/-}$ cells [80]. In another study by the same group, oxidative stress induced more cell death in $GCLM^{-/-}$ primary cerebellar granule neurons (10x higher sensitivity to exogenous oxidative stressors) [76]. Other experiments examined the effects of oxidative stress in $GCLM^{-/-}$ primary co-cultured hippocampal neurons and astrocytes, where neurons alone were more sensitized to oxidative stress and co-cultured astrocytes and neurons were sensitized but to a lesser extent [81]. Furthermore, in vitro blocking of GCL via BSO in rat primary lung epithelial cells led to an increased inflammatory response to lipopolysaccharide insult [82]. Thus, in both acute and chronic models, rodents with impaired GSH generation are sensitized to oxidative stress and inflammation.

Behaviorally, young $GCLM^{-/-}$ mice displayed limited changes in motor and cognitive function [83]. Acute depletion of GSH by ~50% in the brain of rats or mice by treatment with

intra-peritoneal oxidative stressors compared to saline led to small deficits in Y-maze test for memory [84]. Importantly, in an alternative model of neuronal GSH depletion, biochemical deficits were present in at ~2 months, however behavioral deficits were not observed until 11 months. As such, even in animals with drastically impaired redox balance but within an optimal living environment, age is still a factor in determining the response. Therefore, there is a greater need to characterize these animals long term, as all studies performed up to now have focused on younger animals.

Along with behavioral characterization, two related pathways of interest are the redox sensitive AMP-activated protein kinase (AMPK) and mammalian target of rapamyacin (mTOR) protein kinase systems. An overview of the proposed pathways interactions with redox state is seen in Figure 2. These pathways act in opposition to each other, where AMPK is considered the master regulator for cellular energy metabolism while mTOR is integral for growth and differentiation of cells. AMPK is primarily activated by a higher ratio of adenosine monophosphate (AMP) to adenosine triphosphate (ATP), indicating low-energy status and triggering cellular cascades to replenish ATP by increasing fatty acid oxidation and concurrently limiting pathways related to energy storage [85]. AMPK activation can also stimulate autophagy to aid in recapturing energy stores by the breakdown of entire cells or organelles. Finally, inactivation of AMPK can promote energy storage and growth through processes such as gluconeogenesis, fatty acid synthesis, and protein synthesis [85]. While alterations in the AMP:ATP ratio is the primary metabolic signal to active AMPK, more recently AMPK has been found to be redox sensitive and can be activated or inactivated directly or indirectly through redox signaling [86]. AMPK is also a highly researched pathway within the aging field, as

increased activation of AMPK appears to promote several pro-longevity mechanisms, making it an attractive target for biology of aging research.

Opposite of the AMPK pathway, mTOR activation largely leads to the activation of pro-growth pathways resulting in increased cell growth, differentiation, anabolic processes yielding more macromolecules such as lipids, proteins, and organelles, as well as decreased autophagy [87]. As such mTOR is classically though of the master regulator for cell growth and proliferation, and as an almost polar opposite of the AMPK pathway. Activation of mTOR classically occurs through growth factors such as insulin-like growth factor-1 (IGF-1) through a series of upstream protein kinases. Alternatively, mTOR can be inactivated by a blockade of these kinases via the AMPK pathway, highlighting the tight control and interaction between these two metabolic pathways. The biology of aging field is also highly interested in mTOR as various drugs or other interventions that limit mTOR activation have been shown to be pro-longevity in various animal models. There is also recent evidence that mTOR signaling can be modulated by redox state, further highlighting the need to explore this pathway in the present study.

1.5 Goals of the current research

Glutathione is the primary indicator and controller of endogenous redox state, however there is limited research on the effects of lifelong redox dysregulation through systemic glutathione deficits. All current studies have focused on either transient changes in glutathione or only examined young glutathione deficient animals. The long-term effects of glutathione depletion on lifespan, motor function, cognitive function, and overall redox state have not been addressed. Therefore, the proposed studies will focus on exploring the effects of glutathione depletion on motor and cognitive function across the lifespan, primarily by comparing young, adult and old animals with and without glutathione depletion. It is suggested that glutathione depletion will exacerbate age-related decline due to limited defense against reactive oxygen species and disruption of redox status and redox signaling. To further explore the biochemical and longevity effects of glutathione depletion, these studies will also examine the effects of lifelong glutathione depletion on cellular signaling, redox status, and lifespan. Thus the working hypothesis of this study is '**Lifelong glutathione depletion will exacerbate age-related decline in motor and cognitive function, decrease lifespan, and disrupt redox-sensitive proteins'**.

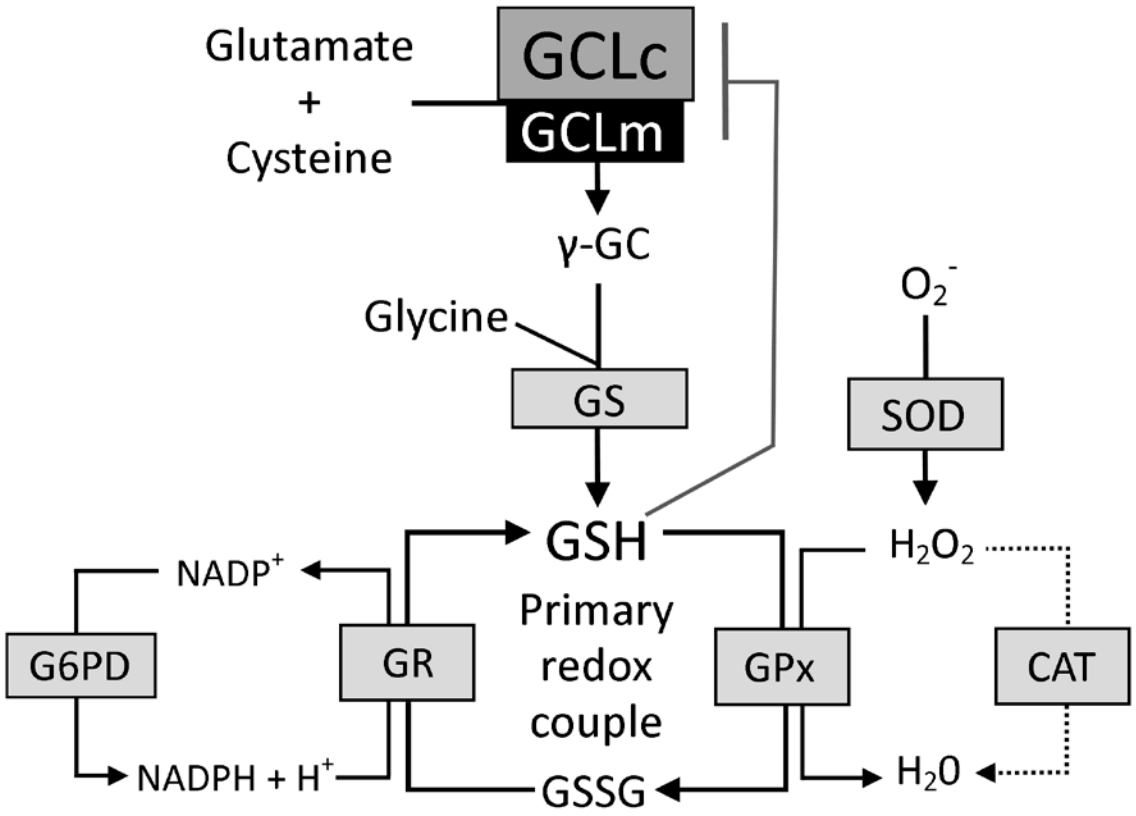

Figure 1: Glutathione (GSH) synthesis pathway and effect of GCLM-/-. The two-subunit holoenzyme glutamate cysteine ligase (GCL) couples glutamate and cysteine to form γ-glutamylcysteine and is the rate-limiting step in GSH synthesis. The GCL catalytic subunit (GCLc) provides all the catalytic function, while the GCL modifier subunit (GCLm) increases affinity for glutamate and decreases feedback inhibition by GSH. Glycine is then added via GSH synthetase (GS) to form GSH. GSH can be oxidized to GSSG to detoxify H_2O_2 generated by conversion of O_2^- to H_2O_2 by superoxide dismutase (SOD). GSSG is regenerated to GSH via glutathione reductase (GR) which concurrently oxidizes NADPH to NADP+. Glucose-6-phosphate dehydrogenase (G6PD) can then reduce NADP+ to NADPH in preparation for continuation of the redox cycling of GSH and GSSG. Alternatively, H_2O_2 can be detoxified via catalase (CAT) or other peroxidases.

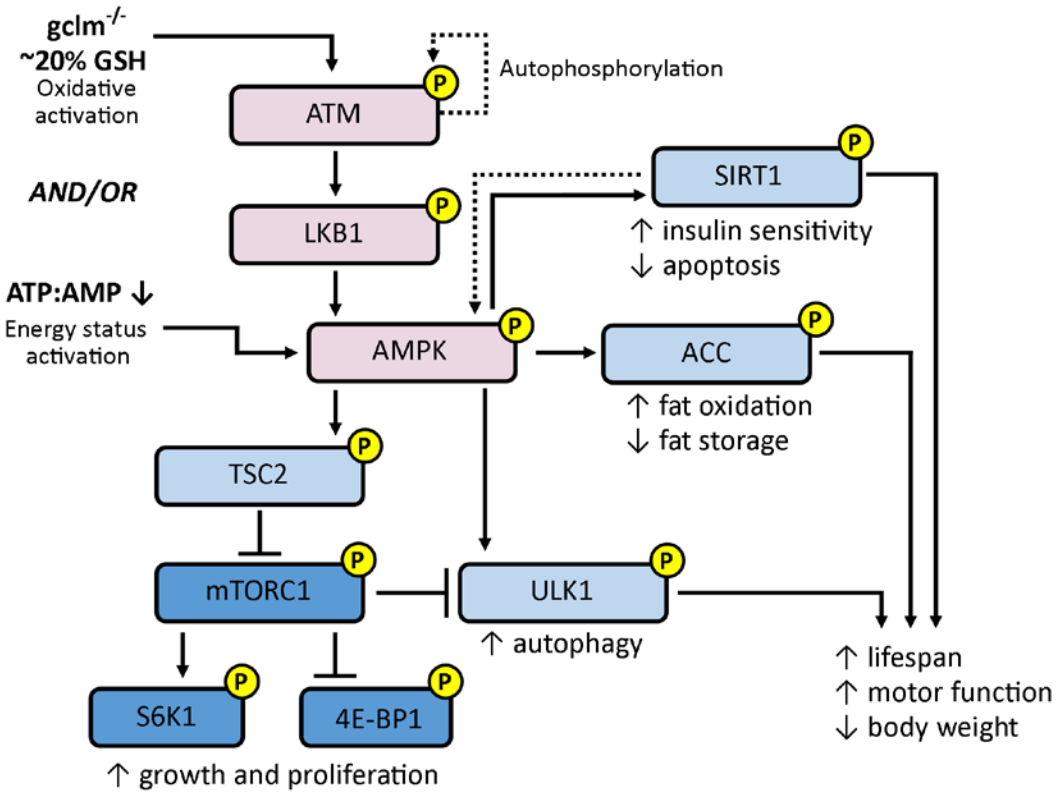

Figure 2. Proposed pathway for interaction of GCLM-/- genotype with AMPK and mTOR pathways. ataxia-telangiectasia mutated kinase (ATM), liver kinase B1 (LKB1), AMP-activated protein kinase (AMPK), tuberous sclerosis complex 2 (TSC2), mammalian target of rapamyacin (mTOR), S6 kinase (S6K1), eukaryotic translation initiation factor 4E)-binding proteins 1 (4E-BP1), unc-51-like kinase 1 (ULK1), acetyl-CoA carboxylase (ACC), and sirtuin-1 (SIRT).

References

1. Sternberg, S.A., et al., *The identification of frailty: a systematic literature review.* J Am Geriatr Soc, 2011. **59**(11): p. 2129-38.
2. Fried, L.P., et al., *Frailty in older adults: evidence for a phenotype.* J Gerontol A Biol Sci Med Sci, 2001. **56**(3): p. M146-56.
3. Rockwood, K., X. Song, and A. Mitnitski, *Changes in relative fitness and frailty across the adult lifespan: evidence from the Canadian National Population Health Survey.* CMAJ, 2011. **183**(8): p. E487-94.
4. United Nations, D.o.E.a.S.A., Population Division, *World Population Ageing 2015.* 2015.
5. Ortman, J.M., V.A. Velkoff, and H. Hogan, *An aging nation: the older population in the United States.* Washington, DC: US Census Bureau, 2014: p. 25-1140.
6. Jaul, E. and J. Barron, *Age-Related Diseases and Clinical and Public Health Implications for the 85 Years Old and Over Population.* Front Public Health, 2017. **5**: p. 335.
7. Crimmins, E.M. and H. Beltran-Sanchez, *Mortality and morbidity trends: is there compression of morbidity?* J Gerontol B Psychol Sci Soc Sci, 2011. **66**(1): p. 75-86.
8. Jin, K., *Modern Biological Theories of Aging.* Aging Dis, 2010. **1**(2): p. 72-74.
9. Commoner, B., J. Townsend, and G.E. Pake, *Free radicals in biological materials.* Nature, 1954. **174**(4432): p. 689-91.
10. Harman, D., *Aging: a theory based on free radical and radiation chemistry.* J Gerontol, 1956. **11**(3): p. 298-300.
11. Freeman, B.A. and J.D. Crapo, *Biology of disease: free radicals and tissue injury.* Lab Invest, 1982. **47**(5): p. 412-26.

12. Brand, M.D., *Mitochondrial generation of superoxide and hydrogen peroxide as the source of mitochondrial redox signaling.* Free Radic Biol Med, 2016. **100**: p. 14-31.

13. Babior, B.M., R.S. Kipnes, and J.T. Curnutte, *Biological defense mechanisms. The production by leukocytes of superoxide, a potential bactericidal agent.* J Clin Invest, 1973. **52**(3): p. 741-4.

14. Meier, B., et al., *Human fibroblasts release reactive oxygen species in response to interleukin-1 or tumour necrosis factor-alpha.* Biochem J, 1989. **263**(2): p. 539-45.

15. McCord, J.M. and I. Fridovich, *The utility of superoxide dismutase in studying free radical reactions. I. Radicals generated by the interaction of sulfite, dimethyl sulfoxide, and oxygen.* J Biol Chem, 1969. **244**(22): p. 6056-63.

16. Sies, H., *Oxidative stress: introductory remarks.* Oxidative stress, 1985.

17. Harman, D., *Free radical theory of aging.* Mutat Res, 1992. **275**(3-6): p. 257-66.

18. Beckman, K.B. and B.N. Ames, *The free radical theory of aging matures.* Physiol Rev, 1998. **78**(2): p. 547-81.

19. Salmon, A.B., A. Richardson, and V.I. Perez, *Update on the oxidative stress theory of aging: does oxidative stress play a role in aging or healthy aging?* Free Radic Biol Med, 2010. **48**(5): p. 642-55.

20. Ott, M., et al., *Mitochondria, oxidative stress and cell death.* Apoptosis, 2007. **12**(5): p. 913-22.

21. Babior, B.M., *Phagocytes and oxidative stress.* Am J Med, 2000. **109**(1): p. 33-44.

22. Schrader, M. and H.D. Fahimi, *Peroxisomes and oxidative stress.* Biochim Biophys Acta, 2006. **1763**(12): p. 1755-66.

23. Schieber, M. and N.S. Chandel, *ROS function in redox signaling and oxidative stress.* Curr Biol, 2014. **24**(10): p. R453-62.

24. Cadenas, E. and K.J. Davies, *Mitochondrial free radical generation, oxidative stress, and aging.* Free Radic Biol Med, 2000. **29**(3-4): p. 222-30.

25. Melov, S., et al., *Extension of life-span with superoxide dismutase/catalase mimetics.* Science, 2000. **289**(5484): p. 1567-9.

26. Sun, J. and J. Tower, *FLP recombinase-mediated induction of Cu/Zn-superoxide dismutase transgene expression can extend the life span of adult Drosophila melanogaster flies.* Mol Cell Biol, 1999. **19**(1): p. 216-28.

27. Migliaccio, E., et al., *The p66shc adaptor protein controls oxidative stress response and life span in mammals.* Nature, 1999. **402**(6759): p. 309-13.

28. Bokov, A., A. Chaudhuri, and A. Richardson, *The role of oxidative damage and stress in aging.* Mech Ageing Dev, 2004. **125**(10-11): p. 811-26.

29. Forster, M.J., et al., *Age-related losses of cognitive function and motor skills in mice are associated with oxidative protein damage in the brain.* Proc Natl Acad Sci U S A, 1996. **93**(10): p. 4765-9.

30. Fukui, K., et al., *Cognitive impairment of rats caused by oxidative stress and aging, and its prevention by vitamin E.* Ann N Y Acad Sci, 2002. **959**: p. 275-84.

31. Keller, J.N., et al., *Evidence of increased oxidative damage in subjects with mild cognitive impairment.* Neurology, 2005. **64**(7): p. 1152-6.

32. Kotulska, K., et al., *Overexpression of copper/zinc-superoxide dismutase in transgenic mice markedly impairs regeneration and increases development of neuropathic pain after sciatic nerve injury.* J Neurosci Res, 2006. **84**(5): p. 1091-7.

33. Jaarsma, D., et al., *Human Cu/Zn superoxide dismutase (SOD1) overexpression in mice causes mitochondrial vacuolization, axonal degeneration, and premature motoneuron death and accelerates motoneuron disease in mice expressing a familial amyotrophic lateral sclerosis mutant SOD1.* Neurobiol Dis, 2000. **7**(6 Pt B): p. 623-43.

34. Shin, J.H., et al., *Aberrant neuronal and mitochondrial proteins in hippocampus of transgenic mice overexpressing human Cu/Zn superoxide dismutase 1.* Free Radic Biol Med, 2004. **37**(5): p. 643-53.

35. Shin, J.H., et al., *Proteome analysis in hippocampus of mice overexpressing human Cu/Zn-superoxide dismutase 1.* Neurochem Int, 2005. **46**(8): p. 641-53.

36. Jang, Y.C. and H. Van Remmen, *The mitochondrial theory of aging: insight from transgenic and knockout mouse models.* Exp Gerontol, 2009. **44**(4): p. 256-60.

37. Schriner, S.E., et al., *Extension of murine life span by overexpression of catalase targeted to mitochondria.* Science, 2005. **308**(5730): p. 1909-11.

38. Sun, J., et al., *Induced overexpression of mitochondrial Mn-superoxide dismutase extends the life span of adult Drosophila melanogaster.* Genetics, 2002. **161**(2): p. 661-72.

39. Cabreiro, F., et al., *Increased life span from overexpression of superoxide dismutase in Caenorhabditis elegans is not caused by decreased oxidative damage.* Free Radic Biol Med, 2011. **51**(8): p. 1575-82.

40. Mittal, C.K. and F. Murad, *Activation of guanylate cyclase by superoxide dismutase and hydroxyl radical: a physiological regulator of guanosine 3',5'-monophosphate formation.* Proc Natl Acad Sci U S A, 1977. **74**(10): p. 4360-4.

41. Ristow, M., et al., *Antioxidants prevent health-promoting effects of physical exercise in humans.* Proc Natl Acad Sci U S A, 2009. **106**(21): p. 8665-70.

42. Ristow, M. and S. Schmeisser, *Extending life span by increasing oxidative stress.* Free Radic Biol Med, 2011. **51**(2): p. 327-36.

43. Sies, H., *Hydrogen peroxide as a central redox signaling molecule in physiological oxidative stress: Oxidative eustress.* Redox Biol, 2017. **11**: p. 613-619.

44. Orr, W.C., et al., *Overexpression of glutamate-cysteine ligase extends life span in Drosophila melanogaster.* J Biol Chem, 2005. **280**(45): p. 37331-8.

45. Legan, S.K., et al., *Overexpression of glucose-6-phosphate dehydrogenase extends the life span of Drosophila melanogaster.* J Biol Chem, 2008. **283**(47): p. 32492-9.

46. Castagne, V., et al., *Low brain glutathione and ascorbic acid associated with dopamine uptake inhibition during rat's development induce long-term cognitive deficit: relevance to schizophrenia.* Neurobiol Dis, 2004. **15**(1): p. 93-105.

47. Bermejo, P., et al., *Peripheral levels of glutathione and protein oxidation as markers in the development of Alzheimer's disease from Mild Cognitive Impairment.* Free Radic Res, 2008. **42**(2): p. 162-70.

48. Wei, Y.H. and H.C. Lee, *Oxidative stress, mitochondrial DNA mutation, and impairment of antioxidant enzymes in aging.* Exp Biol Med (Maywood), 2002. **227**(9): p. 671-82.

49. Kregel, K.C. and H.J. Zhang, *An integrated view of oxidative stress in aging: basic mechanisms, functional effects, and pathological considerations.* Am J Physiol Regul Integr Comp Physiol, 2007. **292**(1): p. R18-36.

50. Grimm, S., et al., *Protein oxidative modifications in the ageing brain: consequence for the onset of neurodegenerative disease.* Free Radic Res, 2011. **45**(1): p. 73-88.

51. Perluigi, M., et al., *Redox proteomics in aging rat brain: involvement of mitochondrial reduced glutathione status and mitochondrial protein oxidation in the aging process.* J Neurosci Res, 2010. **88**(16): p. 3498-507.

52. Dubey, A., et al., *Effect of age and caloric intake on protein oxidation in different brain regions and on behavioral functions of the mouse.* Arch Biochem Biophys, 1996. **333**(1): p. 189-97.

53. Perez, V.I., et al., *Is the oxidative stress theory of aging dead?* Biochim Biophys Acta, 2009. **1790**(10): p. 1005-14.

54. Ferguson, G. and W. Bridge, *Glutamate cysteine ligase and the age-related decline in cellular glutathione: The therapeutic potential of gamma-glutamylcysteine.* Arch Biochem Biophys, 2016. **593**: p. 12-23.

55. Huang, T.T., D. Leu, and Y. Zou, *Oxidative stress and redox regulation on hippocampal-dependent cognitive functions.* Arch Biochem Biophys, 2015. **576**: p. 2-7.

56. Sohal, R.S. and M.J. Forster, *Caloric restriction and the aging process: a critique.* Free Radic Biol Med, 2014. **73**: p. 366-82.

57. Sohal, R.S. and W.C. Orr, *The redox stress hypothesis of aging.* Free Radic Biol Med, 2012. **52**(3): p. 539-55.

58. Rebrin, I., M.J. Forster, and R.S. Sohal, *Effects of age and caloric intake on glutathione redox state in different brain regions of C57BL/6 and DBA/2 mice.* Brain Res, 2007. **1127**(1): p. 10-8.

59. Droge, W. and H.M. Schipper, *Oxidative stress and aberrant signaling in aging and cognitive decline.* Aging Cell, 2007. **6**(3): p. 361-70.

60. Hajjar, I., et al., *Oxidative stress predicts cognitive decline with aging in healthy adults: an observational study.* J Neuroinflammation, 2018. **15**(1): p. 17.

61. Muller, F.L., et al., *Trends in oxidative aging theories.* Free Radic Biol Med, 2007. **43**(4): p. 477-503.

62. Rebrin, I. and R.S. Sohal, *Pro-oxidant shift in glutathione redox state during aging.* Adv Drug Deliv Rev, 2008. **60**(13-14): p. 1545-52.

63. Maher, P., *The effects of stress and aging on glutathione metabolism.* Ageing Research Reviews, 2005. **4**(2): p. 288-314.

64. Fujii, J., et al., *Unveiling the roles of the glutathione redox system in vivo by analyzing genetically modified mice.* J Clin Biochem Nutr, 2011. **49**(2): p. 70-8.

65. Schafer, F.Q. and G.R. Buettner, *Redox environment of the cell as viewed through the redox state of the glutathione disulfide/glutathione couple.* Free Radic Biol Med, 2001. **30**(11): p. 1191-212.

66. Berthiaume, J.M., et al., *Mitochondrial NAD(+)/NADH Redox State and Diabetic Cardiomyopathy.* Antioxid Redox Signal, 2017.

67. McConnachie, L.A., et al., *Glutamate cysteine ligase modifier subunit deficiency and gender as determinants of acetaminophen-induced hepatotoxicity in mice.* Toxicol Sci, 2007. **99**(2): p. 628-36.

68. Diaz-Hung, M.L., et al., *Sensory-motor performance after acute glutathione depletion by L-buthionine sulfoximine injection into substantia nigra pars compacta.* Behav Brain Res, 2014. **271**: p. 286-93.

69. Chi, L., et al., *Depletion of reduced glutathione enhances motor neuron degeneration in vitro and in vivo.* Neuroscience, 2007. **144**(3): p. 991-1003.

70. Morrison, J.P., et al., *Aging reduces responsiveness to BSO- and heat stress-induced perturbations of glutathione and antioxidant enzymes.* Am J Physiol Regul Integr Comp Physiol, 2005. **289**(4): p. R1035-41.

71. Cabungcal, J.H., et al., *Transitory glutathione deficit during brain development induces cognitive impairment in juvenile and adult rats: relevance to schizophrenia.* Neurobiol Dis, 2007. **26**(3): p. 634-45.

72. Garrido, M., et al., *Glutathione depletion and overproduction both initiate degeneration of nigral dopaminergic neurons.* Acta Neuropathol, 2011. **121**(4): p. 475-85.

73. Chen, T.S., J.P. Richie, Jr., and C.A. Lang, *The effect of aging on glutathione and cysteine levels in different regions of the mouse brain.* Proc Soc Exp Biol Med, 1989. **190**(4): p. 399-402.

74. Currais, A. and P. Maher, *Functional consequences of age-dependent changes in glutathione status in the brain.* Antioxid Redox Signal, 2013. **19**(8): p. 813-22.

75. Yang, Y., et al., *Initial characterization of the glutamate-cysteine ligase modifier subunit Gclm(-/-) knockout mouse. Novel model system for a severely compromised oxidative stress response.* J Biol Chem, 2002. **277**(51): p. 49446-52.

76. Giordano, G., et al., *Neurotoxicity of domoic Acid in cerebellar granule neurons in a genetic model of glutathione deficiency.* Mol Pharmacol, 2006. **70**(6): p. 2116-26.

77. Aoyama, K., et al., *Neuronal glutathione deficiency and age-dependent neurodegeneration in the EAAC1 deficient mouse.* Nat Neurosci, 2006. **9**(1): p. 119-26.

78. Jones, D.P., *Redox potential of GSH/GSSG couple: assay and biological significance.* Methods Enzymol, 2002. **348**: p. 93-112.

79. Foller, M., et al., *Functional significance of glutamate-cysteine ligase modifier for erythrocyte survival in vitro and in vivo.* Cell Death Differ, 2013. **20**(10): p. 1350-8.

80. Giordano, G., et al., *Glutathione levels modulate domoic acid induced apoptosis in mouse cerebellar granule cells.* Toxicol Sci, 2007. **100**(2): p. 433-44.

81. Giordano, G., T.J. Kavanagh, and L.G. Costa, *Neurotoxicity of a polybrominated diphenyl ether mixture (DE-71) in mouse neurons and astrocytes is modulated by intracellular glutathione levels.* Toxicol Appl Pharmacol, 2008. **232**(2): p. 161-8.

82. Haddad, J.J., et al., *Inhibition of glutathione-related enzymes augments LPS-mediated cytokine biosynthesis: involvement of an IkappaB/NF-kappaB-sensitive pathway in the alveolar epithelium.* Int Immunopharmacol, 2002. **2**(11): p. 1567-83.

83. Cole, T.B., et al., *Behavioral Characterization of GCLM-Knockout Mice, a Model for Enhanced Susceptibility to Oxidative Stress.* J Toxicol, 2011. **2011**: p. 157687.

84. Dean, O., et al., *Glutathione depletion in the brain disrupts short-term spatial memory in the Y-maze in rats and mice.* Behav Brain Res, 2009. **198**(1): p. 258-62.

85. Mihaylova, M.M. and R.J. Shaw, *The AMPK signalling pathway coordinates cell growth, autophagy and metabolism.* Nat Cell Biol, 2011. **13**(9): p. 1016-23.

86. Emerling, B.M., et al., *Hypoxic activation of AMPK is dependent on mitochondrial ROS but independent of an increase in AMP/ATP ratio.* Free Radic Biol Med, 2009. **46**(10): p. 1386-91.

87. Laplante, M. and D.M. Sabatini, *mTOR signaling at a glance.* J Cell Sci, 2009. **122**(Pt 20): p. 3589-94.

CHAPTER 2

MATERIALS AND METHODS

2.1 Animals

Procedures were approved by the Institutional Animal Care and Use Committee at the University of North Texas Health Science Center (UNT HSC) at Fort Worth, and adhered to NIH guidelines. The mice heterozygous for GCLM (GCLM +/-) were generated on a C57BL/6J (B6.129) background, acquired from Dr. Terrance Kavanagh from University of Washington, rederived and backcrossed at least 7 generations into C57BL/6 mice by Jackson Laboratories. Once in the UNT HSC vivarium, triads of GCLM+/- were mated to obtain wild-type (GCLM+/+) and knock-out (GCLM-/-) littermates. From the in-house breeding colony, male and female mice were housed and aged in groups of 2-4, separated according to sex and genotype, in standard polycarbonate cages (28 x 17 x 12.5 cm) with corncob bedding and ad libitum access to water and standard rodent chow (LabDiet® R&M 5LG6 5S84; catalog number: 1813505 from TestDiet, Richmond, IN), and were maintained at ambient temperature (23 ± 1° C), under a 12-h light/dark cycle starting at 0600.

We maintained a breeding colony to generate animals for behavioral assessment, tissue collection, and an aging cohort to determine lifespan. Some animals were singly housed due to

social incompatibility or death of cage mates, and animals received no enrichment as it can affect lifespan and behavioral outcomes. Animals were identified via a subcutaneously embedded 2 mm x 13 mm Rf scannable chip. Weights were taken bi-monthly for animals not currently in behavior analysis, and weekly for animals undergoing behavior. The day of each animal's death was recorded to allow for lifespan analysis. We performed a post-hoc power analysis for the discrimination reversal test, which historically represents an unfavorable power/sample size for the behavioral battery. Our smallest group with a sample size of 15 for this test had a one-tailed power of more than 94% for detecting an effect of age.

At the target ages of 5, 10, and 20 months for this study, squads of mice from the aging colony were used for behavioral testing or euthanized for biochemical tissue analyses. The specific animal ages were chosen as they include a young, mature adult, and elderly age corresponding to approximately 25, 40, and 75 years for humans according to our lifespan study and age-equivalency conversions [1].

2.2 Neurobehavioral Measures

The series of test comprises tests measuring spontaneous activity, gait, motor, affective and cognitive functions. Administration of the complete test battery required approximately 10 weeks of testing and details of these procedures have been described in previous publications [2].

2.2.1 Elevated Plus Maze

The plus maze is constructed of plexiglass and is elevated three feet above the floor in a dimly illuminated test room and consists of two arms that are open to the room and two that are closed such that the floor is not visible, with the same type of arms facing each other. A

computerized tracking system (ANY-MAZE, Stoelting) was used to record the position of the mice. Shifts in preference for the closed versus open arms under different lighting conditions was used to detect anxiolytic and anxiogenic effects. The mice were tested under a 60-watt spotlight. All mice were acclimated to the darkened room for 5 min prior to testing. Using the tracking system, the number of entries in open or closed arms as well as the time spent in each arm were recorded during a 5 min observation period. An anxiolytic response was defined as an increase in time spent in the open arms of the maze.

2.2.2 Open field

Each testing box consists of a clear chamber (40.5 X 40.5 X 30.5 cm) surrounded by a metal frame lined with photocells, inside a sound-attenuating chamber equipped with a fan, which provides background noise. Each mouse was placed in a chamber for 4 consecutive sessions, each 4 minutes in duration for a total of 16 minutes. While in the chamber, the photobeams are interrupted by the mouse's activity, which is then recorded by the computer. This activity can be categorized into three basic components: vertical, horizontal, and stereotypic behaviors. Rearing, for example, is a vertical behavior. Horizontal behaviors, on the other hand, included such things as running around the chamber. Behaviors, such as grooming, that occur in a repetitive fashion are considered to be stereotypic.

2.2.3 Coordinated Running

The accelerating rotorod is a motor driven treadmill (Model, Omnirotor treadmill, Omnitech Electronics) used to measure coordinated running. The rotorod consists of a nylon cylinder (length 45 cm, diameter 3.2 cm) mounted horizontally, 35.5 cm above a padded surface.

The cylinder is separated into four 11 cm wide compartments, formed by 5 black round plastic dividers, each with a radius of 15 cm. The cylinder rotates (via a microprocessor controlled motor) with an acceleration of 0.5 revolutions per minute (rpm) per second. On a given trial, four mice were placed on the nylon cylinder (one mouse in each compartment). The cylinder is made to rotate and a timer switch is simultaneously activated. Acceleration continues until either 75 rpm is reached or the last animal is unable to perform the running response and has fallen to the padded surface. When the mouse lands on the surface, a photo sensitive switch is tripped and the timer for that compartment stops. The elapsed time is recorded in tenths of a second as the measure of performance on each trial. Mice received two sessions daily for at least seven sessions. The first session of the day began at approximately 0900 h and the second at 1300 h. Each session consisted of four trials with an interval of ten minutes between the successive trials and a minimum of two hours between the two daily sessions. After the seventh session, performance stability was calculated. All mice must reach a "stability criterion" of three consecutive sessions over which the four trial mean latency to fall did not differ by more than 15%. Mice unable to reach criterion were given additional sessions until the criterion was met.

2.2.4 Psychomotor Function

Walk Initiation: A circle is drawn around the mouse, with a radius corresponding to one body length. The time taken by the mouse to escape out of the circle was recorded. The walk initiation test was given in one daily session for four consecutive days.

Alley Turn: The "alleyway" is constructed of black acrylic (14 X 3 X 14 cm) with an open end and a back wall. The mouse was carefully placed inside the alleyway facing the back wall.

The time (sec) for the mouse to turn completely around and face the open end of the alleyway was recorded. Alley turn was given in one daily session for four consecutive days.

Negative Geotaxis: The apparatus is constructed from a hinged clear acrylic sheet (53 X 30 cm) that is covered with a fine black nylon wire mesh (0.10 X 0.10 cm). A wire is attached to the open ends of the board to ensure a maximum incline of 45^0. The mouse was placed in the center of the wire mesh board, facing away from the experimenter. The board is gently inclined to 45° at the end closest to the experimenter. The time (sec.) for the mouse to turn 90° and 180° was recorded. Negative Geotaxis was given in one daily session for four consecutive days.

Wire Suspension: Each mouse was allowed to grip a horizontal wire with the front paws when suspended 27 cm above a padded surface. The latency to tread (reach the wire with their hind legs) and the latency to fall was recorded and averaged over four consecutive daily sessions (2 trials/ day).

Bridge walking: Each mouse was tested for the latency to fall or reach a safe platform after being placed on one of four acrylic bridges, each mounted 50 cm above a padded surface. The bridges differed in diameter (small or large) and shape (round or square), providing four levels of difficulty. Each bridge was presented three times, and the measure of performance is the average latency to fall (up to a maximum of 60 s) across all bridges and for each bridge.

2.2.5 Morris Water Maze

The swim maze test involves acquisition of an ability to swim to a hidden platform from different starting locations, in the presence of only distal cues as to the location, during a series of nine sessions. A spatial learning index was developed to specifically compare subjects in terms of the rate at which they learned the task.

A plastic tank (120 cm dia, 60 cm high) was filled with water opacified with nontoxic paint and maintained at 24 ± 1^0 C. A computerized tracking system (ANY-MAZE-Stoelting) was used to record the position of the mice. Testing was conducted in four phases: (1) a *pretraining phase (straight alley)* in which the mouse learns the simple response components of swimming and standing on the platform hidden below the water surface, (2) a *place discrimination acquisition phase* in which the mouse must learn and remember the location of the platform, (3) a *probe trial retention phase* in which the mouse is tested for retention of the learned behavior after one week of no exposure to the apparatus, (4) a *visible platform phase* in which the mouse was tested for motivation and visual function.

Straight alley pretraining: During these training sessions, a black curtain was placed above the tank to remove visual cues. The animals were placed at the end of the straight alley and must reach the hidden platform at the opposite end within 60 s. Once a mouse has reached the platform, it was allowed to stay on for 10 s before being placed back in the holding apparatus. The mice will receive 5 trials per session with an intertrial interval of 5 minutes. The mice will receive one session a day for 2 days (Friday and Monday).

Place discrimination acquisition: This phase started the day after the last session of training with the straight alley (ex: Tuesday). The curtain was removed and the mice was allowed to use distal cues to locate the platform in the tank. The mice was lowered in the water at one of four starting locations and was given 90 s to find the platform. Once a mouse has reached the platform, it remained on the platform for 30 s prior to removal to the holding apparatus, for a 90 s intertrial interval. Each mouse was given 4-5 platform trials per session. The mice received one session a day for a total of 9 sessions (Tuesday-Friday, Sessions 1-4 and Monday-Friday, Sessions 5-9). The measures of performance for this phase was the distance traveled by the

mouse to reach the platform (path length), speed and duration. From the path length measures, we also used a learning index generated as the averaged performance for sessions 2, 3, and 4. As part of sessions 2, 4, 5, 7, and 9, a probe trial was given as the 5^{th} trial instead of a platform trial. During this trial, the platform was inaccessible to the mice for 30 s. Once the trial was over, the platform was raised and the mice was given 60 s to find it. On this trial, spatial bias for the platform location was evaluated in terms of the (i) percentage of time spent in the platform quadrant, (ii) percentage of time spent within 40- and 20cm diameter annuli surrounding the platform location, and (iii) entries into the platform zone. The purpose of the reappearing platform is to ensure that each trial ends with a successful location of the platform. This decreases the probability of the extinction of the learned behavior and minimizes the potentially disruptive effect of the probe trial upon subsequent performance.

Probe trial retention: After the ninth acquisition session (Friday), mice were returned to their home cage and were not tested for 7 days. On the following Friday, mice were again given a one probe trial lasting 60 s (session 10) during which the platform was not available to the mice. The purpose of this session is to determine whether the mice have retained the learned behavior during the acquisition phase. Measures of performance was identical to the ones used for a probe trial during the acquisition phase, and to compare to the other probe data, the first 30 s were used for analyses.

Visible platform**:** A visual platform test was used in order to assess visual function in rodents. The visible platform test required the mice to swim in an open tank, filled with opacified water, and locate a platform identified only with a small triangular flag (5 cm each side, 11 cm^2) that was raised above the surface of the water (6 cm from the water surface to the bottom of the flag). Ten sessions were administered, each consisting of four trials at 10-min intervals. Two

sessions were performed each day. The second trial did not begin until 2 hours have lapsed from the end of the first trial. On each trial, the mouse had to swim to the platform from a different starting point in the tank. In addition, the platform was moved to a different location before each trial. Thus, the mouse had to learn to associate the location of the flag with the location of the platform. Performance across sessions was measured as path length taken to reach the platform (latency and speed were also analyzed).

2.2.6 Discriminated Reversal

This behavioral test requires mice to adapt to a shift in "set" that has been previously well learned, requiring cognitive flexibility that is often linked to frontal cortical functions. Mice were first trained to make a preemptive response involving a simple discrimination (running to the correct arm of a T-maze), to avoid a punishing stimulus (shock to the feet). Once the discriminated avoidance response has been well learned, a reversal was introduced such that running to the opposite goal arm of the maze was reversed.

The T-Maze is constructed of acrylic (black sides and clear top) and is divided into 3 compartments: a start box (10 x 6.3 x 6 cm), a stem arm (17.5 x 6.3 x 6 cm) and 2 goal arms (14.5 x 6.3 x 6 cm). Each compartment is separated by clear, removable acrylic doors. The floor of the apparatus is a grid floor composed of 3.0 mm diameter rods spaced 7 mm and wired for delivery of mild shock to the feet (0.27 mA was used for this study, comparable to previous studies using C57BL/6 mice, but the level of shock is adjustable). Acquisition phase: The goal of the acquisition phase is for mice to learn a simple arm discrimination using a shock escape paradigm, and to also acquire a learning set for predicting which goal of the T-maze was correct on a given day. During the first session, an initial preference trial was given wherein a shock is

initiated with the mouse in the stem of the maze and then terminated upon entry by the mouse into either goal arm. The correct goal arm was then defined as the arm opposite that chosen. On each trial thereafter (inter-trial time of 60 sec), shock was initiated 5 sec after the opening of the start box door (or immediately upon an entry into the incorrect goal arm) and was terminated after entry into the correct goal arm (maximum time = 60 sec). As an animal learned the task, the latency to find the correct goal arm (escape latency) will decrease. With further learning, the animal will consistently arrive at the correct goal arm within the 5 sec time frame during which no shock is delivered (i.e., the animal no longer is escaping the shock, but has learned to avoid the shock). The latency to enter the correct goal arm was recorded for each trial. Avoidance and discrimination components are scored independently: *Avoidance*= entering either goal within 5 sec; *Correct discrimination*= entering the correct goal without error, regardless of time required; *Correct avoidance*= a correct discrimination within 5-sec. The training session continues until the mouse has made a correct avoidance on four out of five consecutive trials, with the last two correct or has reached a maximum of 25 trials. Reversal phases: Upon completion of the acquisition phase, the mice was returned to their home cage for one hour prior to the first reversal session. The test was conducted the same way as the acquisition phase, with the exception of the information trial; the correct arm will automatically be set as the opposite arm from the one on the previous session. The second reversal will start one hour after the end of the first one. The same criterion as for the acquisition phase for completion of the session was applied. In one day, a mouse was tested on 3 sessions (1 acquisition, 2 reversals). The performance of the mice was primarily measured as the average number of trials taken to reach criterion across the 3 sessions, as it has shown to be age-sensitive. However, other measures was

analyzed such as mean numbers of avoidances, correct discriminations (i.e., correct turns) and correct avoidances for each session, during the first 5 trials of reversal.

2.2.7 Auditory Startle (Hearing Acuity)

The musculoskeletal startle reflex to auditory stimuli of various intensities was determined using a standard testing system (SA Lab, San Diego Instruments) that employs an electromagnetic force transducer. For the auditory startle test, a mouse was placed inside an acrylic cylinder and presented with a series of mixed-frequency noise bursts (0, 90, 100, 110, 120 or 140 dB). Each acoustic signal (lasting 20 ms) was presented 12 times in a counterbalanced series, for a total of 72 trials. The amplitude of the startle reflex was defined as the peak response to each auditory intensity within a 250-ms time window that began with the stimulus presentation.

2.2.8 Porsolt Forced Swim (Depression-like behavioral test)

For the forced swim test, a 25 cm x 76 cm cylindric acrylic tank is filled with water (24±1°C). Water level is approximately 15 cm below the top of the cylinder, so the mouse cannot escape but is able to freely swim. The forced swim test has been used effectively as a primary screen for antidepressants drugs and studying affective changes in rodents. The forced swim test consisted of a single trial in which the mouse is placed in the tank for a total of 6 min. The immobility time after the first 2 min was recorded using a stop watch. The typical behavior as seen in rodents was that when put in the tank they struggle initially and then usually float or do minimal possible movements to keep their head above the water which was recorded as immobility time.

2.2.9 Fear Conditioning

The test apparatus is constructed of Plexiglas (dimensions: 19 w x 18 d x 24 cm h) within a larger sound attenuated chamber. For context conditioning session, the flooring is electrified stainless steel rods, and the walls have vertical stripes. Shock is delivered via the rod floor. For novel context (NC) test session and loud sound (CS) test session, the flooring is smooth, white Plexiglas, and the walls are white. A dim light illuminates the chamber, and a fan provides ventilation. A camera is mounted in the ceiling of the apparatus and records the animal's behavior, with the Any-maze (Stoelting) software monitoring freezing behavior. A 10% ethanol or 10% vinegar solution is used to clean between animals, masking other animal scents and giving alternated smells for the various testing sessions.

Procedures:	**Time (in seconds) of each phase of program**				
Conditioning:	0-120 (explore)	120-135 (CS) 133-135 (US)	135-255 (explore)	255-270 (CS) 268-270 (US)	270-300 (consolidation)
CC Test:	0-300 (conditioning context, freezing to conditioning context assay)				
Novel C Test:	0-180 (novel context, freezing to novel context assay)				
Novel C + CS Test:	180-360 (novel context with CS, freezing to CS assay)				

Table 1. Fear conditioning protocol

Day 1: The fear conditioning procedure consisted of placing a mouse in an unfamiliar environment (known as the conditioning context or CC) and then administering a brief foot shock (0.7 mA for 2 seconds). Just prior to the foot shock, the mouse was presented with a loud sound (known as the conditioned stimulus or CS). There was 2 pairings of the loud sound and foot shock in the 5-min session. We expect that the mouse will learn several things from its foot shock exposure, including 1) an association between the conditioning context and shock; 2) an

association between a loud sound and shock; and 3) anxiety in subsequent new situations. The response of a rodent that is exposed to a fearful situation is to become completely still, a behavior known as 'freezing'. So, we used freezing behavior as a gauge of the strength of the fear conditioning experience.

Day 2, Test 1: Twenty-four hours after fear conditioning, the mouse was returned to the conditioning context (CC) for a 5-min test in which time spent freezing was measured. If a rodent is still for most of the 5-min test, we can assume that the mouse learned that the fear conditioning context is a dangerous place and responded by freezing. The mouse was returned to its home cage after this test.

Day 2, Test 2: One hour after Test 1, the mouse was placed in a novel context (NC), different from the conditioning context and one in which the animal has never experienced any unpleasant events. For this 3-min test, freezing was again measured. An anxious animal might freeze some, even though the context was not in of itself fearful. The mouse remained in this novel context for the next test.

Day 2, Test 3: Immediately after Test 1, while the mouse was still in the novel context (NC), the loud sound (CS) that was paired with the foot shock was presented for 3 min. During that 3-min period, freezing was measured. A mouse that had learned a connection between sound and shock would expect foot shock to follow the loud sound and would freeze for much of the test.

2.3 Biochemical Measurements

At the target ages aforementioned, tail bleed was performed on the mice just prior to euthanization. Blood was collected in tube containing EDTA and was spun at 5,000G for 10

min, and plasma was saved and snap frozen in liquid nitrogen for future measurements of inflammatory markers. Once blood was collected, the mice were euthanized by cervical dislocation and tissues were collected. Brain from individual mouse was dissected into six regions (cerebral cortex, cerebellum, midbrain, brainstem, striatum, and hippocampus), liver, skeletal muscle, heart, kidneys, lungs and snap frozen in liquid nitrogen. For the purpose this study we will focus on biochemical measures in key brain regions (cortex, cerebellum, striatum) related to behavioral testing, as well as skeletal muscle and liver tissue for systemic function and in relation to motor function.

2.3.1 Tissue Homogenization

Ten percent tissue homogenates were prepared using an antioxidant buffer (5mM sodium phosphate, pH 7.4, 5mM EDTA, 2mM BHT) containing proteases and phosphatases inhibitors (CST, #5872) The samples were then centrifuged at 10000 G for 15 min at 4°C, after which the supernatant was reserved for protein concentration and Western blot analyses. Protein concentration was determined according to the Pierce BCA method (ThermoFisher, Waltham, MA). The assay was performed in triplicate within a 96 well plate, with a standard curve of bovine serum albumin (BSA). Tissue homogenate was added to individual wells and then 200 uL of Reagent C (50:1 Reagent A:Reagent B) was added to each well. Samples were then incubated for 30 min at 37° C and read in a spectrophotometer at 562 nm.

2.3.2 Plasma Inflammatory Markers

Commercial sandwich-based enzyme linked immunosorbent assays (ELISA) were used to determine plasma IL6 and TNF-α (R&D Quantikine). Samples were added to a pre-coated 96

well plate, incubated for 2 hours, washed 5x, incubated with conjugate for 2 hours, washed 5x, incubated with substrate solution (color agent) for 30 min, the reaction was stopped via acid and then read within 30 min at 540 nm via a spectrophotometric plate reader.

2.3.3 Redox state

Samples for redox state measurement were snap frozen in liquid nitrogen, then pulverized and homogenized in liquid nitrogen via mortar and pestle. Samples were shipped frozen on dry ice to the Oklahoma Nathan Shock Center – Redox Biology Core for determination of redox state measures. Redox state (GSH, NADPH, NADH) was determined via high-performance liquid chromatography. The levels of GSH, GSSG, NADH, NAD, NADPH, and NADP in cerebellum, cortex, striatum, and skeletal muscle were quantified using reverse-phase HPLC and electrochemical detection. Proteins were precipitated upon incubation on ice (5.0 min) followed by centrifugation (10 min at 16,000 g). The supernatant was filtered (0.45-μm syringe filters) and metabolites were resolved by HPLC and quantified by electrochemical detection (Shimadzu HPLC system, ESA Coularray electrochemical detector 5600A set at 750 mV). Metabolites were eluted through a C18 column (Phenomenex Luna C18(2), 100 Å, 3 μm, 150×4.6 mm) at 0.5 ml/min using an isocratic mobile phase consisting of 25 mM NaH2PO4, 0.5 mM 1-octane sulfonic acid, 4% acetonitrile, pH 2.7. Metabolite concentrations were calculated by employing standard curves constructed from peak areas.

2.3.4 Antibodies

The following previously validated primary antibodies were used: rabbit anti-mTOR (1:1000, #2983S) , rabbit anti-AMPK-a (1:1000, #5831S), rabbit anti-LC3B (1:1000, #2775S),

rabbit anti-p-AMPK-a (1:1000, #2535S), rabbit anti-p-mTOR (1:1000, #2971S), and rabbit anti-GAPDH (1:1000, #2118) from Cell Signaling Technologies (Danvers, MA, USA). Secondary antibody was goat anti-rabbit IgG-HRP (1:5000, #7074S), from Cell Signaling Technologies (Danvers, MA, USA).

2.3.5 Semi-quantitative Immunoblotting

Forty micrograms of total proteins were loaded and electrophoretically separated for 70 min at 100 mV then transferred to nitrocellulose membrane (Bio Rad, USA) overnight at 4°C at 30 mV. The membranes were blocked with 5% dehydrated milk in a 1X TBS buffer solution containing 0.1% Tween 20 (TBST), then incubated on a rotator for 1 h at room temperature with the primary antibodies (in TBST). After washing with TBST, the membranes were incubated for 2 h at room temperature with the secondary antibody (in TBST). Membranes were imaged on a Biorad ChemiDoc XRS+ with ECL western blotting detection reagents (CST SignalFire Plus ECL). Quantification was performed by densitometry using BioRads ImageLab software and values were corrected for background and normalized for GAPDH density.

2.3.6 Statistical Analysis

Data analysis of the behavioral data involved three-way analyses of variance (ANOVA) with Sex, Age, and Genotype as between group factors for each independent measure using the car package in R. Furthermore, variables from behavioral tests with multiple sessions or biochemistry from multiple brain regions were analyzed with a repeated measures three-way analyses of variance (with Session, Week, or Month as the within group factor). Planned individual comparisons between different age groups (5, 10, or 20 months), sex (male or female),

and genotype (GCLM+/+ and GCLM-/-) were performed using a single degree-of-freedom F tests involving the error term from the overall ANOVA. Survival curves were fitted using the Kaplan-Meier method, and lifespans were compared using the Cox Proportional Hazard Model using the survminer and survival R packages. The α level was set at 0.05 for all analyses. R 3.5 (R Foundation, Vienna, Austria) was used to perform all analyses.

2.4 References

1. Fox, J. G., Barthold, S., Davisson, M., Newcomer, C. E., Quimby, F. W., & Smith, A. (2006). *The mouse in biomedical research: normative biology, husbandry, and models* (Vol. 3). Elsevier.

2. de Fiebre NC, Sumien N, Forster MJ, de Fiebre CM. Spatial learning and psychomotor performance of C57BL/6 mice: age sensitivity and reliability of individual differences. Age (Dordr). 2006;28(3):235-53. Epub 2006/09/01. doi: 10.1007/s11357-006-9027-3. PubMed PMID: 22253492; PMCID: 3259155.

CHAPTER 3

RESULTS

3.1 Survival

The effects of Sex, Age, and Genotype on Kaplan-Meier probabilities of survival time are presented in Fig. 1. In both males and females, median lifespan of the GCLM-/- mice was extended 5-8% (1-2 months) and maximum lifespan was extended 7-14% (2-4 months), and there was no difference between males and females survivorship. In female GCLM-/- especially, there was a delay in initial mortality compared to female GCLM+/+. A Cox proportional hazards analysis revealed a significant effect of Genotype ($p < 0.01$) but no effect of Sex ($p = 0.9$) or interaction between Sex and Genotype ($p = 0.6$).

3.2 Body Weight and Food Intake

The effects of Sex, Age, and Genotype on body weight throughout the lifespan are presented in Fig. 2A. In both males and females, GCLM-/- mice weighed less across the lifespan, and males weighed more than Genotype-matched females. A repeated measures ANOVA revealed significant between-subject main effects of Sex ($p < 0.0001$) and Genotype ($p < 0.0001$), and a main within-subjects effect of Month ($p < 0.001$). There were also interactions of Sex * Genotype ($p < 0.01$) and Month * Sex ($p < 0.0001$), Month * Genotype ($p < 0.001$), and Month * Sex * Genotype ($p < 0.01$).

The effects of Sex, Age, and Genotype on bodyweight during behavior are presented in Fig.2B. In both males and females, the GCLM-/- mice weighed less, males weighed more than Age- and Genotype-matched females, and there was no effect of behavior on body weight. A three-way repeated measures ANOVA revealed significant main effects of Sex ($p < 0.001$), Age ($p < 0.05$), and Genotype ($p < 0.001$), but no within-group effect of Week ($p = 0.95$). There were significant interactions of Sex * Age ($p < 0.01$), Age * Genotype ($p < 0.05$), Sex * Week ($p < 0.001$) and Age * Week ($p < 0.001$), but no other interactions (all ps > 0.5).

The effects of Sex, Age, and Genotype on food intake during behavior are presented in Fig. 3. Food intake increased at 20 months in male and female mice of both Genotypes. In males only, GCLM-/- mice ate more food at 10 months and less food at 20 months than Age-matched GCLM+/+. A three-way ANOVA revealed a significant main effect of Age ($p < 0.0001$), and significant interactions of Sex*Age ($p < 0.05$), Age*Genotype ($p < 0.001$), and Sex*Age*Genotype ($p < 0.05$).

3.3 Elevated Plus Maze

The effects of Sex, Age, and Genotype on time spent in the open arms of the elevated plus maze are presented in Fig. 4. In GCLM+/+ groups, there was no difference with Age in the males, but the 10 and 20 months females spent less time in the open arms compared to the 5 month group. In GCLM-/- groups, the 10 and 20 months male mice spent less time in the open arms than the 5 month group, while no Age effect were observed in females. GCLM-/- mice spent more time in open arms than the Age-matched GCLM+/+ at 5 and 20 months in males and at 10 and 20 months in females. A three-way ANOVA revealed a significant main effects of Sex ($p < 0.0001$), Age ($p < 0.01$), and Genotype ($p < 0.0001$), and an interaction between

Sex, Age, and Genotype ($p < 0.01$).

The effects of Sex, Age, and Genotype on total distance traveled in the elevated plus maze are presented in Fig. 5. A moderate decline in total distance was observed across Age in GCLM+/+ mice especially the females, while there was no Age-related decline in GCLM-/-. GCLM-/- traveled as far or more than age- and sex-matched GCLM+/+ mice, especially in 10 and 20 months females. A three-way ANOVA revealed a significant main effect of Age ($p < 0.05$) and Genotype ($p < 0.01$), but no interactions between Sex, Age, and Genotype (all ps > 0.2).

3.4 Open Field

The effects of Sex, Age, and Genotype on total distance traveled in the open field are presented in Fig. 6. Total distance travelled was higher in 20 month old male and female GCLM+/+ compared to 10 month mice. In GCLM-/-, total distance travelled increased only in females at 20 months compared to 5 months, and to a greater extent than in 20 month old female GCLM+/+. A three-way ANOVA revealed a significant main effects of Age ($p < 0.0001$), and Genotype ($p < 0.05$), but no interactions between Sex, Age, and Genotype (all ps > 0.1).

The effects of Sex, Age, and Genotype on vertical activity in the open field are presented in Fig. 7. Vertical activity was higher in 20 month old male and female GCLM+/+ compared to 5 and 10 months. In GCLM-/-, vertical activity increased only in females at 20 months compared to 10 months, and to a greater extent than in 20 month old female GCLM+/+. A three-way ANOVA revealed a significant main effects of Sex ($p < 0.05$), Genotype ($p < 0.001$), approached significance for Age ($p = 0.06$), and had a significant interaction for Age *

Genotype ($p < 0.05$), but no other interactions between Sex, Age, and Genotype (all ps > 0.1).

The effects of Sex, Age, and Genotype on time spent in the margin zone of the open field are presented in Fig. 8. In both male and female GCLM+/+ margin time did not vary with age. GCLM-/- had limited age-related changes and differential Sex-related changes, where males spent less time in the margin than sex- or age-matched GCLM+/+. A three-way ANOVA revealed a significant main effects of Sex ($p < 0.01$), and interactions between Sex * Genotype ($p < 0.05$) and Age * Genotype ($p < 0.05$), but no other interactions of Sex, Age, and Genotype (all ps > 0.08).

The effects of Sex, Age, and Genotype on time spent in the center zone of the open field are presented in Fig. 9. In female GCLM+/+ center time decreased in 10 month mice and increased back up by 20 month, while there was no change with age in males. GCLM-/- had limited age-related changes and differential sex-related changes, where males spent more time in the center than sex- or age-matched GCLM+/+. A three-way ANOVA revealed a significant main effects of Sex ($p < 0.01$), and interactions between Sex * Genotype ($p < 0.05$) and Age * Genotype ($p < 0.05$), but no other interactions of Sex, Age, and Genotype (all ps > 0.08).

3.5 Psychomotor Function

3.5.1 Walk Initiation

The effects of Sex, Age, and Genotype on walk initiation are presented in Fig. 10. Latency to walk was higher at 10 and 20 months in male and female GCLM+/+ than at 5 months. In GCLM-/- age-related changes were smaller than in the GCLM+/+ and only significant at 20 months in males. A three-way ANOVA revealed significant main effects of Age ($p < 0.01$) and Genotype ($p < 0.05$), but there was no main effect of Sex and no

interactions between Sex, Age, and Genotype (all ps >= 0.3).

3.4.2 Alley Turn

The effects of Sex, Age, and Genotype on alley turn are presented in Fig. 11. For male and female GCLM+/+ mice latency to turn was higher at 10 and 20 months than at 5 months, though the age effect was larger in males. There was no major changes with age in GCLM-/- male mice, while an age effect was apparent at 20 month for the females. A three-way ANOVA revealed significant main effects of Sex, Age, and Genotype (all ps < 0.01), but no interactions of Sex, Age, or Genotype (all ps > 0.2).

3.5.3 Negative Geotaxis

The effects of Sex, Age, and Genotype on negative geotaxis are presented in Fig. 12. Latency to turn in GCLM+/+ declined with age at 10 and 20 months in males, but increased with age at 10 and 20 months in females. In GCLM-/- there was no age-related effects in males and females. A three-way ANOVA revealed a significant main effect of Sex ($p < 0.05$), Age ($p < 0.05$), but no main effect of Genotype ($p > 0.7$), and only an interaction of Sex * Age * Genotype ($p < 0.01$).

3.5.4 Wire tread and fall

The effects of Sex, Age, and Genotype on latency to tread are presented in Fig. 13. In GCLM+/+ latency to tread increased mainly between 5 and 10 month for males and gradually at 10 and 20 months for females. While GCLM-/- also had age changes it was mostly between 10 and 20 months for both sexes. GCLM-/- took shorter latencies to tread that the GCLM+/+ at 5

and 10 months, but there was no difference between the two genotypes at 20 months. A three-way ANOVA revealed significant main effect of Sex ($p < 0.01$), Age ($p < 0.001$), and Genotype ($p < 0.001$), with interactions of Age * Genotype ($p < 0.01$) and Sex * Age * Genotype ($p < 0.05$).

The effects of Sex, Age, and Genotype on latency to fall from a wire are presented in Fig. 14. In GCLM+/+, latency to fall decreased mostly between 5 and 10 month in males, while there were no changes in females. In GCLM-/-, latency to fall was decreased mostly between 10 and 20 months for both sexes. A three-way ANCOVA revealed significant main effects of Age ($p < 0.05$) and Weight ($p < 0.05$), and a significant interaction for Age * Genotype ($p < 0.01$, but there was no main effect of Sex or Genotype and no interaction between Sex and Genotype or Sex * Age * Genotype (all ps >/= 0.11).

3.5.5 Bridge walking

The effects of Sex, Age, and Genotype on overall average latency to fall from an elevated bridge are presented in Fig. 15. Latency to fall in male and female GCLM+/+ decreased mostly between 5 and 10 months, and to a greater extent in males. In GCLM-/-, latency to fall was mostly decreased between 10 and 20 months in both sexes. A three-way ANCOVA revealed a significant main effect of Age ($p < 0.001$), but there were no main effects of Sex, Genotype, or weight and no interactions between Sex, Age, or Genotype (all ps > 0.1). As we observed significant differences across the total bridge performance, we further examined bridge by breaking results up into each bridge difficulty.

The effects of Sex, Age, and Genotype across session on latency to fall from an elevated bridge across bridge difficulty are presented in Fig. 16. Latency to fall decreased as bridge difficulty increased in all groups. At 5 and 20 months, all mice performed similarly

regardless of sex or genotype with the old mice having shorter latencies. At 10 months, the male GCLM-/- mice had higher latencies on all bridges than the GCLM+/+, while it was only on the most difficult bridge that a separation between genotype was observed in females. It is noteworthy that the males had shorter latencies than females. There was a significant within groups effect of Session ($p < 0.0001$), but no significant interactions of Session with Sex, Age, or Genotype (all ps > 0.05).

3.6 Rotorod

The effects of Sex, Age, and Genotype on the last session latency to fall from a rotating rod are presented in Fig. 17. Latency to fall in GCLM+/+ decreased with age at 10 and 20 months only in males, with no age-related decline in females. In both male and female GCLM-/, latency to fall decreased with Age at 10 and 20 months, but to a lesser extent than GCLM+/+ at 10 months. A three-way ANOVA revealed a significant main effect of Sex ($p < 0.001$), Age ($p < 0.001$), and Genotype ($p < 0.01$), and a significant interaction of Age * Genotype, but there were no other interactions between Sex, Age, or Genotype (all ps >/= 0.07).

To determine whether these differences happened in the learning phase or maximum performance phase on these animals, the data were plotted by session and presented in Fig. 18. All groups increased latency to fall across session. Latencies increased across sessions as the mice learned to run on the rotating rod. Differences in performance seem to stem from maximum performance rather than learning. Rate of learning (sessions 1-4) are similar when comparing within age and sex groups, however it is clear that the GCLM-/- at 5 and 10 months reach a high plateau of performance. This effect disappears in the 20 month old group. There was a significant within groups effect of Session ($p < 0.0001$), and significant interactions for

Sex * Session ($p < 0.01$), Age * Session ($p < 0.0001$), Genotype * Session ($p < 0.0001$), and Age * Genotype * Session ($p < 0.01$), but no other significant interactions of Session with Sex, Age, or Genotype (all ps > 0.3).

3.7 Morris Water Maze

The effects of Sex, Age, and Genotype across session on path length to target site are presented in Fig. 19. Path length to the target site decreased across session in all groups. Path length was higher in both male and female GCLM+/+ and GCLM-/- at 10 and 20 months compared to 5 months. There was no differences between the genotypes at any ages. A three-way repeated measures ANOVA revealed significant between groups main effects of Age ($p < 0.05$), but no main effects of Sex or Genotype (ps > 0.18), and no significant interactions (all ps > 0.4). There was a significant within groups effect of Session ($p < 0.0001$), but no other significant interactions of Session with Sex, Age, or Genotype (all ps > 0.2).

The effects of Sex, Age, and Genotype across session on latency to target site are presented in Fig. 20. Latency to the target site decreased across session in all groups. In both male and female GCLM+/+ and GLCM-/- latency to target site increased with age at 10 and 20 months. A three-way repeated measures ANOVA revealed significant between groups main effects of Age ($p < 0.001$) but no main effect of Sex or Genotype ($p > 0.2$), and no significant interactions of Sex, Age, and Genotype ($p > 0.6$). There was a significant within groups effect of Session ($p < 0.0001$), but no significant interactions of Session with Sex, Age, or Genotype (all ps > 0.2).

The effects of Sex, Age, and Genotype across session on average swim speed are

presented in Fig. 21. Swim speed decreased with Age in GCLM+/+ at 10 and 20 months for both males and females. In GCLM-/- swim speed decreased with age at 10 months only in females, but at 20 months in both males and females. Swim speed was higher at 10 months in GCLM-/- males compared to sex-matched GCLM+/+. A three-way repeated measures ANOVA revealed significant between groups main effects of Age ($p < 0.05$) but no other main effects or interactions of Sex, Age, or Genotype (all ps > 0.1).. There was a significant within groups effect of Session ($p < 0.0001$), but no significant interactions of Session with Sex, Age, or Genotype (all ps > 0.2).

The effects of Sex, Age, and Genotype across session on percent time within the target quadrant are presented in Fig. 22. Time spent in the target quadrant varied by session, but was not affected by sex, age or genotype. A three-way repeated measures ANOVA revealed no significant between groups main effects of Sex, Age, or Genotype ($p > 0.19$), and no significant interaction of Sex, Age, or Genotype (all ps > 0.67). There was a significant within groups effect of Session ($p < 0.0001$), and significant interactions for Age * Session ($p < 0.05$) and Sex *Age * Session ($p < 0.05$), but no other significant interactions of Session with Sex, Age, or Genotype (all ps > 0.1).

The effects of Sex, Age, and Genotype across session on percent time spent in the annulus 40 are presented in Fig. 23. Time spent in the annulus 40 increased with session in all groups. Time spent in the annulus 40 in GCLM+/+ and GCLM-/- decreased with age at 10 and 20 months for male and females. A three-way repeated measures ANOVA revealed significant between groups main effects of Age ($p < 0.0001$), but no main effects of Sex or Genotype (ps > 0. 3), and no significant interactions of Sex, Age, or Genotype (all ps > 0.4). There was a significant within groups effect of Session ($p < 0.0001$) and significant interaction for Sex *

Age *Session ($p < 0.01$), but no other significant interactions of Session with Sex, Age, or Genotype (all ps > 0.1).

The effects of Sex, Age, and Genotype across session on percent time spent in the annulus 20 are presented in Fig. 24. Time spent in the annulus 20 increased across session in all groups. Time spent in the annulus 20 in GCLM+/+ decreased with age in both males and females. In GCLM-/-, time spent by males in the annulus 20 decreased with age at 10 and 20 months in males, but was lower at 5 months in females than males. A three-way repeated measures ANOVA revealed significant between groups main effects of Age ($p < 0.01$), but no main effects of Sex or Genotype (ps > 0.06), and no significant interactions of Sex, Age, or Genotype (all ps > 0.2). There was a significant within groups effect of Session ($p < 0.0001$), but no significant interactions of Session with Sex, Age, or Genotype (all ps > 0.1).

The effects of Sex, Age, and Genotype across session on percent time spent in the target site are presented in Fig. 25. Time spent in the target site increased across session in all groups. In GCLM+/+ time spent in the target site decreased with age in 10 and 20 month old males and females. In GCLM-/-, time spent in the target site did not change with age, and in 5 month old females was lower than age- matched female GCLM+/+. A three-way repeated measures ANOVA revealed significant between groups main effects of Age ($p < 0.01$), but no main effects of Sex or Genotype (ps > 0.2), and a significant interaction of Age * Genotype ($p < 0.05$), but no other significant interactions of Sex, Age, or Genotype (all ps > 0.1). There was a significant within groups effect of Session ($p < 0.0001$) and significant interaction for Age * Genotype * Session ($p < 0.01$), but no other significant interactions of Session with Sex, Age, or Genotype (all ps > 0.1).

The effects of Sex, Age, and Genotype across session on target site entries are presented

in Fig. 26. Target site entries increased across session in all groups. In GCLM+/+ target entries decreased with age at 10 and 20 months in both males and females. In GCLM-/-, target entries decreased with age at 10 and 20 months in males, but not in females which were lower at 5 months than age-matched female GCLM+/+. A three-way repeated measures ANOVA revealed significant between groups main effects of Age ($p < 0.0001$), but no main effects of Sex or Genotype (ps > 0. 3), and a significant interaction of Age * Genotype, but no other significant interactions of Sex, Age, or Genotype (all ps > 0.2). There was a significant within groups effect of Session ($p < 0.0001$) and significant interaction for Age * Genotype * Session ($p < 0.05$), but no other significant interactions of Session with Sex, Age, or Genotype (all ps > 0.1).

3.8 Visible Platform

The effects of Sex, Age, and Genotype across session latency to the visible platform are presented in Fig. 27. Latency to target site decreased across session in all groups. There were no age effects in male or female GCLM+/+ or GCLM-/-, but in male 10 month GCLM+/+ latency to target site was higher than age- and sex-matched GCLM-/-. A three-way repeated measures ANOVA revealed significant between groups main effects of Genotype ($p < 0.0001$), but no main effects of Sex or Age (ps > 0.05), and no significant interactions of Sex, Age, or Genotype (all ps > 0.2). There was a significant within groups effect of Session ($p < 0.0001$) and significant interaction for Genotype * Session ($p < 0.01$), but no other significant interactions of Session with Sex, Age, or Genotype (all ps > 0.1).

The effects of Sex, Age, and Genotype across session on path length to the visible platform are presented in Fig. 28. Path length to target site decreased across session in all groups.

There were no age effects in male GCLM+/+ or GCLM-/-. In females, GCLM+/+ and GCLM-/- path length decreased with age at 20 months. A three-way repeated measures ANOVA revealed significant between groups main effects of Age ($p < 0.05$), but no main effects of Sex or Genotype (ps > 0.5), and a significant interaction of Sex * Age * Genotype ($p < 0.01$), but no other significant interactions of Sex, Age, or Genotype (all ps > 0.2). There was a significant within groups effect of Session ($p < 0.0001$) and significant interaction for Age * Session ($p < 0.001$), Sex * Genotype * Session ($p < 0.05$), and Sex * Age * Genotype * Session ($p < 0.01$), but no other significant interactions of Session with Sex, Age, or Genotype (all ps > 0.05).

The effects of Sex, Age, and Genotype across session on average swim speed during the visible platform test are presented in Fig. 29. Swim speed increased across session for 5 and 10 month old groups. Swim speed decreased with age at 20 months in male and female GCLM+/+ and GCLM-/-. A three-way repeated measures ANOVA revealed significant between groups main effects of Age ($p < 0.05$), but no main effects of Sex or Genotype (ps > 0.5), and a significant interaction of Sex * Age * Genotype ($p < 0.05$), but no other significant interactions of Sex, Age, or Genotype (all ps > 0.2). There was a significant within groups effect of Session ($p < 0.0001$) and significant interaction for Age * Session ($p < 0.001$), but no other significant interactions of Session with Sex, Age, or Genotype (all ps > 0.05).

3.9 Auditory Startle

The effects of Sex, Age, and Genotype on force production during auditory startle test are presented in Fig. 30. Force production increased as sound intensity increased in all groups. In male GCLM+/+ and GCLM-/-, force production was lower at 10 and 20 months compared to 5 months, while in female force production was lower only at 20 months.. A three-way repeated

measures ANOVA revealed significant between group main effects of Age ($p < 0.01$), and interactions for Sex * Age ($p < 0.01$), but no other main effects or interactions (all ps > 0.4). There was a significant within group effect of Session ($p < 0.0001$), and significant interactions of Age * Session ($p < 0.0001$), Sex * Age * Session ($p < 0.01$), and Age * Genotype * Session ($p < 0.0001$) but no other significant interactions of Session with Sex, Age, or Genotype (all ps > 0.44).

3.10 Discrimination Reversal

The effects of Sex, Age, and Genotype on number of trials to reach avoidance criterion in the discrimination-avoidance test are presented in Fig. 31. In both male and female GCLM+/+ and GLCM-/-, the number of trials to reach avoidance criterion increased with age at 20 months. Trials to reach criterion decreased for each session in all groups. A three-way repeated measures ANOVA revealed significant between group main effects of Age ($p < 0.0001$), but no interactions for Sex, Age, or Genotype (all ps > 0.2). There was a significant within group effect of Session ($p < 0.0001$), and significant interactions of Sex * Session ($p < 0.01$), but no other significant interactions of Session with Sex, Age, or Genotype (all ps > 0.2).

The effects of Sex, Age, and Genotype on number of trials to the previously trained arm in the discrimination-avoidance test are presented in Fig. 32. In both male GCLM+/+ and GLCM-/-, the number of trials to the previously trained arm increased with age at 20 months, however 20 month GCLM+/+ had fewer trials to the previously trained arm than 20 month GCLM-/- and was not different than 5 month GCLM+/+. Trials to the previously trained arm decreased for each session in all groups. A three-way repeated measures ANOVA revealed significant between group main effects of Age ($p < 0.001$), but no interactions for Sex, Age, or Genotype (all ps >

0.3). There was a significant within group effect of Session ($p < 0.0001$), but no significant interactions of Session with Sex, Age, or Genotype (all ps > 0.2).

The effects of Sex, Age, and Genotype on recall of the previously trained arm in the discrimination avoidance test are presented in Fig. 33. There were no significant changes for recall percentage. A three-way repeated measures ANOVA revealed no significant between group main effects or interactions (all ps > 0.1), although Age approached significance ($p = 0.055$). There was no significant within group effect of Session ($p > 0.1$), and no significant interactions of Session with Sex, Age, or Genotype (all ps > 0.1).

The effects of Sex, Age, and Genotype on number of correct turns in the first five trials in the discrimination-avoidance test are presented in Fig. 34. In both male and female GCLM+/+ and GLCM-/-, the number of correct turns in the first 5 trials decreased with Age at 20 months. The number of correct turns was increased in session 3 for all groups. A three-way repeated measures ANOVA revealed significant between group main effects of Age ($p < 0.01$), but no interactions for Sex, Age, or Genotype (all ps > 0.3). There was a significant within group effect of Session ($p < 0.0001$), and significant interactions of Age * Session ($p < 0.05$), but no other significant interactions of Session with Sex, Age, or Genotype (all ps > 0.4).

The effects of Sex, Age, and Genotype on number of trials to reach four of five correct turns, independent of avoidance criterion in the discrimination-avoidance test are presented in Fig. 35. In male GCLM+/+ and GLCM-/-, the number of trials to reach 4 of 5 correct turns increased with age at 20 months. In female GCLM +/+ the number of trials did not increase at 20 months, but did in female GCLM-/-. The trials to reach 4 of 5 correct turns decreased in session 3 for all male groups, but did not decrease in 10 month female GCLM-/- or 20 month female GCLM+/-. A three-way repeated measures ANOVA revealed significant between group main

effects of Age ($p < 0.001$), but no interactions for Sex, Age, or Genotype (all ps > 0.2). There was a significant within group effect of Session ($p < 0.0001$), but no significant interactions of Session with Sex, Age, or Genotype (all ps > 0.1).

The effects of Sex, Age, and Genotype on number of trials to consecutive correct turns in the discrimination-avoidance test are presented in Fig. 36. In male GCLM+/+ and GLCM-/-, the number of trials to consecutive correct turns increased with age at 20 months. In females, the number of trials to consecutive correct turns increased with age at 20 months only in GCLM-/-. Trials to consecutive correct turns increased at session 2 then decreased at session for all groups. A three-way repeated measures ANOVA revealed significant between group main effects of Age ($p < 0.01$), but no interactions for Sex, Age, or Genotype (all ps > 0.4). There was a significant within group effect of Session ($p < 0.0001$), and significant interactions of Age * Session ($p < 0.05$), but no other significant interactions of Session with Sex, Age, or Genotype (all ps > 0.4).

3.11 Forced Swim Test

The effects of Sex, Age, and Genotype time spent immobile in the forced swim test are presented in Fig. 37. In male and female GCLM+/+, immobility time decreased with age especially by 20 months. In GCLM-/-, immobility time decreased with age in males, but not in females. Male GCLM-/- had higher immobility time at 20 months than the age- and sex-matched GCLM+/+. A three-way ANOVA revealed significant between group main effects of Age ($p < 0.0001$), and a significant interaction between Sex * Age ($p < 0.05$), but no other interactions for Sex, Age, or Genotype (all ps > 0.1).

3.12 Fear Conditioning

The effects of Sex, Age, and Genotype on freezing time in the fear conditioning test are presented in Fig. 38. In male and female GCLM+/+ context-dependent freezing time increased with age at 10 months. In male and female GCLM+/+ and GCLM-/-, conditioned stimulus-dependent freezing decreased with age at 20 months. For context-dependent freezing time, a three-way ANOVA revealed significant main effects of Age ($p < 0.0001$) and Genotype ($p < 0.01$), but no significant interaction between Sex, Age, or Genotype (all $ps > 0.1$). For conditioned-dependent freezing time, a three-way ANOVA revealed significant main effects of Age ($p < 0.0001$) and Genotype ($p < 0.01$), but no significant interactions between Sex, Age, or Genotype (all $ps > 0.05$).

In male GCLM+/+ context-dependent freezing time increased with age at 10 months, while in female GCLM-/- novel context-dependent freezing increased with age at 10 and 20 months. In male and female GCLM+/+ and GCLM-/-, conditioned stimulus-dependent freezing decreased with age at 20 months, however at 5 and 10 months GCLM-/- conditioned stimulus-dependent freezing time was lower than sex- and age-matched GCLM+/+. For novel-dependent freezing time, a three-way ANOVA revealed significant main effects of Age ($p < 0.01$), and significant interactions of Age * Genotype ($p < 0.01$) and Sex * Age * Genotype ($p < 0.05$), but no other significant interaction between Sex, Age, or Genotype (all $ps > 0.5$). For conditioned-dependent freezing time, a three-way ANOVA revealed significant main effects of Age ($p < 0.0001$) and Genotype ($p < 0.01$), but no significant interactions between Sex, Age, or Genotype (all $ps > 0.05$).

A three-way repeated measures ANOVA revealed significant between group main effects of Age ($p < 0.0001$), Genotype ($p < 0.001$), but no significant interaction between Sex, Age, or

Genotype (all ps > 0.05). There was a significant within groups main effect of Session ($p < 0.0001$), significant interactions of Age * Session ($p < 0.0001$) and Genotype * Session ($p < 0.05$), but no other interactions of Sex, Age, or Genotype with Session (all ps > 0.05).

3.13 Redox status measures

3.13.1 Liver

The effect of Sex, Age, and Genotype on liver GSH are presented in Fig 39. In both male and female GCLM-/- mice, GSH levels were ~80% lower than age-matched GCLM+/+ mice across the lifespan. Overall, GSH levels were higher in females than in males, especially at 5 and 10 months. A three-way ANOVA revealed significant main effects of Sex ($p < 0.01$) and Genotype ($p < 0.05$), but no significant interaction of Sex, Age, or Genotype (all ps > 0.05).

3.13.2 Skeletal Muscle

The effects of Sex, Age, and Genotype on skeletal muscle NADH are presented in Fig. 40. While not significant, the levels of NADH were lower in both male and female GCLM-/- when compared to age-matched GCLM+/+. A three-way ANOVA revealed no significant main effects or interactions for NADH (all ps > 0.29).

The effects of Sex, Age, and Genotype on skeletal muscle NADPH are presented in Fig. 41. The levels of NADPH seemed to be lower in young and old male GCLM-/- compared to Age-matched GCLM+/+, however a three-way ANOVA did not reveal any significant main effects or interactions for NADH (all ps > 0.32).

3.13.3 Cortex

The effects of Sex, Age, and Genotype on cortex GSH are presented in Fig. 42. Young GCLM-/- mice had lower GSH than GCLM+/+, but GSH was not different between Genotypes at adult or old ages. Cortex GSH was higher in females than males at 10 and 20 months in both GCLM+/+ and GCLM-/-. A three-way ANOVA revealed significant main effects of Age ($p < 0.01$), Genotype ($p < 0.01$), and a significant interaction of Age * Genotype ($p < 0.05$), but no other interactions of Sex, Age, or Genotype (all ps > 0.38).

The effects of Sex, Age, and Genotype on cortex NADH are presented in Fig. 43. NADH increased with age at 10 and 20 months for GCLM-/- mice, but only at 20 months for GCLM+/+. NADH levels were much lower at 10 months in GCLM+/+. A three-way ANOVA revealed significant main effects of Age ($p < 0.01$), but no significant interactions of Sex, Age, or Genotype (all ps > 0.6).

The effects of Sex, Age, and Genotype on cortex NADPH are presented in Fig. 44. NADPH was not affected by sex or age in GCLM+/+ mice, but female GCLM-/- mice had age-related increases in NADPH at 10 and 20 months. A three-way ANOVA revealed no significant main effects (all ps > 0.5) or significant interactions of Sex, Age, or Genotype (all ps > 0.4).

3.13.4 Cerebellum

The effects of Sex, Age, and Genotype on cerebellum GSH are presented in Fig. 45. Genotype GSH was much lower in 5 month old female GCLM-/- compared to GCLM+/+ but no other Genotype differences were observed. GSH in female GCLM+/+ mice at 10 and 20 months were lower than at 5 months, but no age differences were observed in GCLM-/- mice. A three-way ANOVA revealed significant main effects of Sex ($p < 0.001$), and significant interactions of

Sex * Age ($p < 0.05$) and Sex * Genotype ($p < 0.05$) but no other interactions of Sex, Age, or Genotype (all ps > 0.1).

The effects of Sex, Age, and Genotype on cerebellum NADH are presented in Fig. 46. NADH levels were lower at 5 and 10 months for male GCLM-/- mice compared to GCLM+/+ but only at 5 months for females. At 5 and 10 months, female GCLM+/+ had lower NADH than age- and genotype-matched males. Age effects were only observed in GCLM+/+ mice. A three-way ANOVA revealed significant main effects of Age ($p < 0.001$) and Genotype ($p < 0.05$), and significant interactions for Sex * Age ($p < 0.05$) and Age * Genotype ($p < 0.05$), but no other interactions of Sex, Age, or Genotype (all ps > 0.1).

The effects of Sex, Age, and Genotype on cerebellum NADPH are presented in Fig. 47. NADPH levels in male GCLM-/- mice were lower at 5 and 10 months than in GCLM+/+, but only at 5 months in female mice. NADPH levels were lower at 10 and 20 months in female GCLM+/+ but only at 20 months in male GCLM+/+ mice compared to sex-matched 5 month old GCLM+/+. A three-way ANOVA revealed a significant main effect of Genotype ($p < 0.05$), but no significant interactions of Sex, Age, or Genotype (all ps > 0.1).

3.13.5 Striatum

The effects of Sex, Age, and Genotype on striatum GSH are presented in Fig. 48. No consistent differences between groups were observed. A three-way ANOVA revealed no significant main effects (all ps > 0.15) or significant interactions of Sex, Age, or Genotype (all ps > 0.06).

The effects of Sex, Age, and Genotype on striatum NADH are presented in Fig. 49.

NADH increased with age at 10 and 20 months for GCLM+/+ mice, but only at 10 months for GCLM-/-. NADH was higher was higher in GCLM-/- males at all ages, but only at 5 and 10 months in females. A three-way ANOVA revealed significant main effects of Age ($p < 0.05$), but no significant interactions of Sex, Age, or Genotype (all ps > 0.2).

The effects of Sex, Age, and Genotype on striatum NADPH are presented in Fig. 50. NADPH increased at 10 and 20 month GCLM+/+ males, but no age-effects were observed in GCLM-/- mice. NADPH in 5 month GCLM+/+ mice was substantially lower than in age- and genotype-matched females. A three-way ANOVA revealed significant main effects of Sex ($p < 0.05$) and Age ($p < 0.01$), but no significant interactions of Sex, Age, or Genotype (all ps > 0.09).

3.14 Immunoblot analyses

3.14.1 Skeletal Muscle

The effects of Sex, Age, and Genotype on skeletal muscle ratios p-mTOR/mTOR are presented in Fig. 51 (representative blots in Fig. 62). While there was no difference with age or genotype in males, p-mTOR/m-TOR ratios seem to decline with age regardless of genotype. However, a three-way ANOVA did not reveal any significant main effects of Sex, Age, or Genotype (all ps > 0.1), or significant interactions between Sex, Age, or Genotype (all ps > 0.2).

The effects of Sex, Age, and Genotype on skeletal muscle ratios of p-AMPK/AMPK are presented in Fig. 52 (representative blots in Fig. 62). Ratios seem to increase with age in males, and decrease in females, regardless of genotype. However, a three-way ANOVA did not reveal any significant main effects of Sex, Age, or Genotype (all ps > 0.1) or significant interactions between Sex, Age, or Genotype (all ps > 0.2).

The effects of Sex, Age, and Genotype on skeletal muscle ratios LC3B-I/LC3B-II are

presented in Fig. 53 (representative blots in Fig. 62). No significant effects were observed in males, and the ratios seem to decrease with age in females. But a three-way ANOVA did not support these observations (no main effects of Sex, Age, or Genotype (all ps > 0.1), and no significant interactions between Sex, Age, or Genotype (all ps > 0.2)).

3.14.2 Cortex

The effects of Sex, Age, and Genotype on cortex ratios of p-mTOR/mTOR are presented in Fig. 54 (representative blots in Fig. 63). There did not seem to be any differences with age, genotype or sex on these ratios. A three-way ANOVA revealed no significant main effects of Sex, Age, or Genotype (all ps > 0.1), and no significant interactions between Sex, Age, or Genotype (all ps > 0.2).

The effects of Sex, Age, and Genotype on cortex ratios of p-AMPK/AMPK are presented in Fig. 55 (representative blots in Fig. 63). There was no observable differences between any of the groups. A three-way ANOVA revealed no significant main effects of Sex, Age, or Genotype (all ps > 0.1), and no significant interactions between Sex, Age, or Genotype (all ps > 0.2).

The effects of Sex, Age, and Genotype on cortex ratios of LC3B-II/LC3B-I are presented in Fig. 56 (representative blots in Fig. 63). This ratio seems to increase with age in males and decrease in females, regardless of genotype. However, a three-way ANOVA did not support any significant main effects of Sex, Age, or Genotype (all ps > 0.1), or significant interactions between Sex, Age, or Genotype (all ps > 0.2).

3.14.3 Cerebellum

The effects of Sex, Age, and Genotype on cerebellum ratios of p-mTOR/mTOR are

presented in Fig. 57 (representative blots in Fig. 64). There was no differences between any of the groups. A three-way ANOVA revealed no significant main effects of Sex, Age, or Genotype (all ps > 0.1), and no significant interactions between Sex, Age, or Genotype (all ps > 0.2).

The effects of Sex, Age, and Genotype on cerebellum ratios of p-AMPK/AMPK are presented in Fig. 58 (representative blots in Fig. 64). The ratio was decreased in 20 month old male mice, regardless of Genotype. Ratios seemed higher in GCLM-/- female mice compared to GCLM+/+ at 5 and 10 months. However, a three-way ANOVA did not support any significant main effects of Sex, Age, or Genotype (all ps > 0.06), or significant interactions between Sex, Age, or Genotype (all ps > 0.3).

The effects of Sex, Age, and Genotype on cerebellum ratios of LC3B-II/LC3B-I are presented in Fig. 59 (representative blots in Fig. 64). In males, this ratio was higher at 10 months compared to 5 months GCLM+/+. Age-related decreased in this ratio was only observed in GCLM-/- females. A three-way ANOVA revealed significant main effects of Sex ($p < 0.05$) and Age ($p < 0.05$), and no significant interactions between Sex, Age, or Genotype (all ps > 0.1).

3.15 Inflammation

3.15.1 TNF-a

The effects of Sex, Age, and Genotype on plasma TNF-α are presented in Fig. 60. In male and female GCLM+/+ TNF-α increased at 10 and 20 months. In GCLM-/- mice it increased to similar extents at 10 months but was higher than GCLM+/+ at 20 months. Female GCLM+/+ and GCLM-/- mice had lower inflammation at 20 months than age- and genotype-matched mice. For TNF-α levels, a three-way ANOVA revealed significant main effects of Age ($p < 0.0001$) but no other main effects (all ps > 0.6). Only a significant interaction between Sex * Age ($p < 0.01$) was

observed.

3.15.2 IL-6

The effects of Sex, Age, and Genotype on plasma IL-6 are presented in Fig. 61. No significant differences were observed. For IL-6 inflammation, a three-way ANOVA revealed no significant main effects (all ps > 0.16) or significant interaction between Sex, Age, or Genotype (all ps > 0.4).

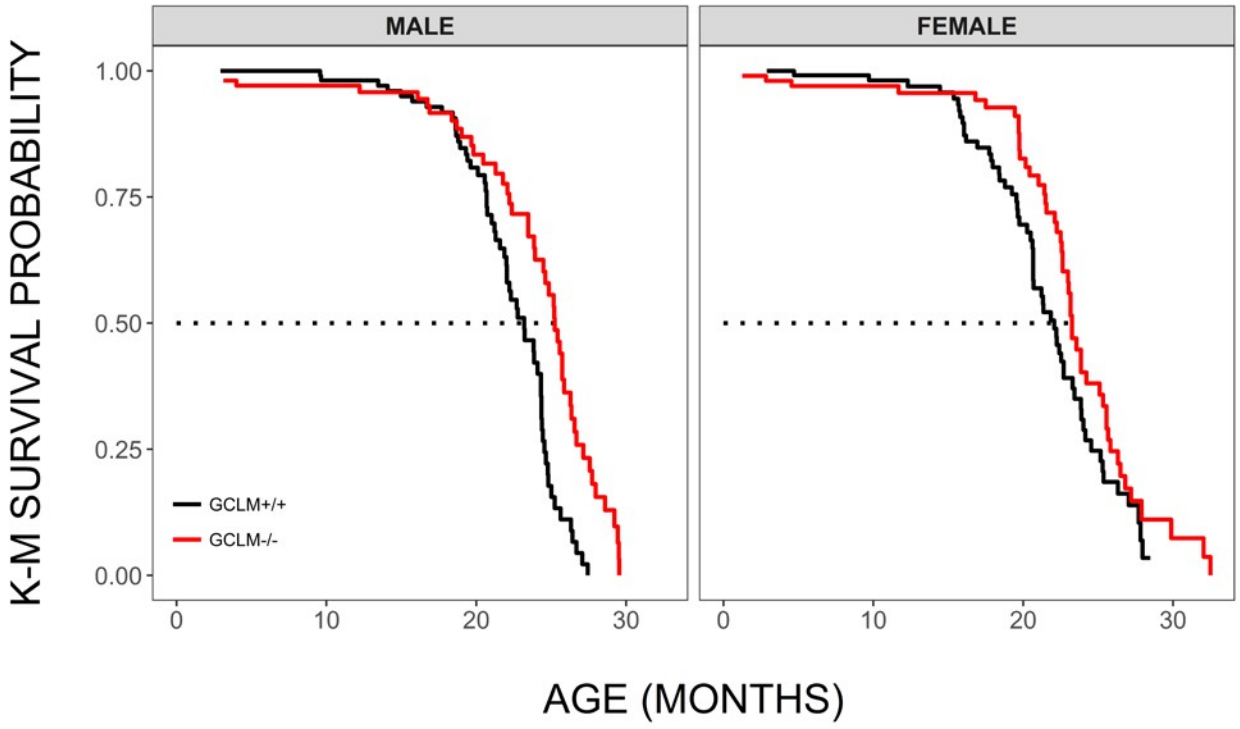

Figure 1. Effects of Sex and Genotype on Kaplan-Meier (K-M) survival probability. All mice were included in the lifespan analysis. N = 101 – 126/group (total = 455).

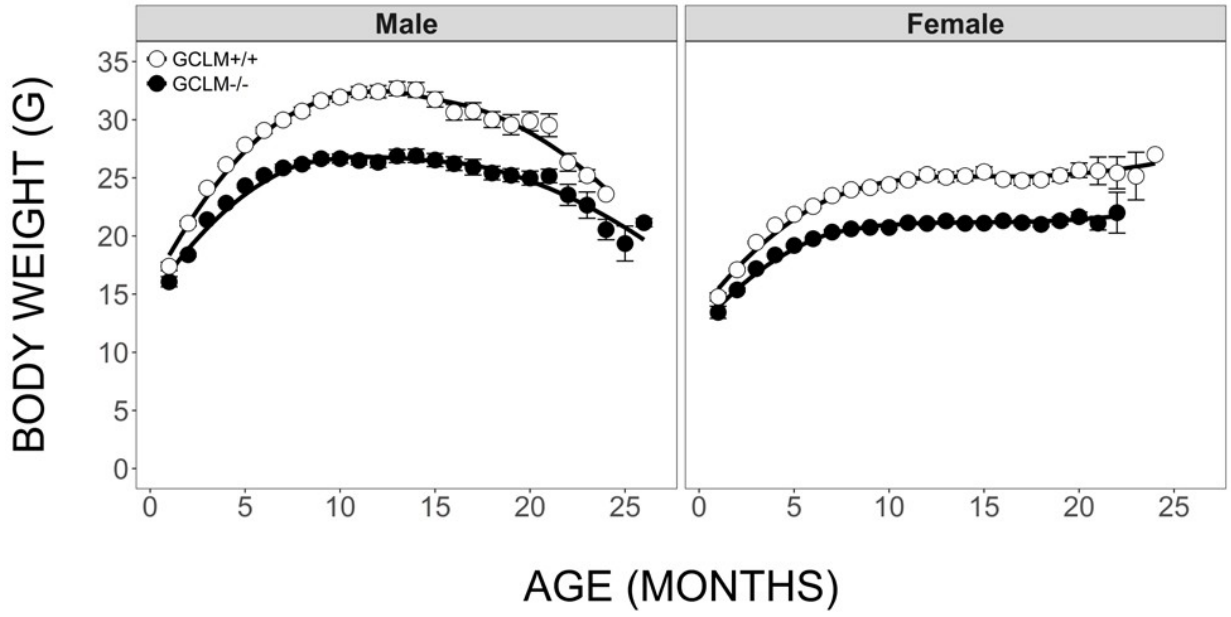

Figure 2A. Effects of Sex, Age, and Genotype on body weight across the lifespan. Each value represents the mean + SEM of (101-126/group, total = 455) mice.

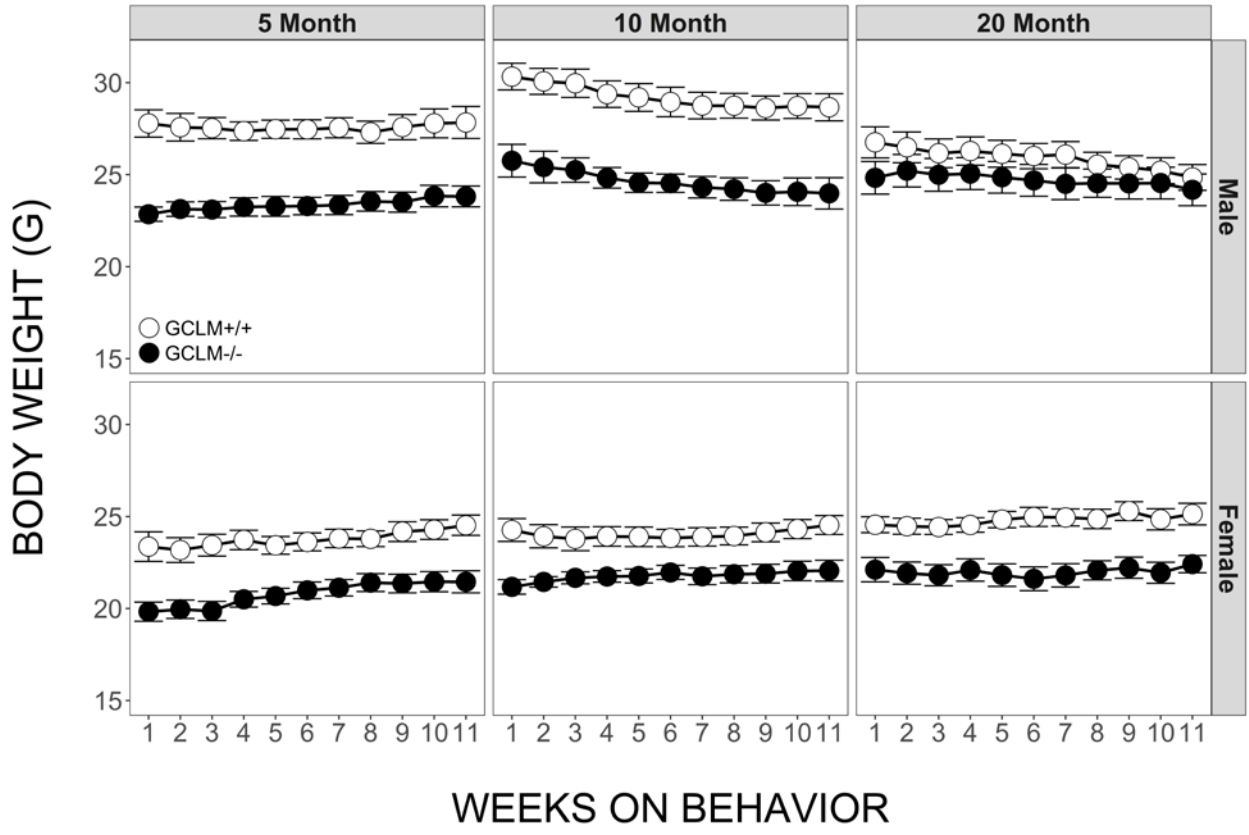

Figure 2B. Effects of Sex, Age, and Genotype on body weight during behavior. Each value represents the mean + SEM of (n = 15-21) mice.

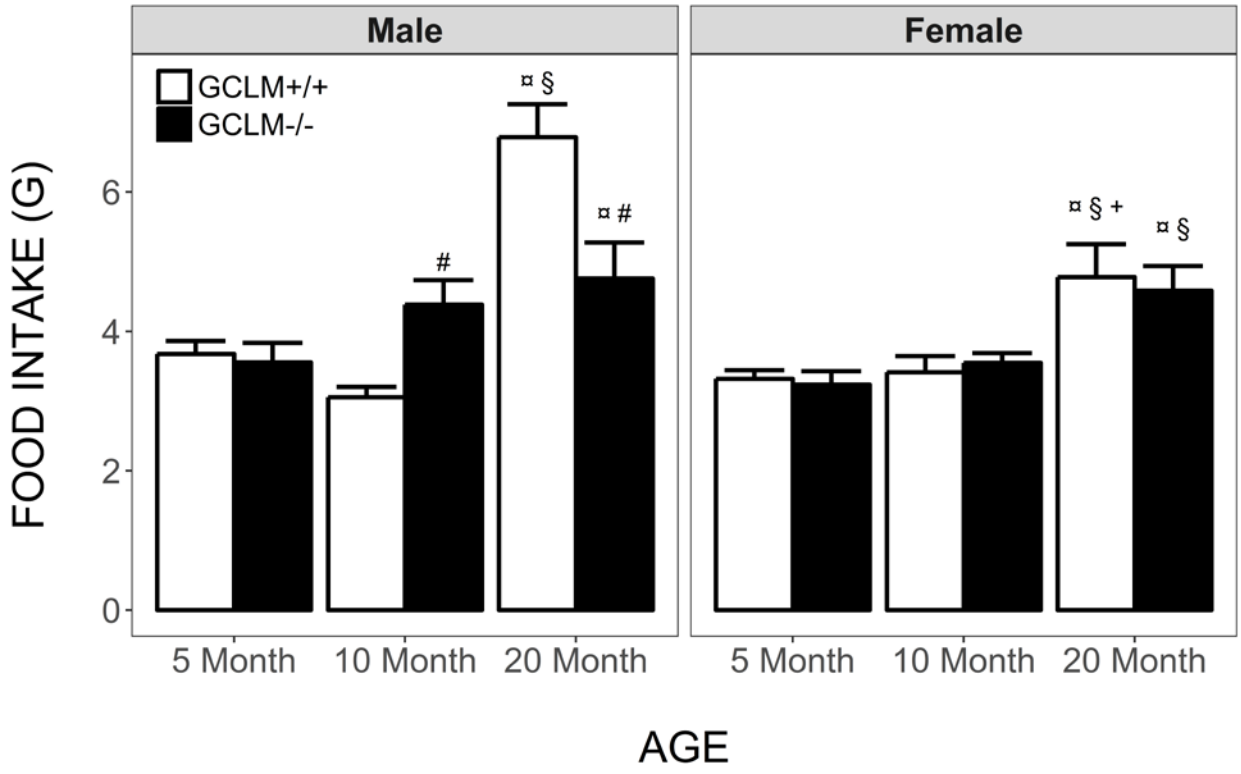

Figure 3. Effects of Sex, Age and Genotype on food intake during behavior in young (5 month), adult (10 month), and old (20 month) GCLM+/+ and GCLM-/- mice. Each value represents the mean + SEM of (n = 15-21) mice. + $p < 0.05$ compared to age and genotype-matched males; ¤ $p < 0.05$ compared to genotype and sex-matched young; § $p < 0.05$ compared to genotype and sex-matched 10 adult; # $p < 0.05$ compared to age and sex-matched GCLM+/+ mice.

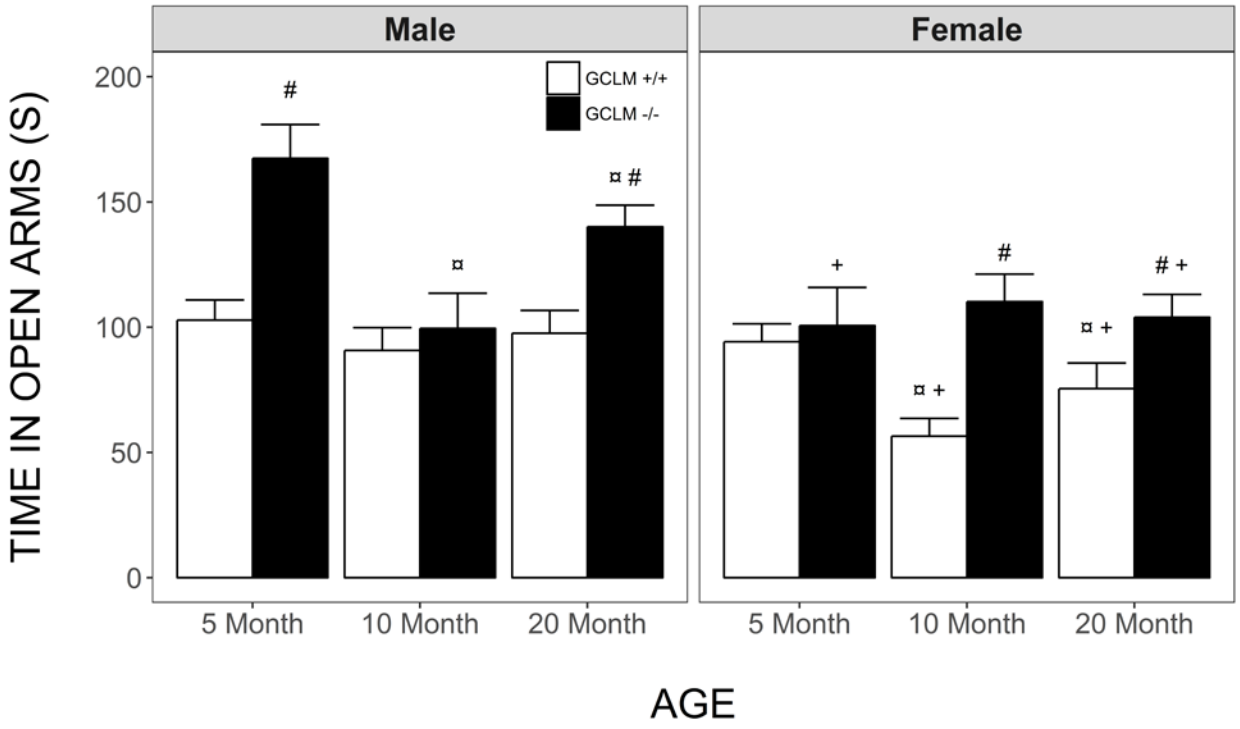

Figure 4. Effects of Sex, Age and Genotype on time spent in the open arms of the elevated plus maze in young (5 month), adult (10 month), and old (20 month) GCLM+/+ and GCLM-/- mice. Each value represents the mean + SEM of (n = 15-21) mice. + $p < 0.05$ compared to age and genotype-matched males; ¤ $p < 0.05$ compared to genotype and sex-matched young; # $p < 0.05$ compared to age and sex- matched GCLM+/+ mice.

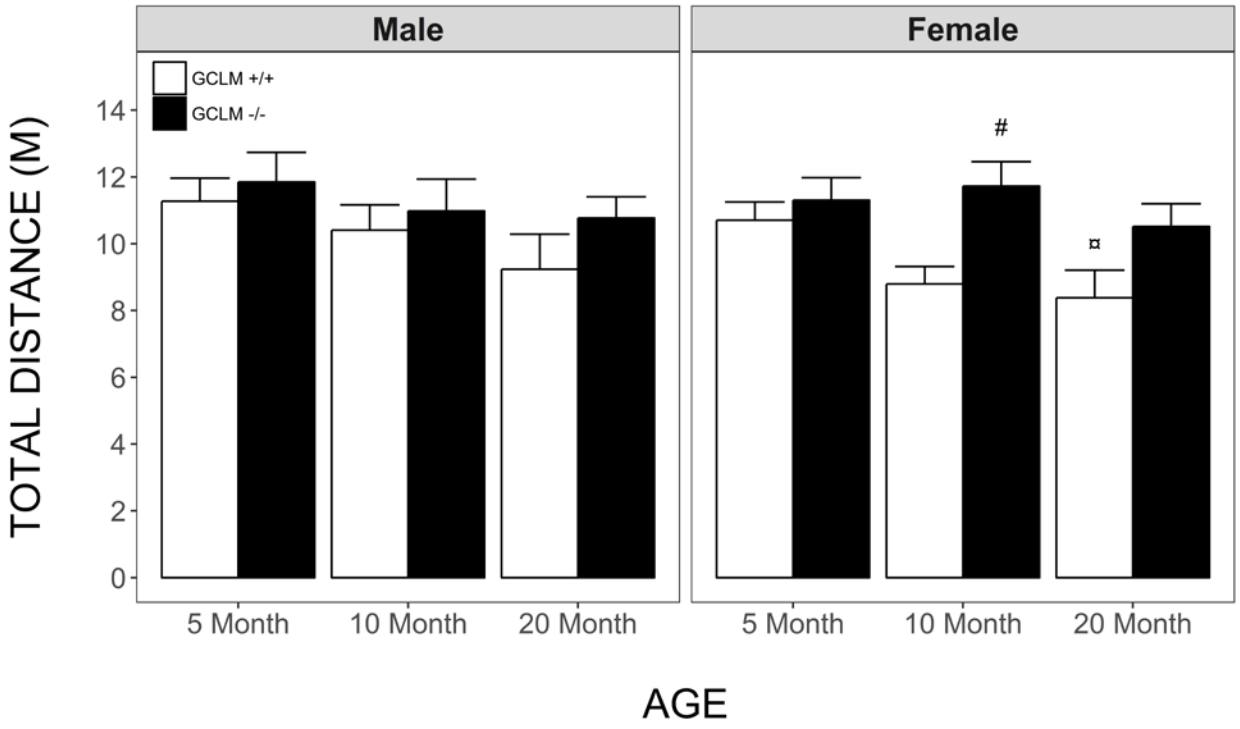

Figure 5. Effects of sex, age and genotype on total distance traveled in the elevated plus maze in young (5 month), adult (10 month), and old (20 month) GCLM+/+ and GCLM-/- mice. Each value represents the mean + SEM of (n = 15-21) mice. ¤ $p < 0.05$ compared to genotype and sex-matched young; # $p < 0.05$ compared to age and sex-matched GCLM+/+ mice.

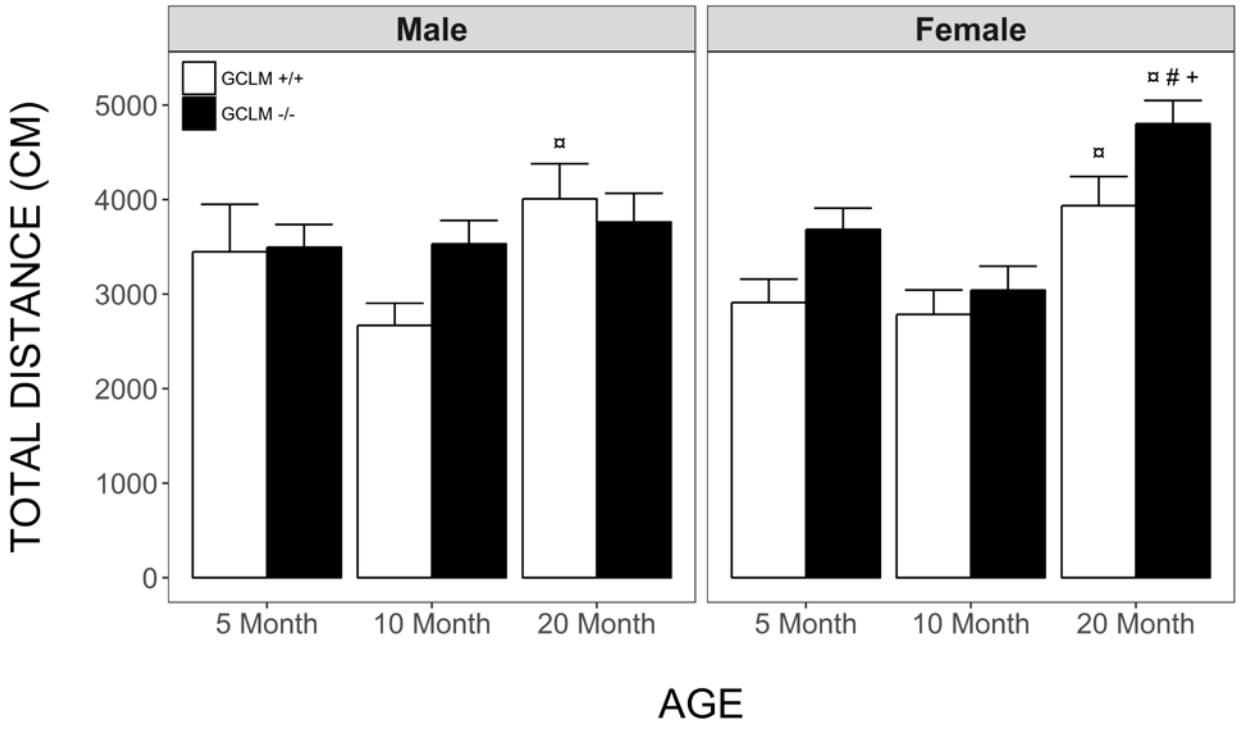

Figure 6. Effects of sex, age and genotype on total distance traveled in the open field in young (5 month), adult (10 month), and old (20 month) GCLM+/+ and GCLM-/- mice. Each value represents the mean + SEM of (n = 15-21) mice. ¤ $p < 0.05$ compared to genotype and sex-matched young; + $p < 0.05$ compared to age and genotype-matched males.

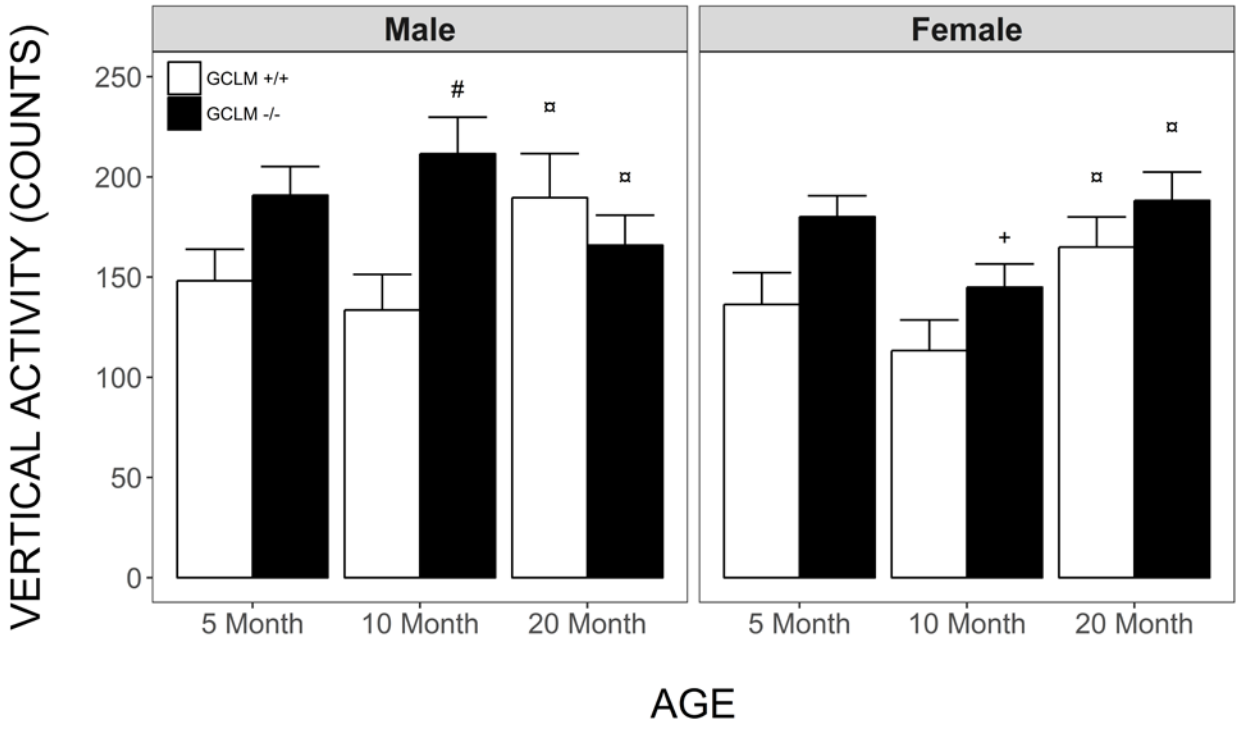

Figure 7. Effects of sex, age and genotype on vertical activity in the open field in young (5 month), adult (10 month), and old (20 month) GCLM+/+ and GCLM-/- mice. Each value represents the mean + SEM of (n = 15-21) mice. ¤ $p < 0.05$ compared to genotype and sex-matched young; + $p < 0.05$ compared to age and genotype-matched males.

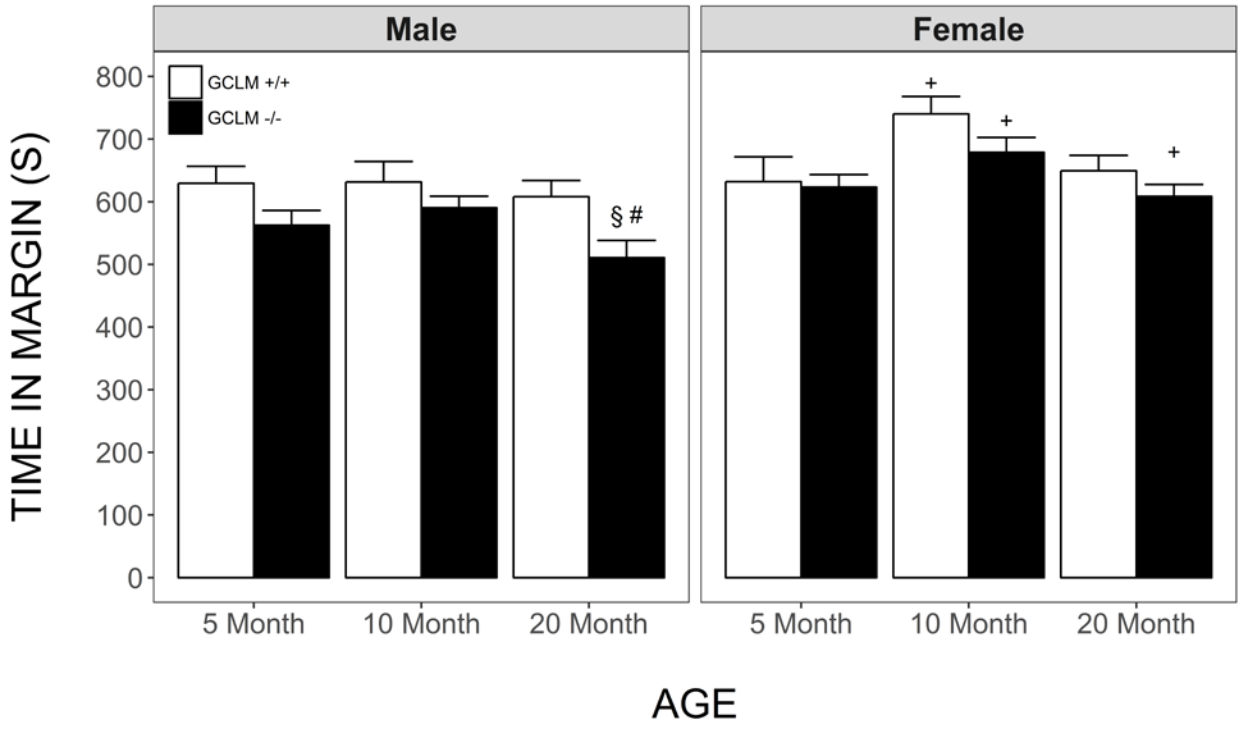

Figure 8. Effects of sex, age and genotype time spent in the margin of the open field in young (5 month), adult (10 month), and old (20 month) GCLM+/+ and GCLM-/- mice. Each value represents the mean + SEM of (n = 15-21) mice. § $p < 0.05$ compared to genotype and sex-matched 10 adult; # $p < 0.05$ compared to age and sex-matched GCLM+/+ mice; + $p < 0.05$ compared to age and genotype-matched males.

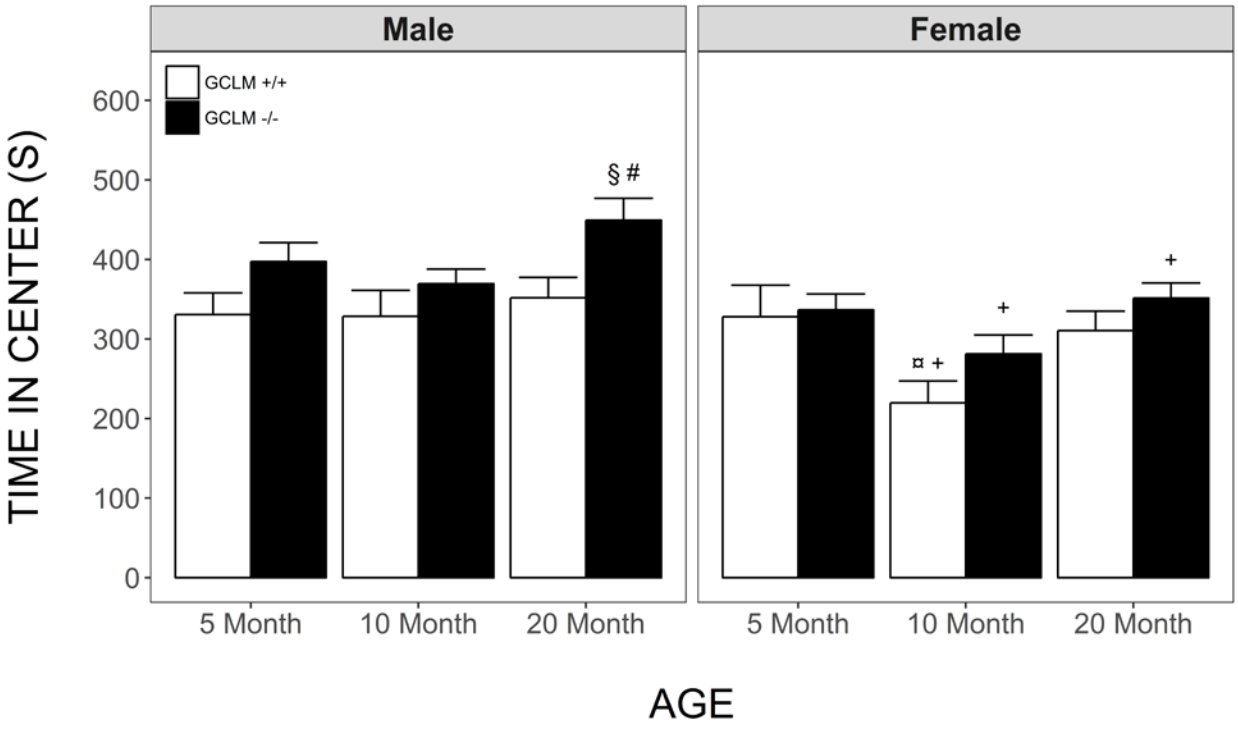

Figure 9. Effects of sex, age and genotype time spent in the center of the open field in young (5 month), adult (10 month), and old (20 month) GCLM+/+ and GCLM-/- mice. Each value represents the mean + SEM of (n = 15-21) mice. ¤ $p < 0.05$ compared to genotype and sex-matched young; § $p < 0.05$ compared to genotype and sex-matched 10 adult; # $p < 0.05$ compared to age and sex-matched GCLM+/+ mice; + $p < 0.05$ compared to age and genotype-matched males.

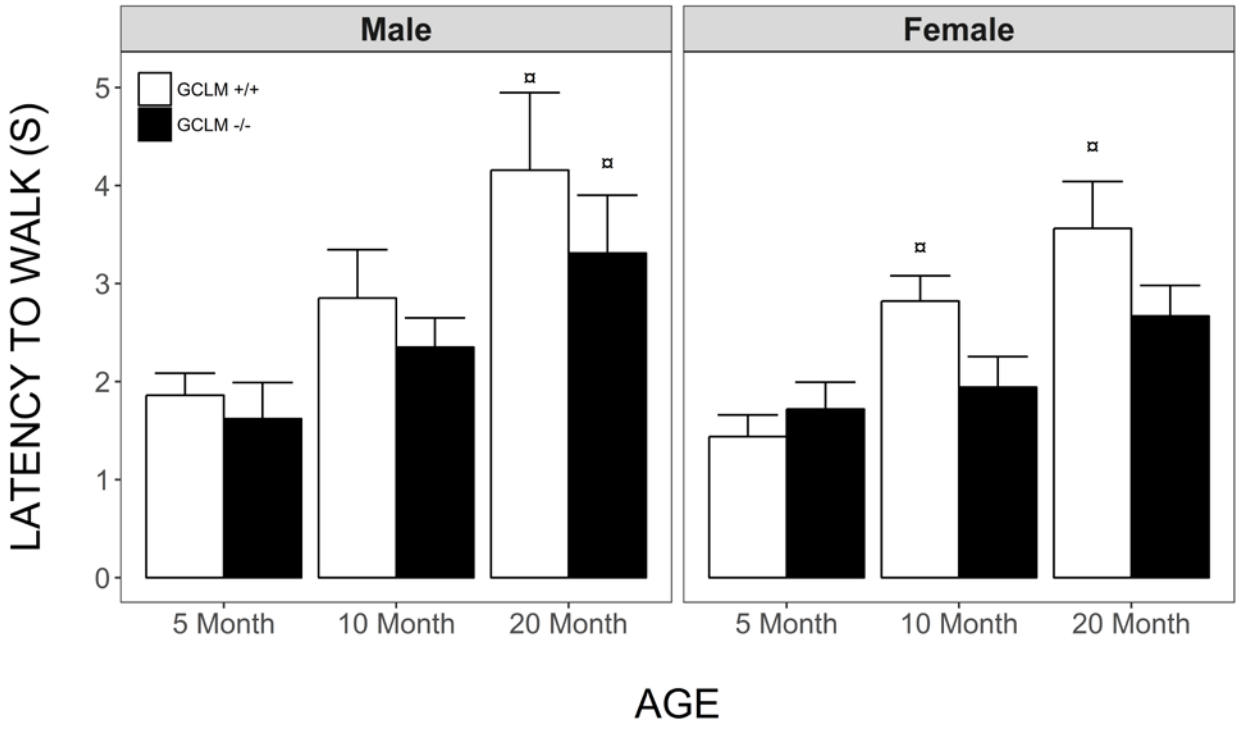

Figure 10. Effects of sex, age and genotype on latency to walk initiation in young (5 month), adult (10 month), and old (20 month) GCLM+/+ and GCLM-/- mice. Each value represents the mean + SEM of (n = 15-23) mice. ¤ $p < 0.05$ compared to genotype and sex-matched young.

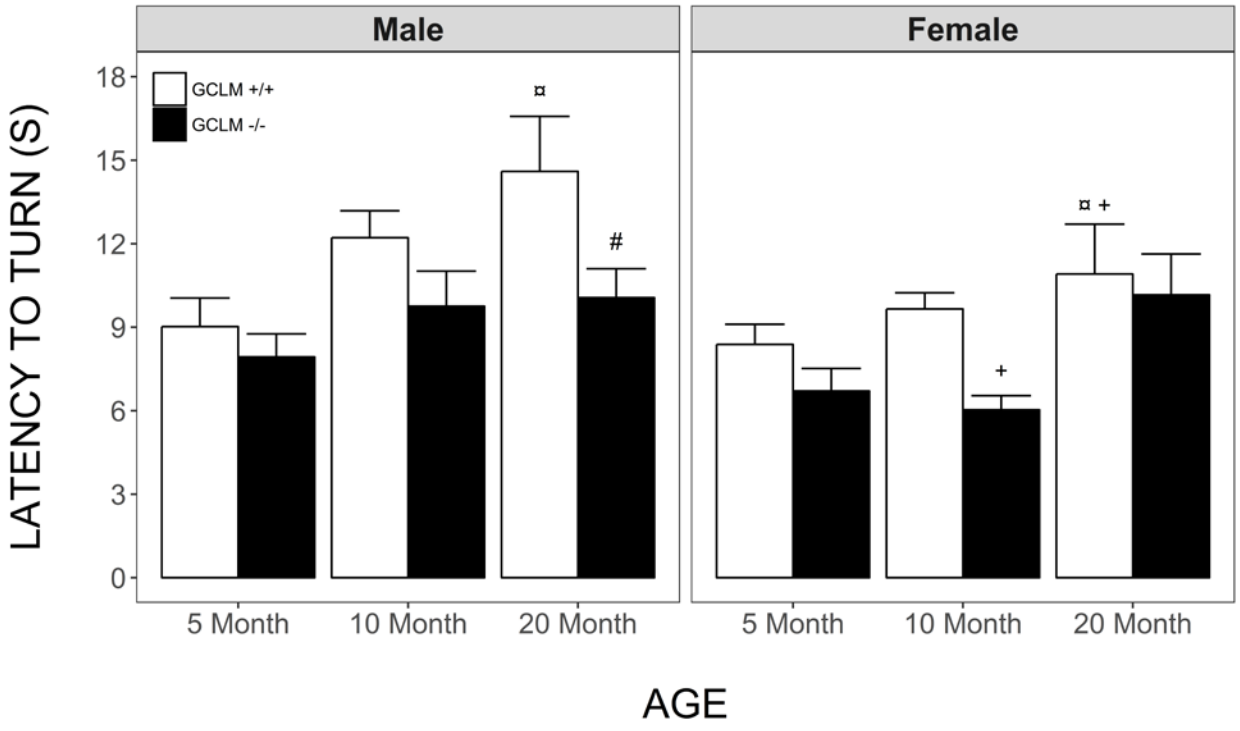

Figure 11. Effects of sex, age and genotype on latency to turn inside the alley in young (5 month), adult (10 month), and old (20 month) GCLM+/+ and GCLM-/- mice. Each value represents the mean + SEM of (n = 15-23) mice. ¤ $p < 0.05$ compared to genotype and sex-matched young; # $p < 0.05$ compared to age and sex-matched GCLM+/+ mice; + $p < 0.05$ compared to age and genotype-matched males.

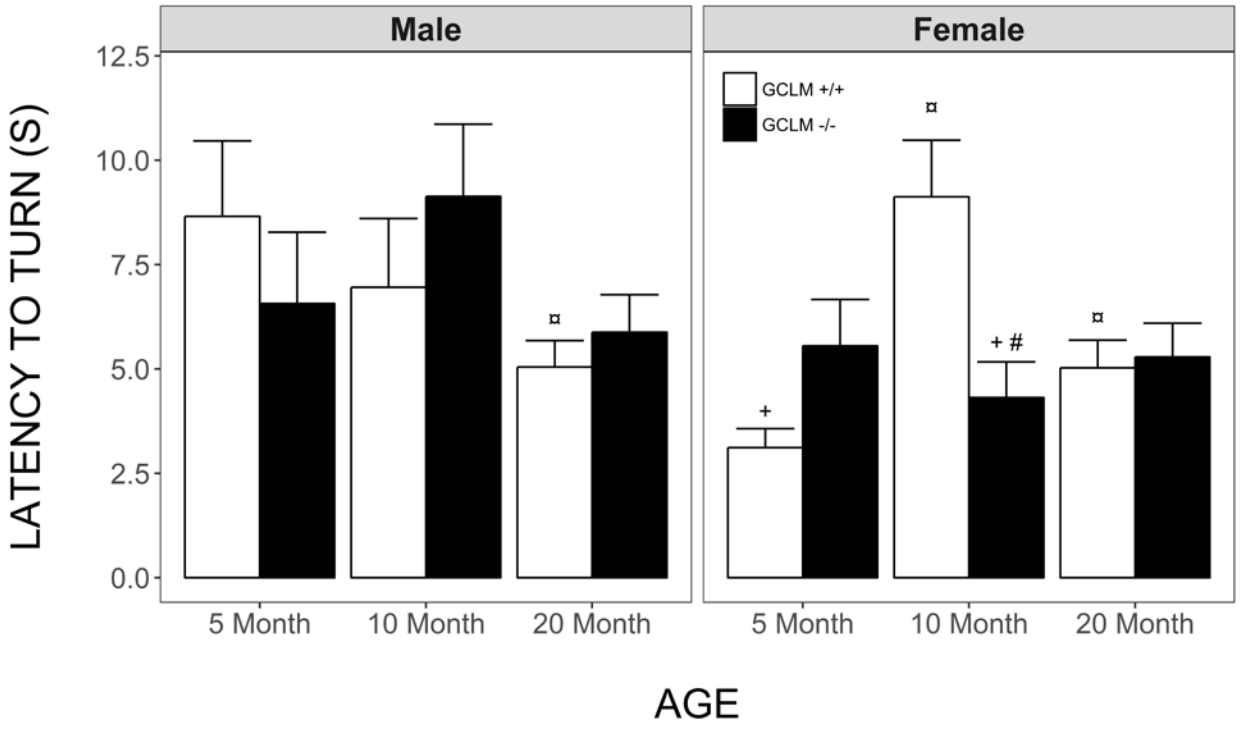

Figure 12. Effects of sex, age and genotype on latency to turn 90 degrees on the negative geotaxis wire grid in young (5 month), adult (10 month), and old (20 month) GCLM+/+ and GCLM-/- mice. Each value represents the mean + SEM of (n = 15-23) mice. ¤ $p < 0.05$ compared to genotype and sex-matched young; # $p < 0.05$ compared to age and sex-matched GCLM+/+ mice; + $p < 0.05$ compared to age and genotype-matched males.

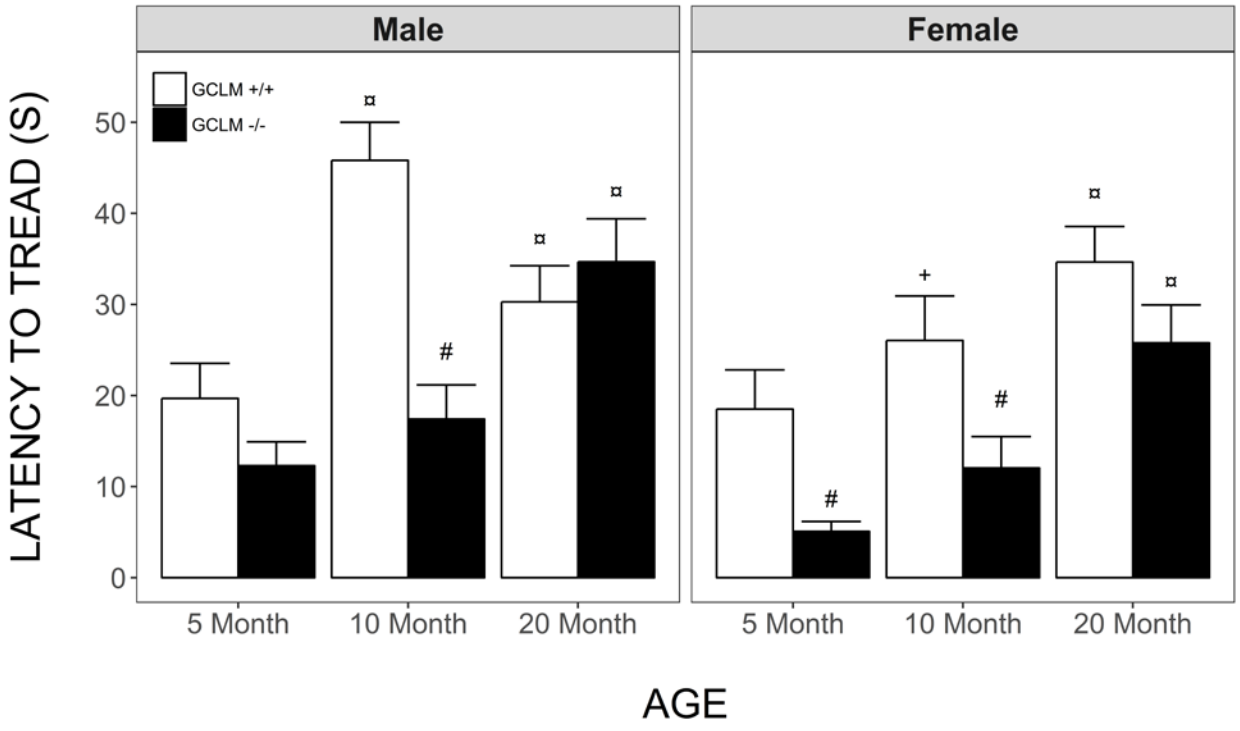

Figure 13. Effects of sex, age and genotype on latency to tread during wire suspension in young (5 month), adult (10 month), and old (20 month) GCLM+/+ and GCLM-/- mice. Each value represents the mean + SEM of (n = 15-23) mice. ¤ $p < 0.05$ compared to genotype and sex-matched young; # $p < 0.05$ compared to age and sex-matched GCLM+/+ mice; + $p < 0.05$ compared to age and genotype-matched males.

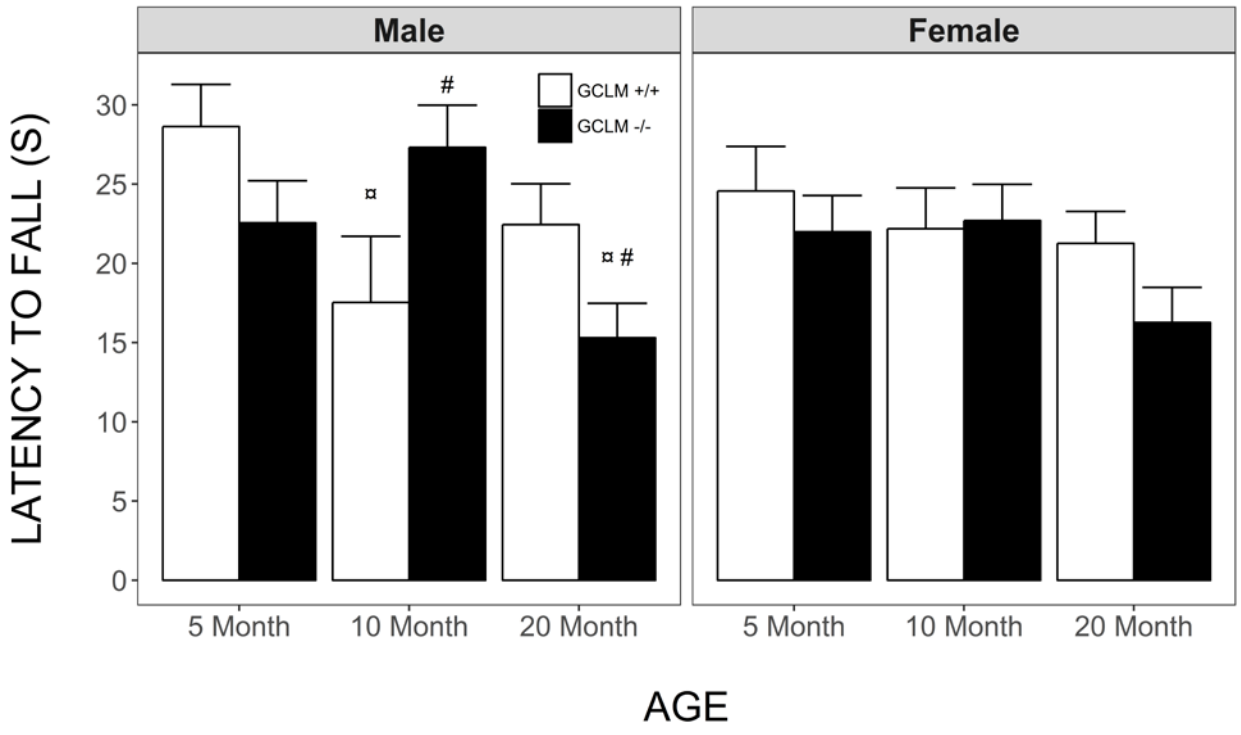

Figure 14. Effects of sex, age and genotype on latency to fall during wire suspension in young (5 month), adult (10 month), and old (20 month) GCLM+/+ and GCLM-/- mice. Each value represents the mean + SEM of (n = 15-23) mice. ¤ $p < 0.05$ compared to genotype and sex-matched young; # $p < 0.05$ compared to age and sex-matched GCLM+/+ mice.

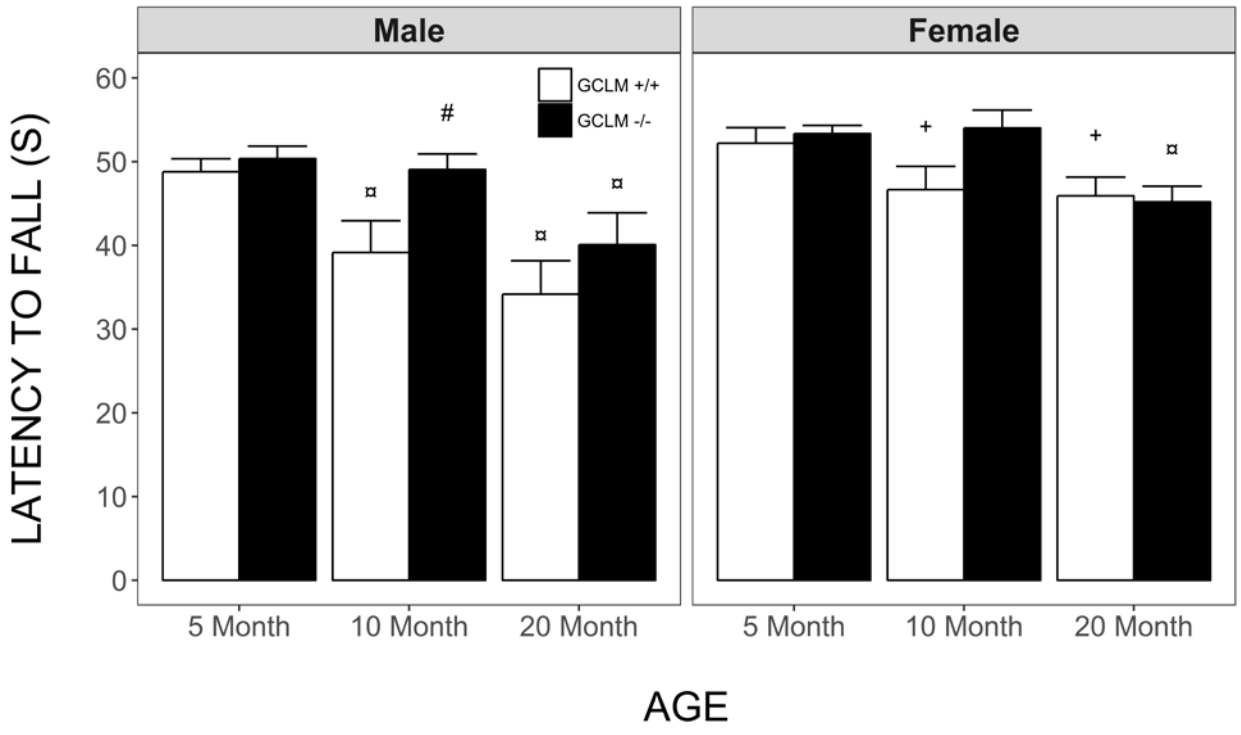

Figure 15. Effects of sex, age and genotype on overall latency to fall from an elevated bridge in young (5 month), adult (10 month), and old (20 month) GCLM+/+ and GCLM-/- mice. Each value represents the mean + SEM of (n = 15-23) mice. ¤ $p < 0.05$ compared to genotype and sex-matched young; # $p < 0.05$ compared to age and sex-matched GCLM+/+ mice; + $p < 0.05$ compared to age and genotype-matched males.

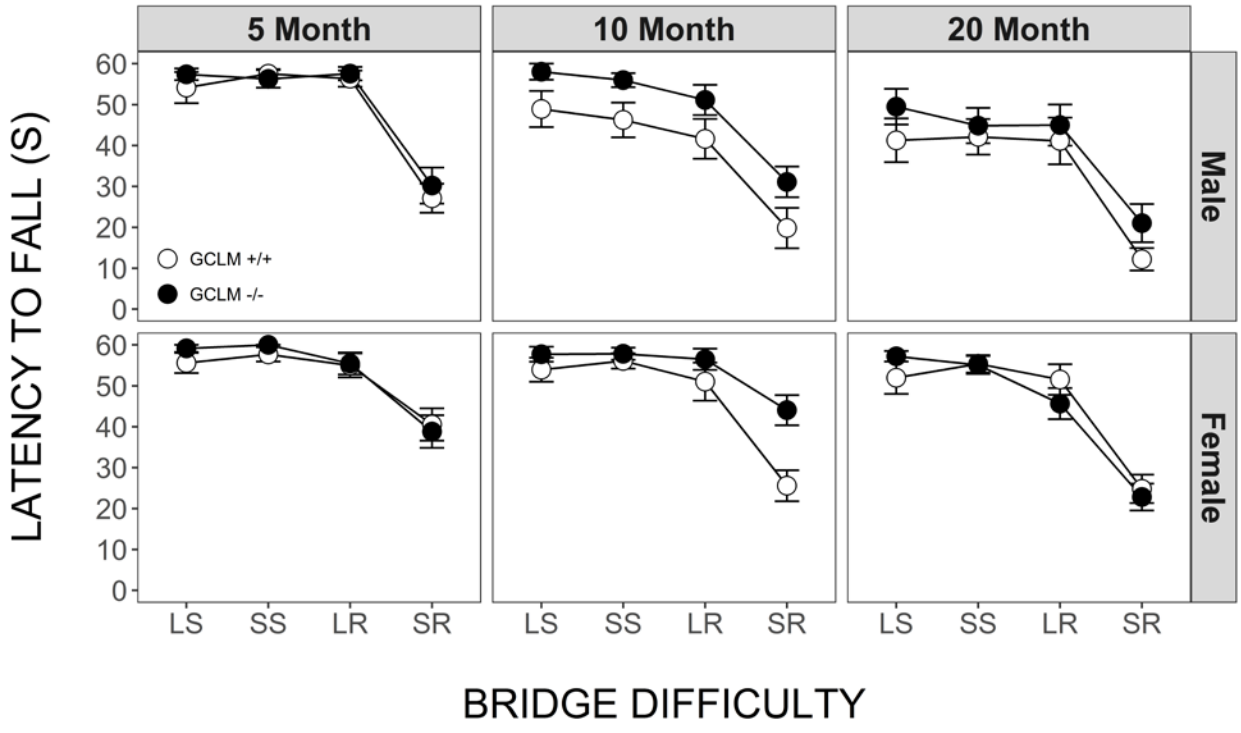

Figure 16. Effects of sex, age and genotype on latency to fall from an elevated bridge by bridge difficulty in young (5 month), adult (10 month), and old (20 month) GCLM+/+ and GCLM-/- mice. Bridge difficulty increased from large square (LS), to small square (SS), to large round (LR), and to small round (SR). Each value represents the mean + SEM of (n = 15-23) mice.

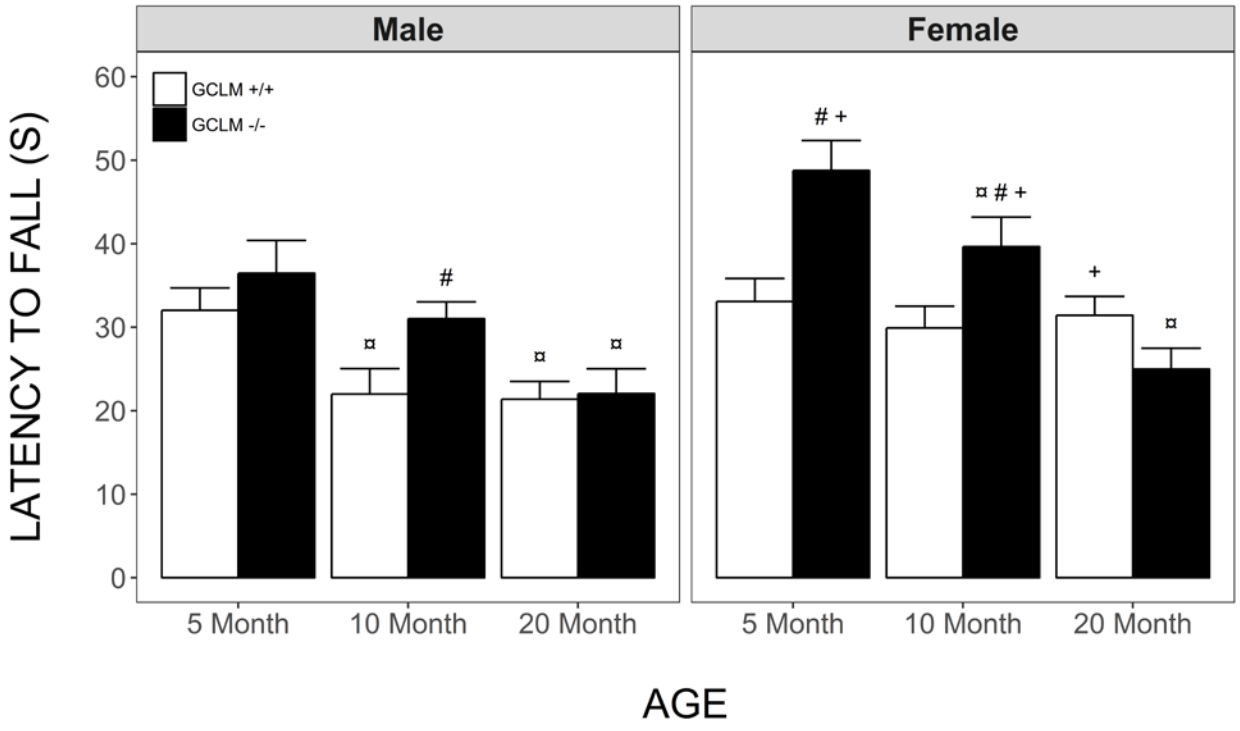

Figure 17. Effects of sex, age and genotype on overall latency to fall from the rotorod in young (5 month), adult (10 month), and old (20 month) GCLM+/+ and GCLM-/- mice. Each value represents the mean + SEM of (n = 15-23) mice. ¤ $p < 0.05$ compared to genotype and sex-matched young; # $p < 0.05$ compared to age and sex-matched GCLM+/+ mice; + $p < 0.05$ compared to age and genotype-matched males.

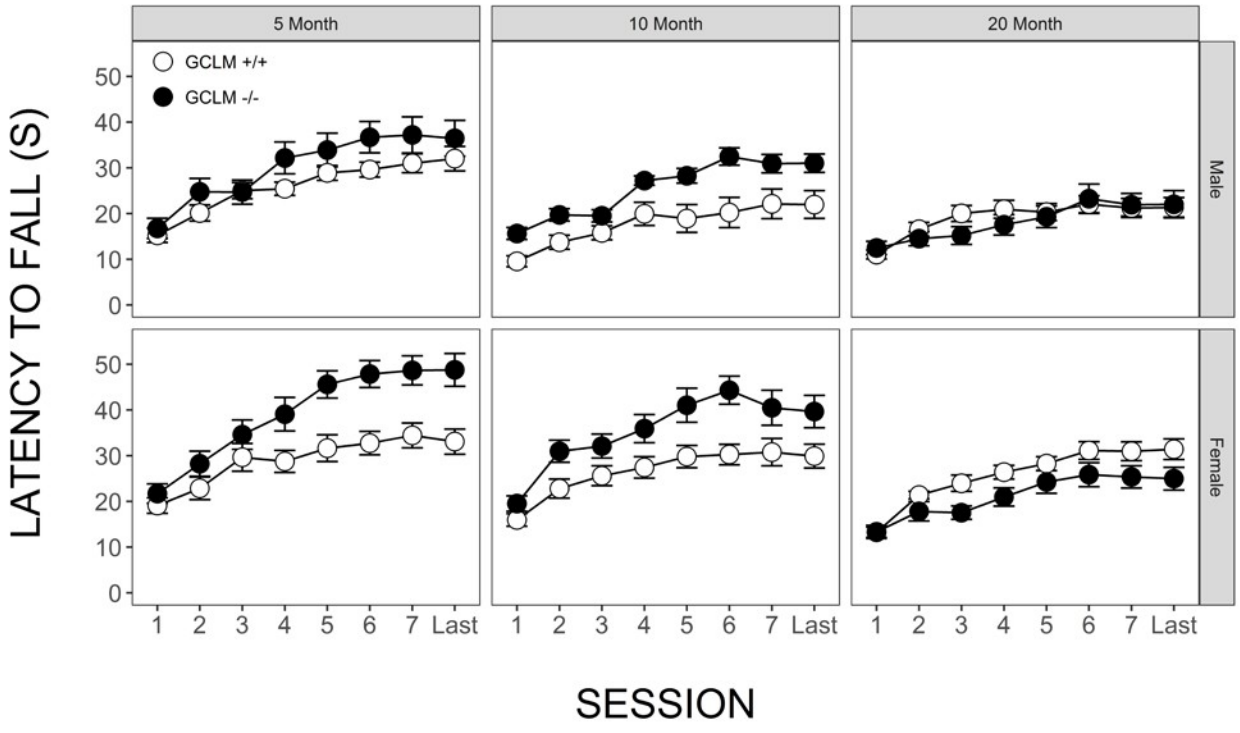

Figure 18. Effects of sex, age and genotype on latency to fall from the rotorod by session in young (5 month), adult (10 month), and old (20 month) GCLM+/+ and GCLM-/- mice. Each value represents the mean + SEM of (n = 15-23) mice.

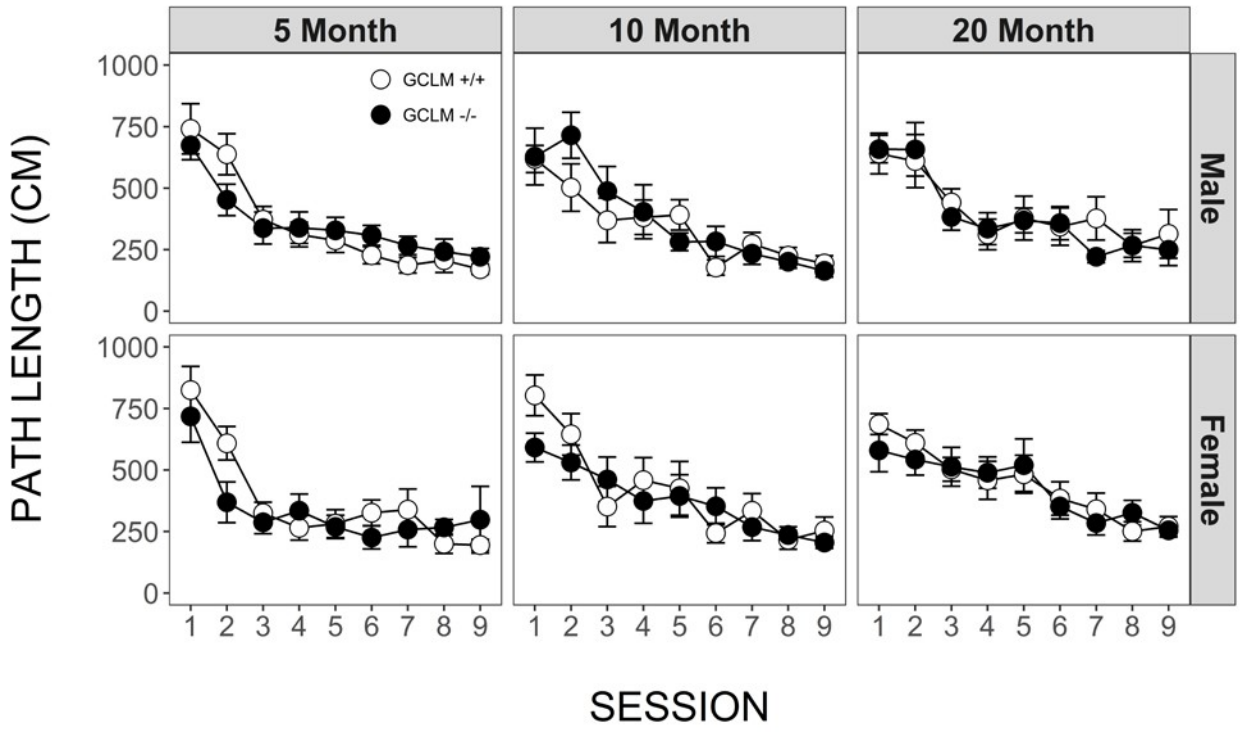

Figure 19. Effects of sex, age and genotype on average path length to completion during the Morris water maze in young (5 month), adult (10 month), and old (20 month) GCLM+/+ and GCLM-/- mice. Each value represents the mean + SEM of (n = 15-23) mice.

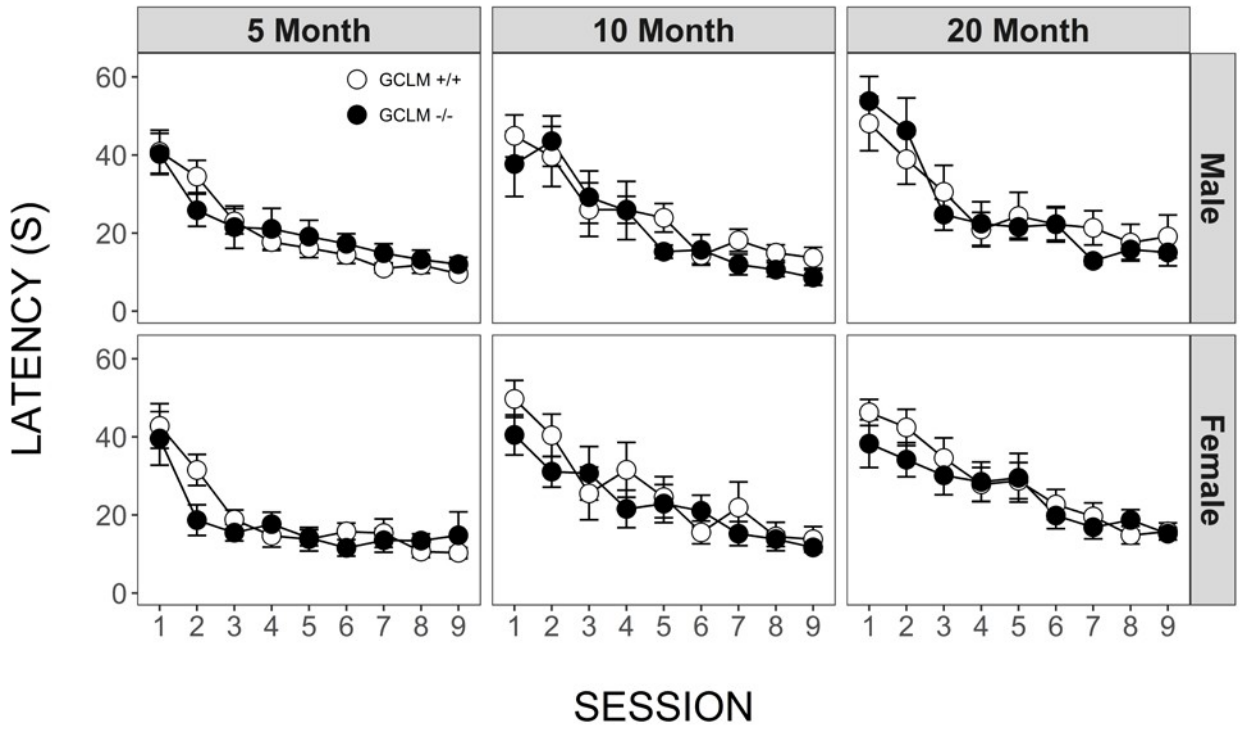

Figure 20. Effects of sex, age and genotype on average latency to completion during the Morris water maze in young (5 month), adult (10 month), and old (20 month) GCLM+/+ and GCLM-/- mice. Each value represents the mean + SEM of (n = 15-23) mice.

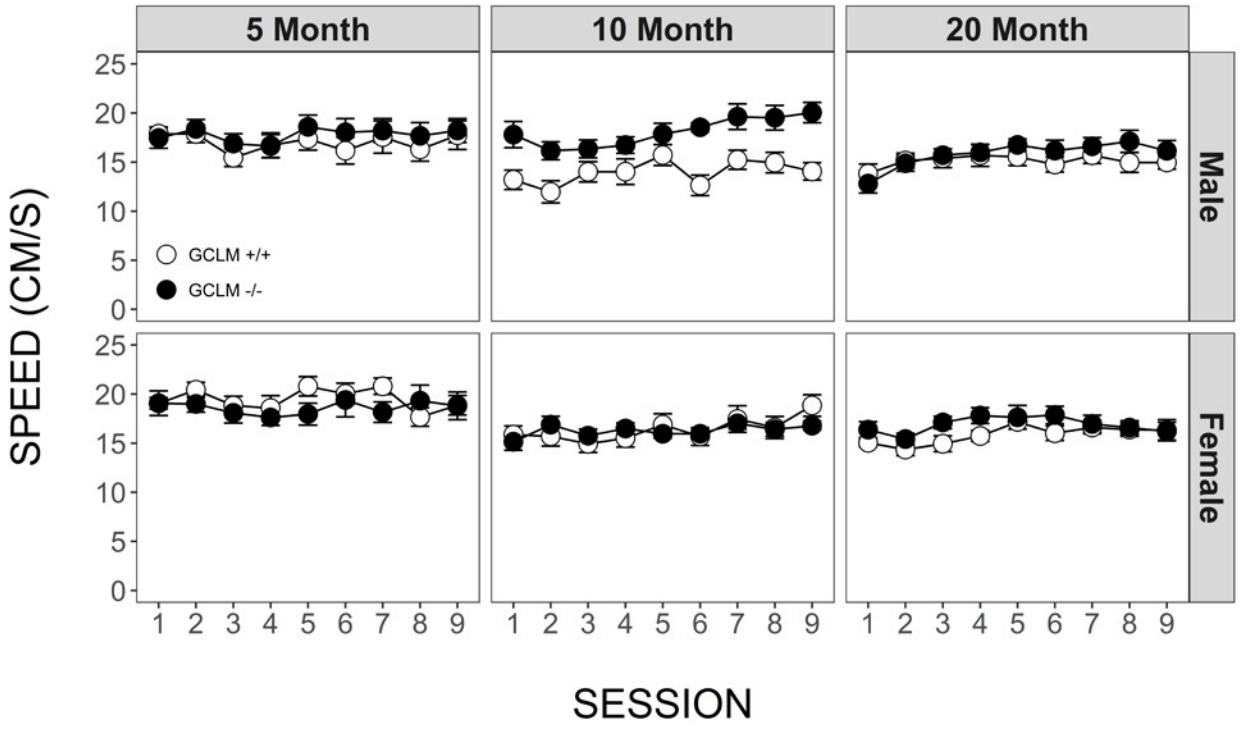

Figure 21. Effects of sex, age and genotype on average swim speed during the morris water maze in young (5 month), adult (10 month), and old (20 month) GCLM+/+ and GCLM-/- mice. Each value represents the mean + SEM of (n = 15-23) mice.

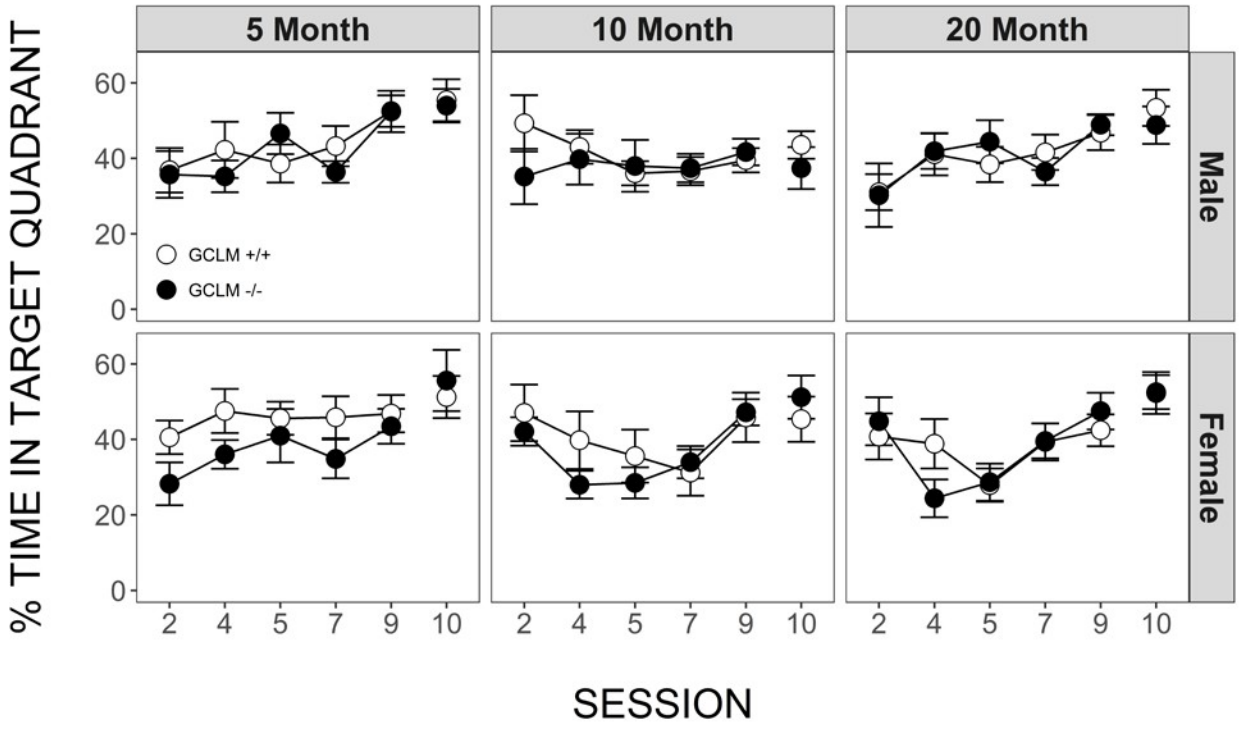

Figure 22. Effects of sex, age and genotype on time in target quadrant during probe sessions in young (5 month), adult (10 month), and old (20 month) GCLM+/+ and GCLM-/- mice. Each value represents the mean + SEM of (n = 15-23) mice.

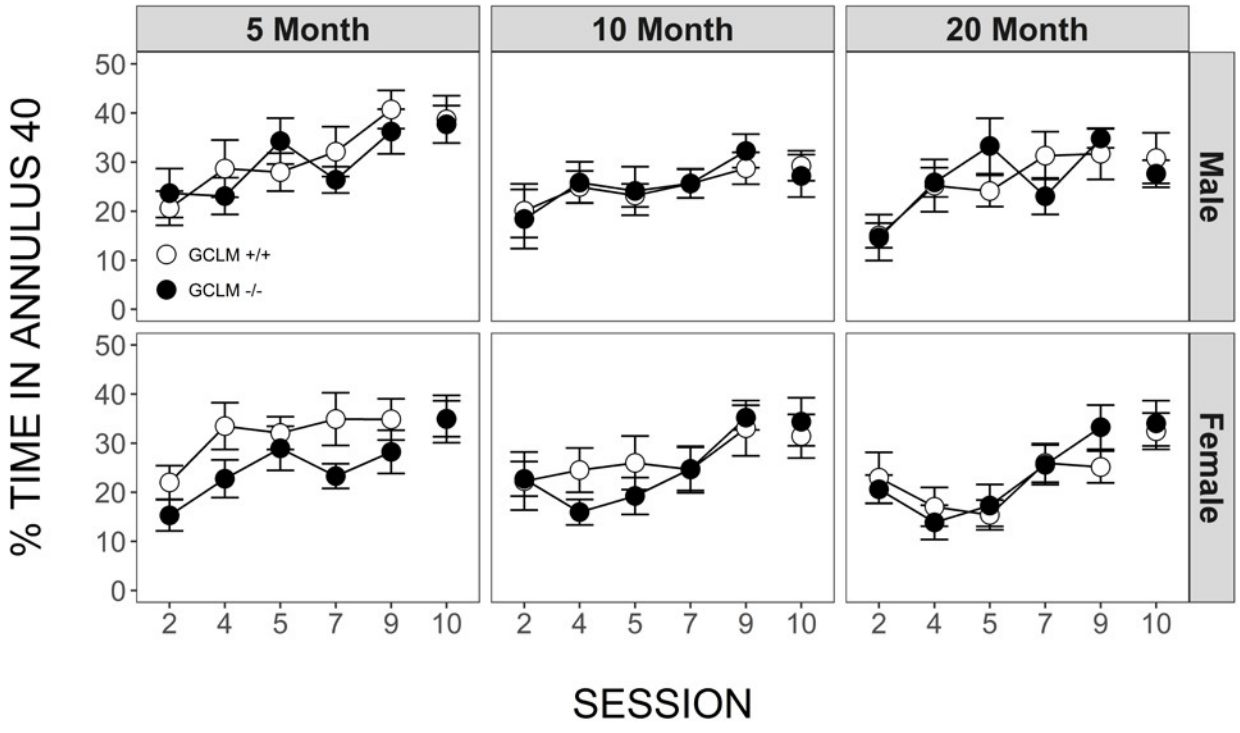

Figure 23. Effects of sex, age and genotype on time in target annulus 40 during probe sessions in young (5 month), adult (10 month), and old (20 month) GCLM+/+ and GCLM-/- mice. Each value represents the mean + SEM of (n = 15-23) mice.

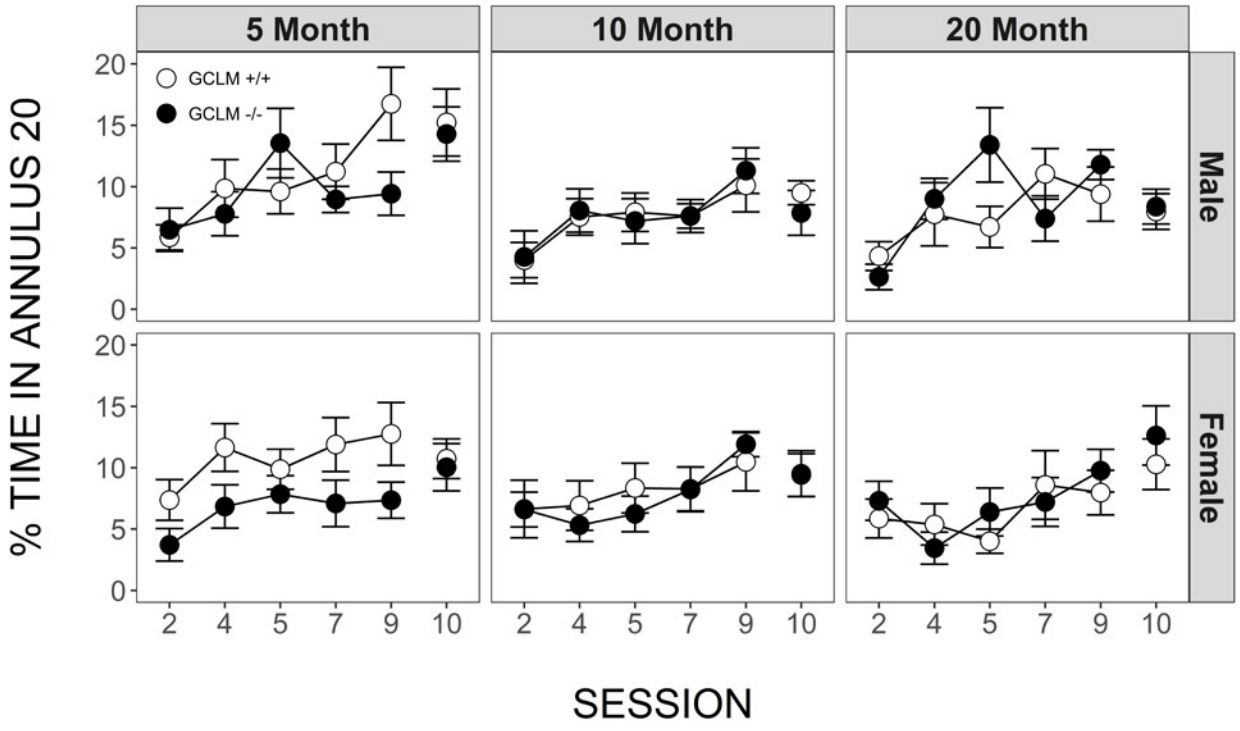

Figure 24. Effects of sex, age and genotype on time in annulus 20 during probe sessions in young (5 month), adult (10 month), and old (20 month) GCLM+/+ and GCLM-/- mice. Each value represents the mean + SEM of (n = 15-23) mice.

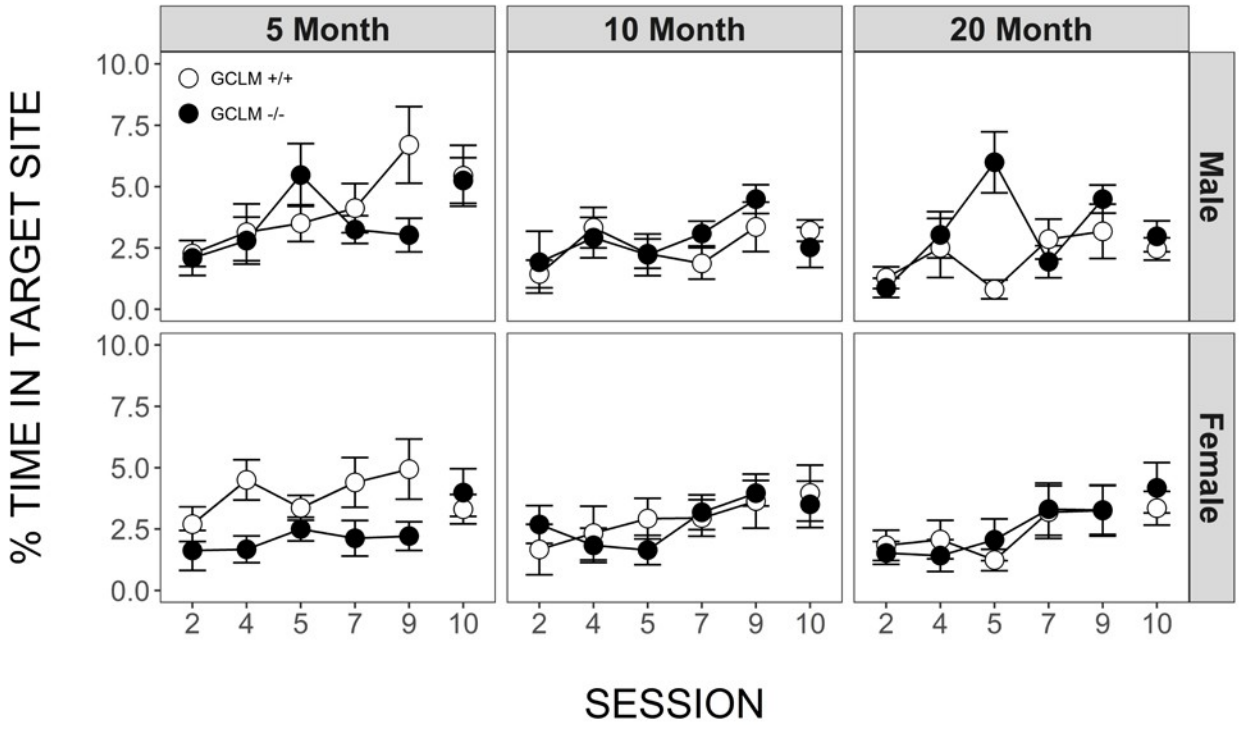

Figure 25. Effects of sex, age and genotype on time in target site during probe sessions in young (5 month), adult (10 month), and old (20 month) GCLM+/+ and GCLM-/- mice. Each value represents the mean + SEM of (n = 15-23) mice.

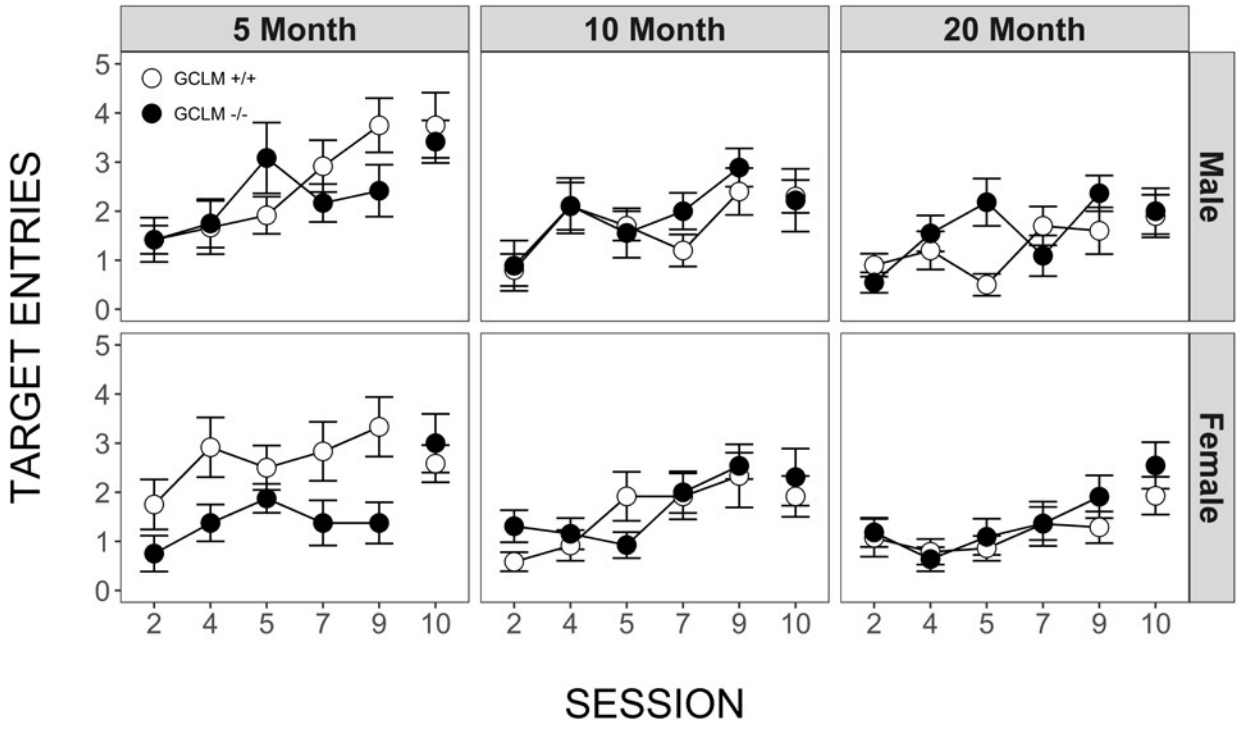

Figure 26. Effects of sex, age and genotype on target entries during probe sessions in young (5 month), adult (10 month), and old (20 month) GCLM+/+ and GCLM-/- mice. Each value represents the mean + SEM of (n = 15-23) mice.

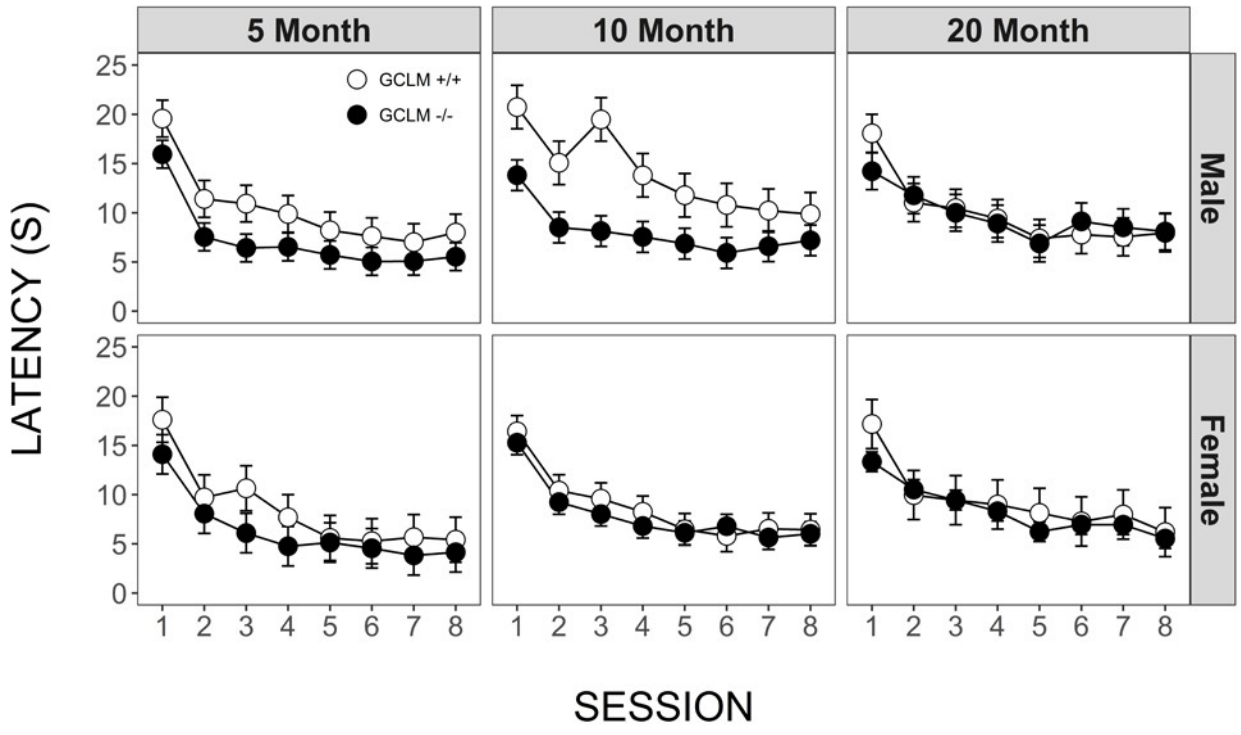

Figure 27. Effects of sex, age and genotype on average time to target across visible platform sessions in young (5 month), adult (10 month), and old (20 month) GCLM+/+ and GCLM-/- mice. Each value represents the mean + SEM of (n = 15-23) mice.

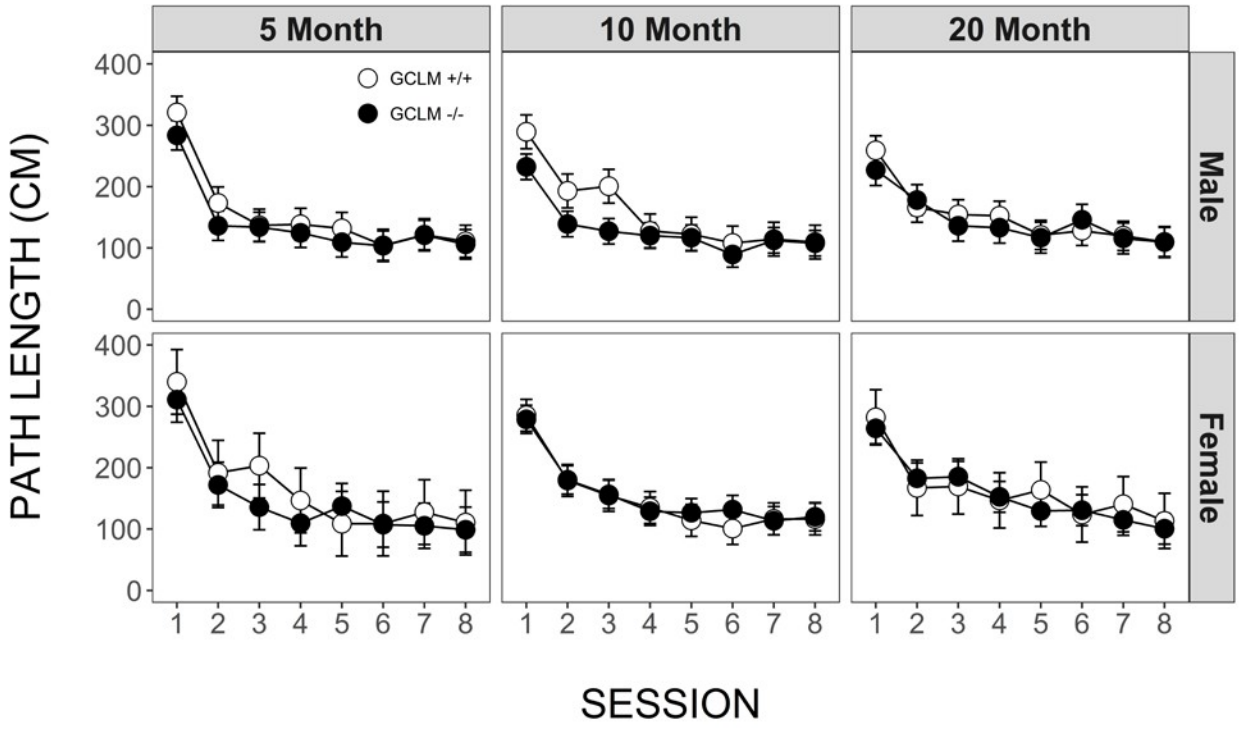

Figure 28. Effects of sex, age and genotype on average path length to target across visible platform sessions in young (5 month), adult (10 month), and old (20 month) GCLM+/+ and GCLM-/- mice. Each value represents the mean + SEM of (n = 15-23) mice.

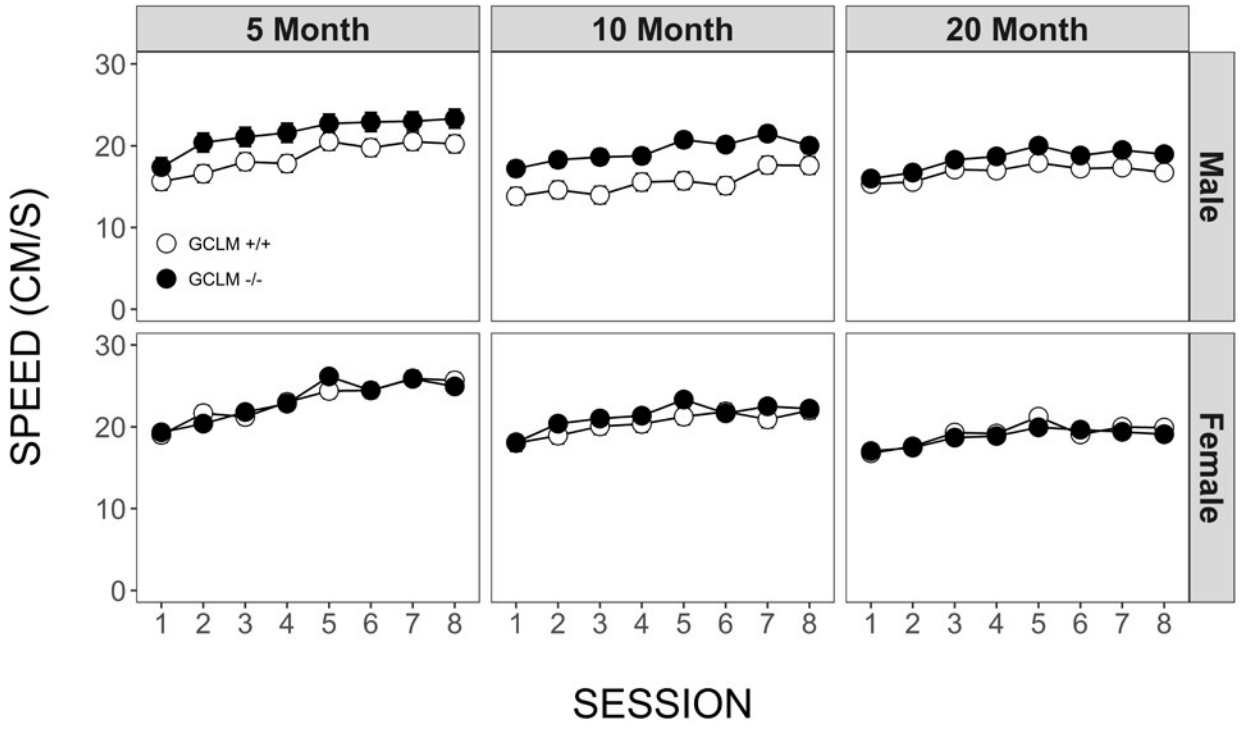

Figure 29. Effects of sex, age and genotype on average swim speed during visible platform sessions in young (5 month), adult (10 month), and old (20 month) GCLM+/+ and GCLM-/- mice. Each value represents the mean + SEM of (n = 15-23) mice.

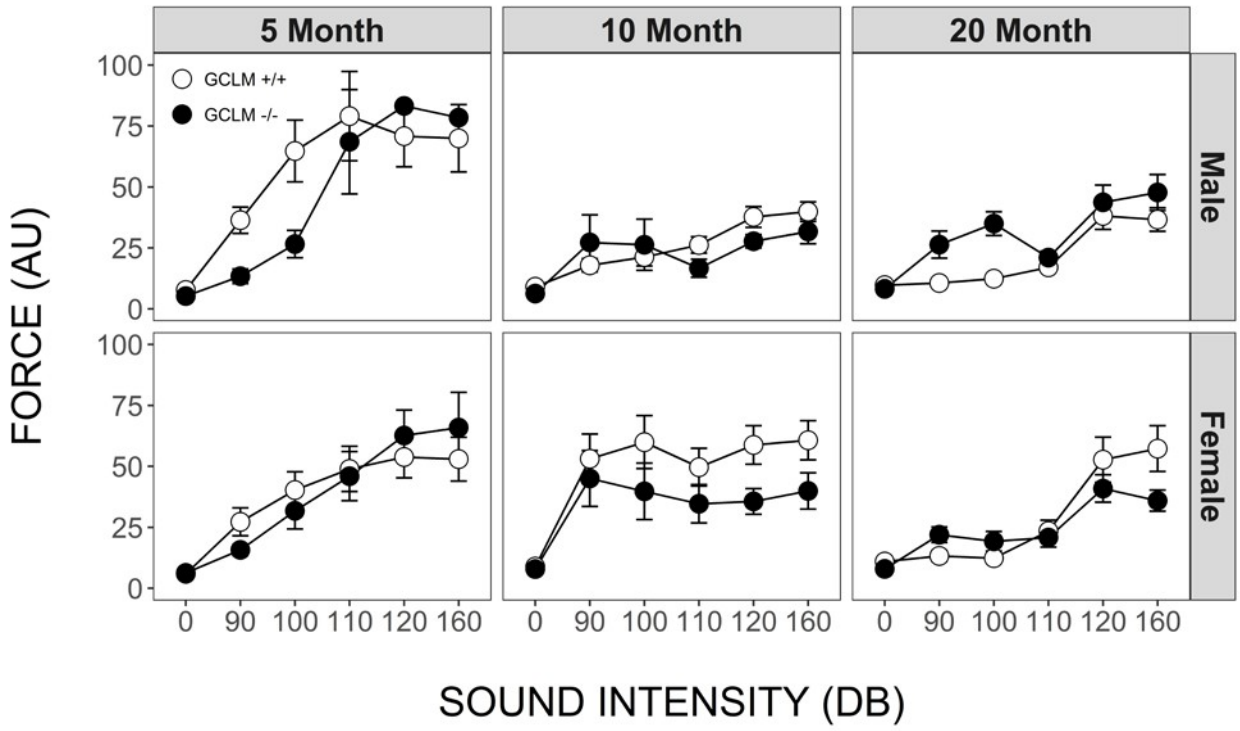

Figure 30. Effects of sex, age and genotype on force production in the auditory startle test in young (5 month), adult (10 month), and old (20 month) GCLM+/+ and GCLM-/- mice. Each value represents the mean + SEM of (n = 15-23) mice.

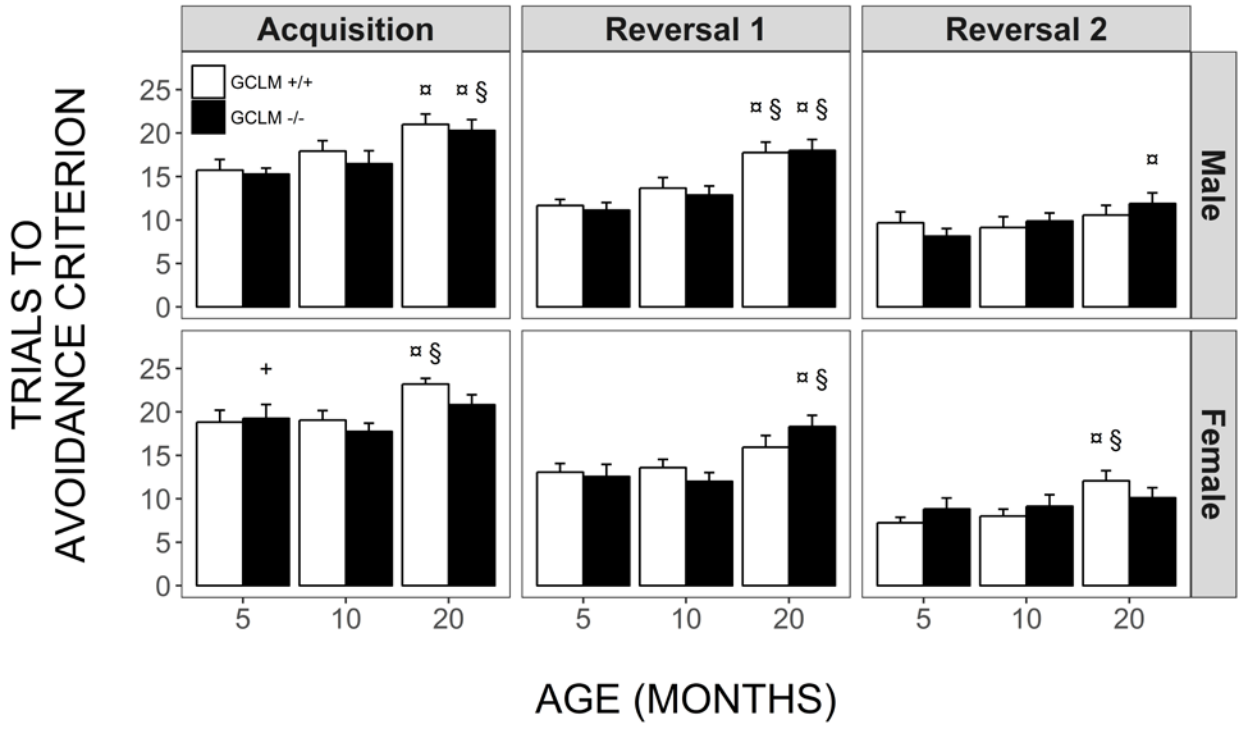

Figure 31. Effects of sex, age and genotype on number of trials to reach avoidance criterion in the discrimination-avoidance test in young (5 month), adult (10 month), and old (20 month) GCLM+/+ and GCLM-/- mice. Each value represents the mean + SEM of (n = 15-23) mice. ¤ $p < 0.05$ compared to genotype and sex-matched young; § $p < 0.05$ compared to genotype and sex-matched 10 adult; + $p < 0.05$ compared to age and genotype-matched males.

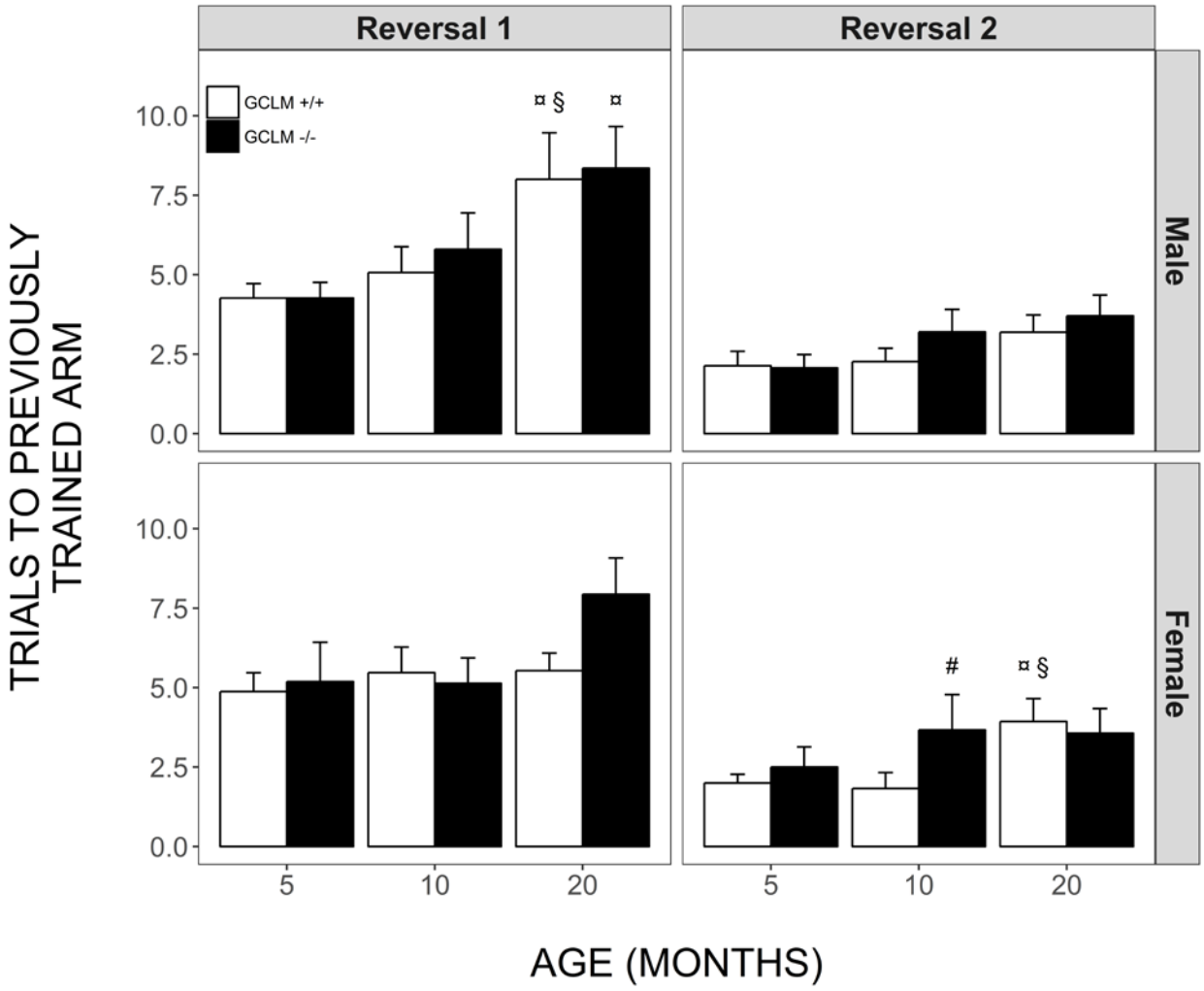

Figure 32. Effects of sex, age and genotype on number of trials to the previously trained arm in the discrimination-avoidance test in young (5 month), adult (10 month), and old (20 month) GCLM+/+ and GCLM-/- mice. Each value represents the mean + SEM of (n = 15-23) mice. ¤ $p < 0.05$ compared to genotype and sex-matched young; § $p < 0.05$ compared to genotype and sex-matched 10 adult; # $p < 0.05$ compared to age and sex-matched GCLM+/+ mice.

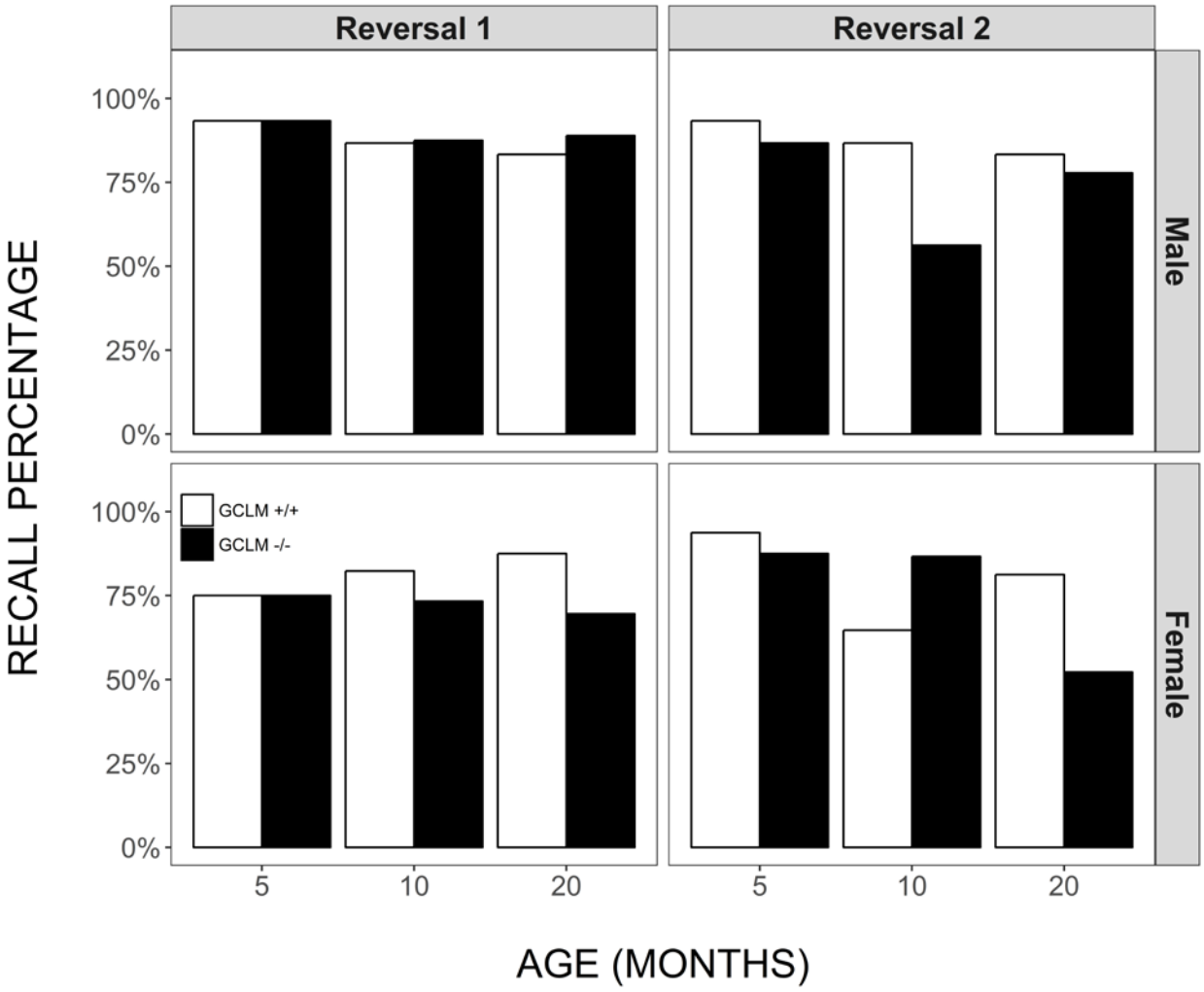

Figure 33. Effects of sex, age and genotype on recall of previously trained arm in the discrimination- avoidance test in young (5 month), adult (10 month), and old (20 month) GCLM+/+ and GCLM-/- mice. Each value represents the mean + SEM of (n = 15-23) mice.

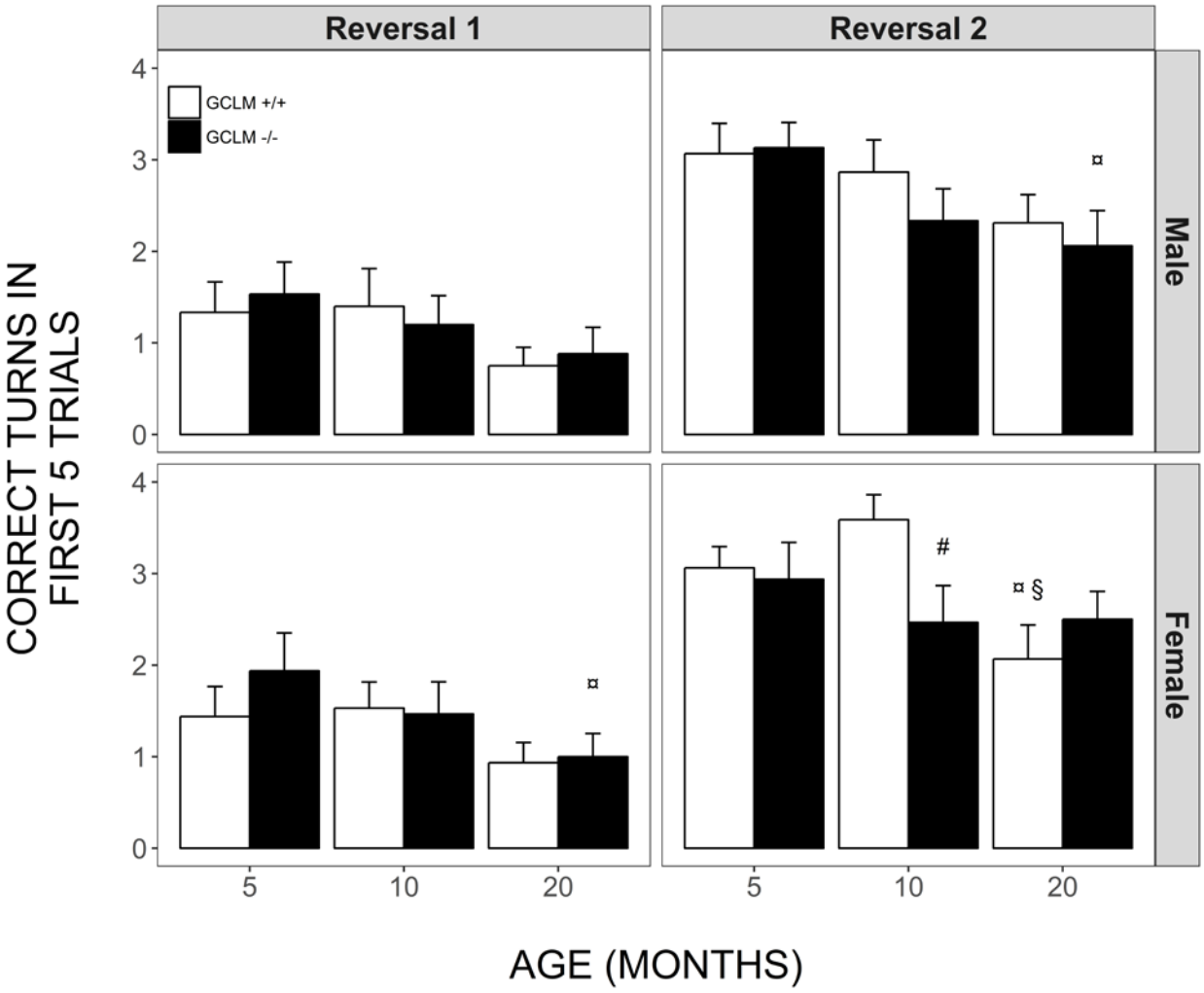

Figure 34. Effects of sex, age and genotype on number of correct turns in the first five trials in the discrimination-avoidance test in young (5 month), adult (10 month), and old (20 month) GCLM+/+ and GCLM-/- mice. Each value represents the mean + SEM of (n = 15-23) mice. ¤ $p < 0.05$ compared to genotype and sex-matched young; § $p < 0.05$ compared to genotype and sex-matched 10 adult; # $p < 0.05$ compared to age and sex-matched GCLM+/+ mice.

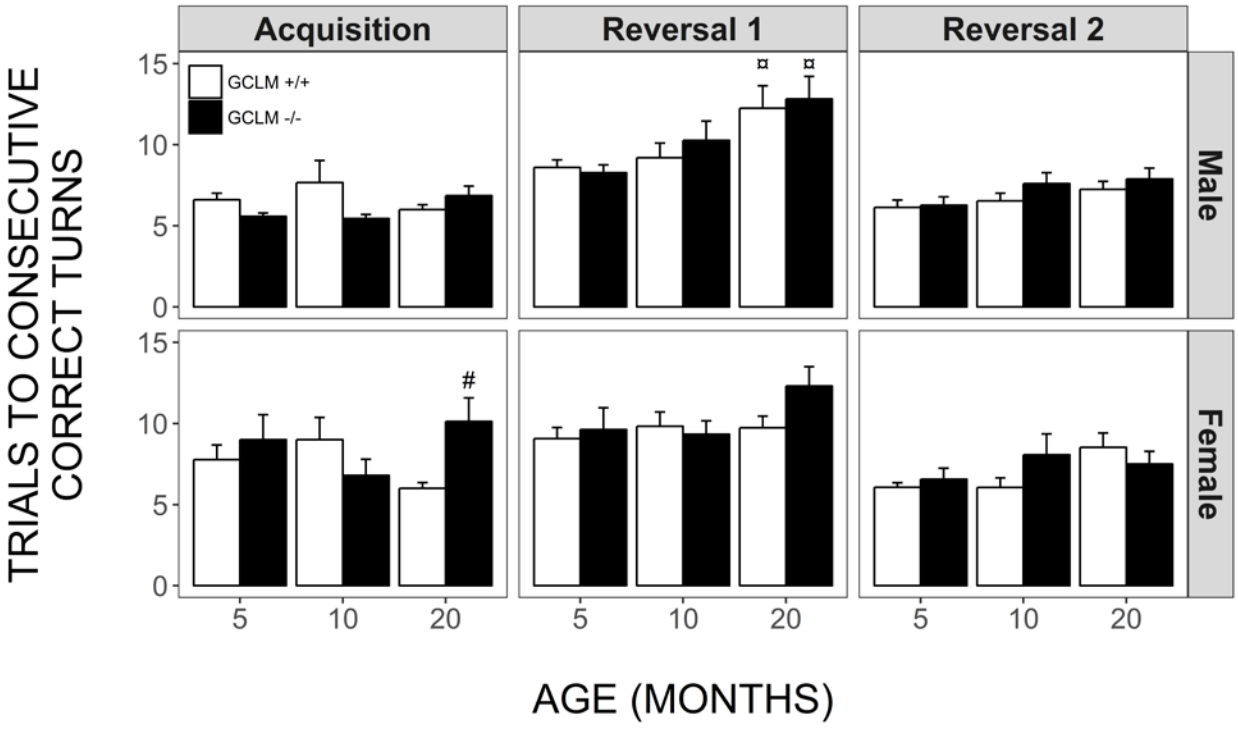

Figure 35. Effects of sex, age and genotype on number of trials to reach four of five correct turns, independent of avoidance criterion in the discrimination-avoidance test in young (5 month), adult (10 month), and old (20 month) GCLM+/+ and GCLM-/- mice. Each value represents the mean + SEM of (n = 15-23) mice. ¤ $p < 0.05$ compared to genotype and sex-matched young; # $p < 0.05$ compared to age and sex-matched GCLM+/+ mice.

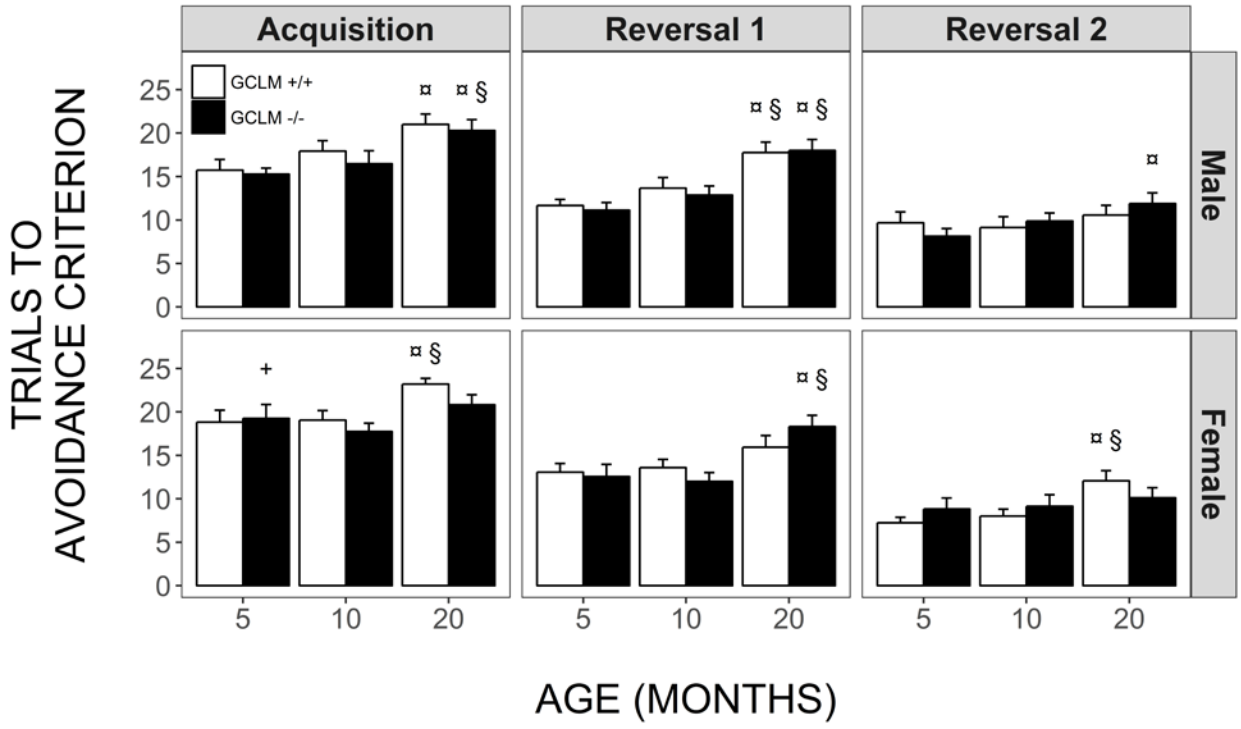

Figure 36. Effects of sex, age and genotype on number of trials to consecutive correct turns in the discrimination-avoidance test in young (5 month), adult (10 month), and old (20 month) GCLM+/+ and GCLM-/- mice. Each value represents the mean + SEM of (n = 15-23) mice. ¤ $p < 0.05$ compared to genotype and sex-matched young; § $p < 0.05$ compared to genotype and sex-matched 10 adult.

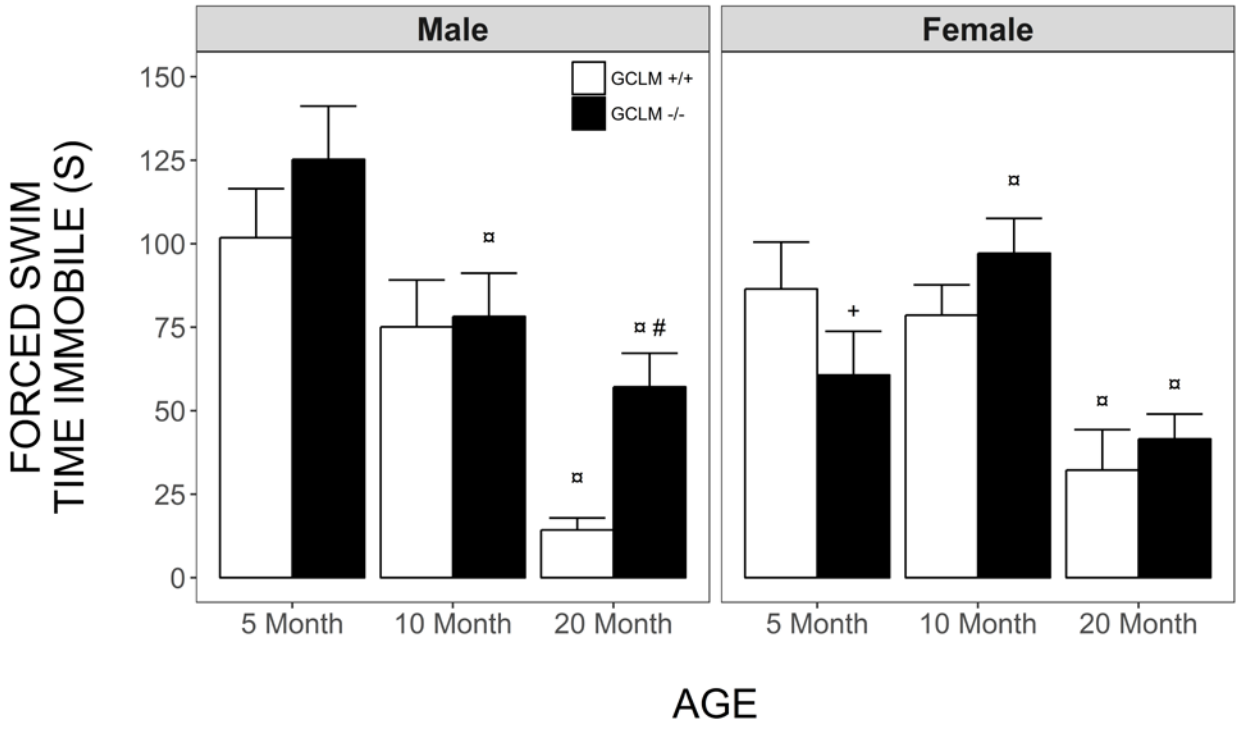

Figure 37. Effects of sex, age and genotype on time spent immobile in the forced swim test in young (5 month), adult (10 month), and old (20 month) GCLM+/+ and GCLM-/- mice. Each value represents the mean + SEM of (n = 15-23) mice. ¤ $p < 0.05$ compared to genotype and sex-matched young; # $p < 0.05$ compared to age and sex-matched GCLM+/+ mice; + $p < 0.05$ compared to age and genotype-matched males.

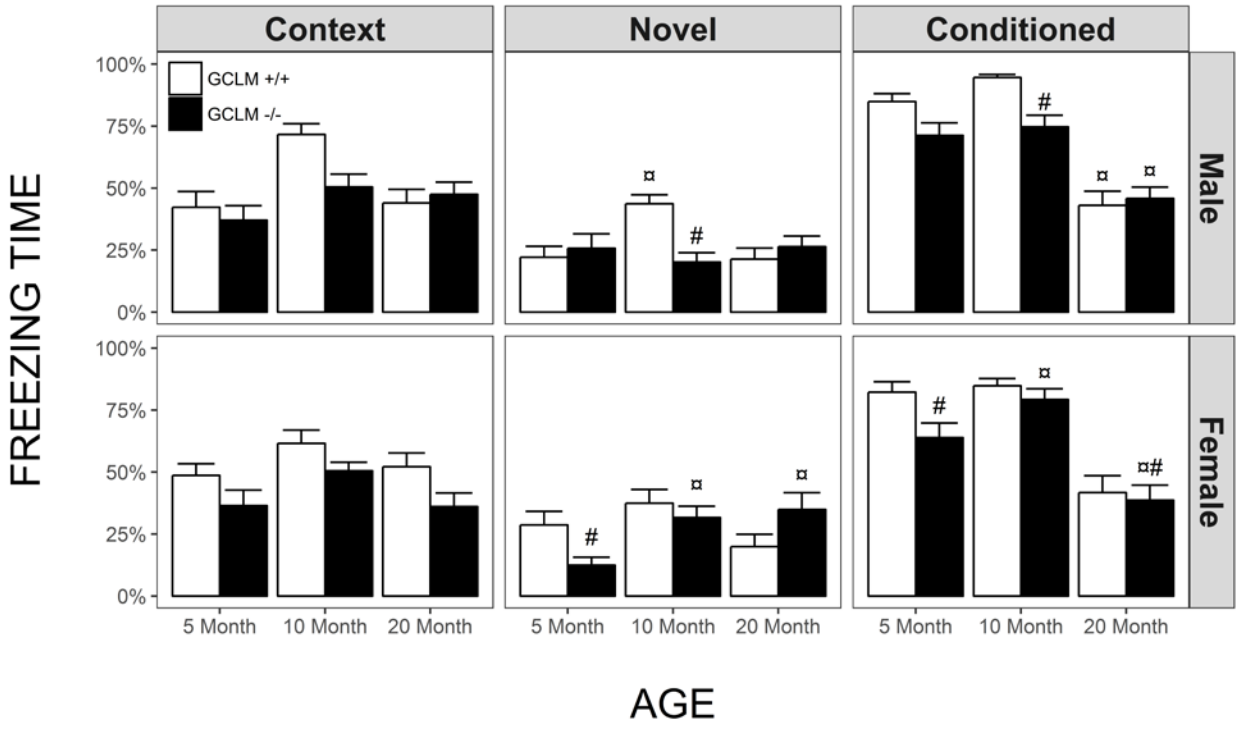

Figure 38. Effects of sex, age and genotype on freezing time in the fear conditioning test in young (5 month), adult (10 month), and old (20 month) GCLM+/+ and GCLM-/- mice. Each value represents the mean + SEM of (n = 15-23) mice. ¤ $p < 0.05$ compared to genotype and sex-matched young; # $p < 0.05$ compared to age and sex-matched GCLM+/+ mice.

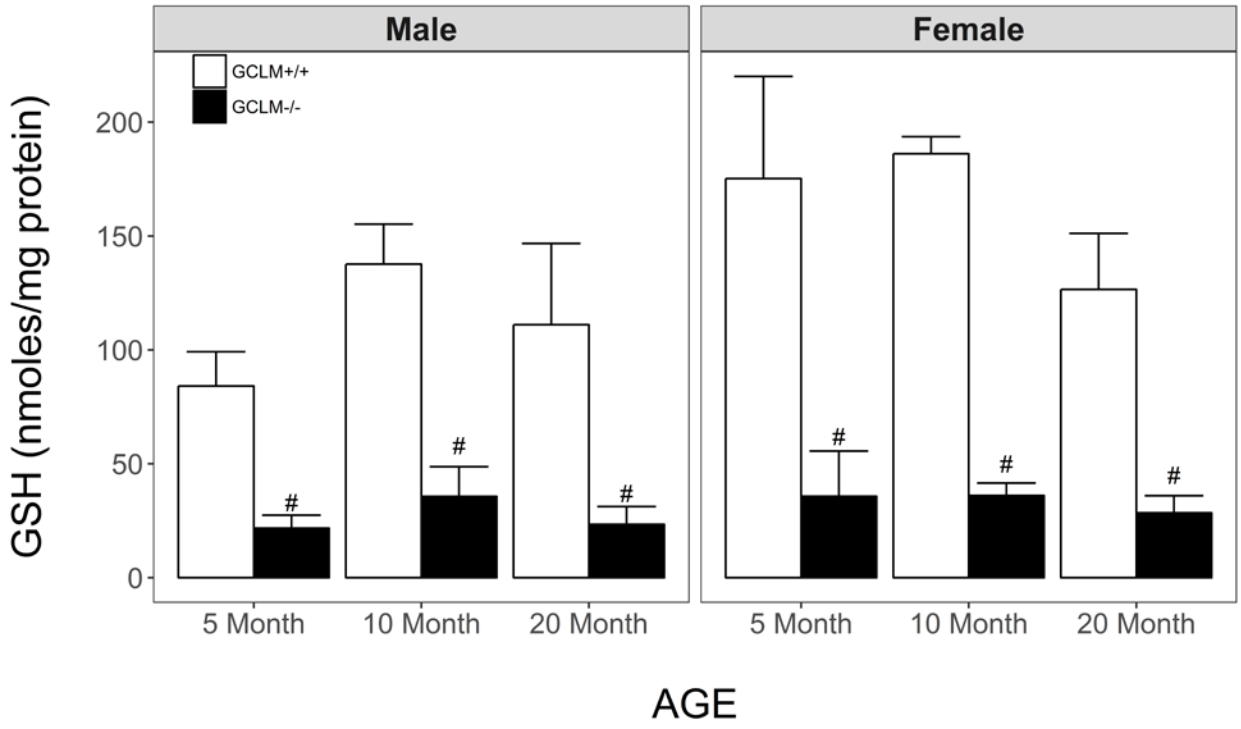

Figure 39. Effects of sex, age and genotype on liver GSH in young (5 month), adult (10 month), and old (20 month) GCLM+/+ and GCLM-/- mice. Each value represents the mean + SEM of (n = 6) mice. # $p < 0.05$ compared to age and sex-matched GCLM+/+ mice.

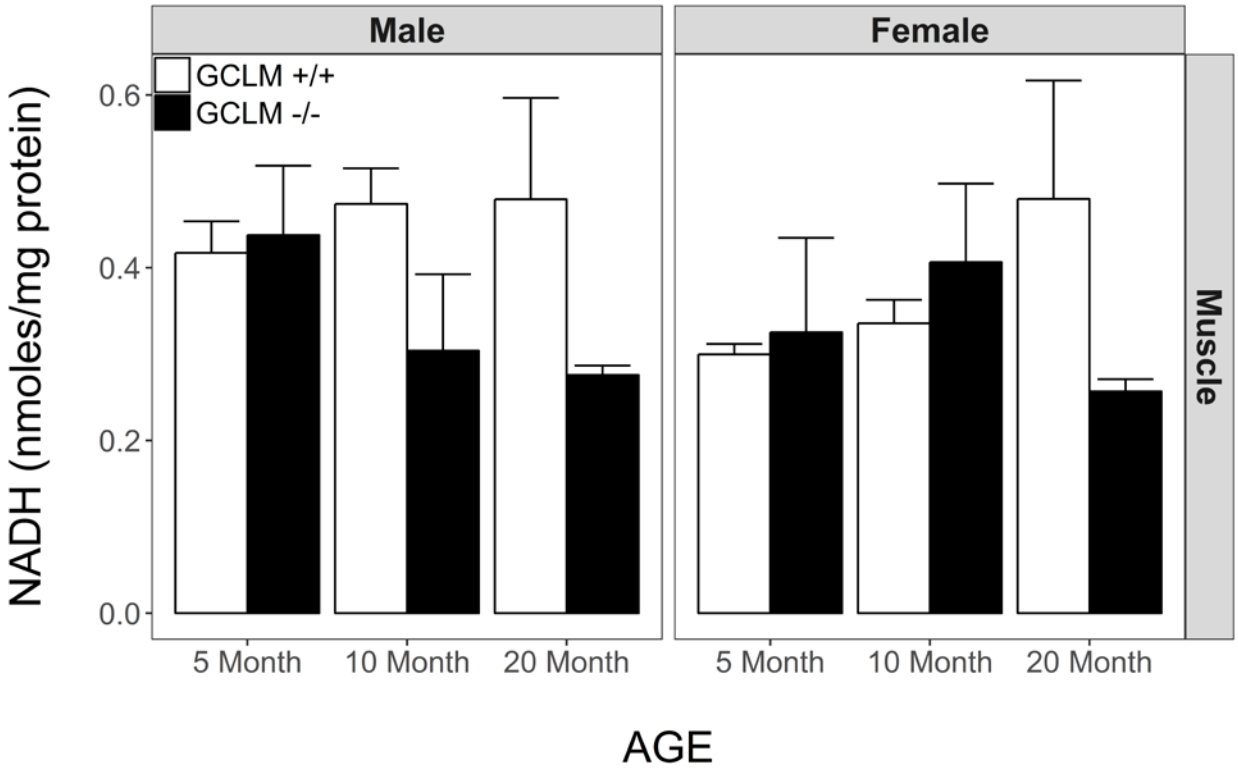

Figure 40. Effects of sex, age and genotype on skeletal muscle NADH in young (5 month), adult (10 month), and old (20 month) GCLM+/+ and GCLM-/- mice. Each value represents the mean + SEM of (n = 3) mice.

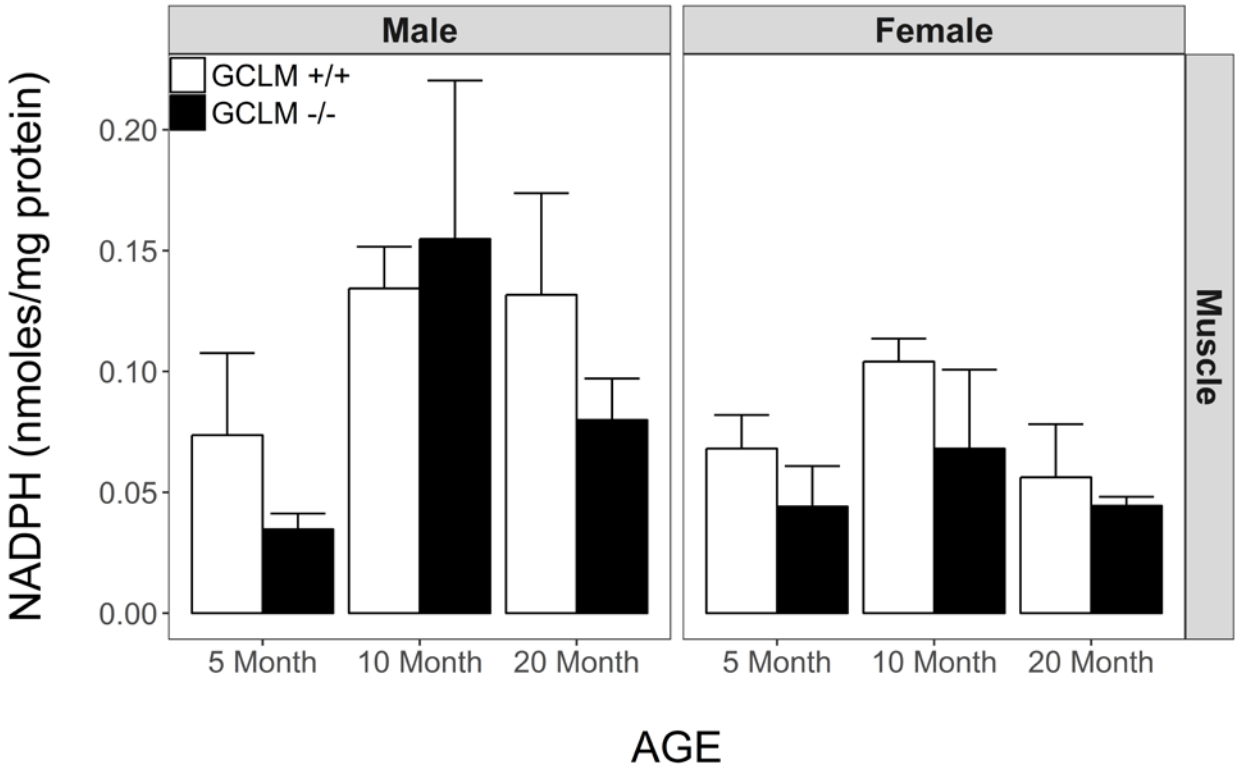

Figure 41. Effects of sex, age and genotype on skeletal muscle NADPH in young (5 month), adult (10 month), and old (20 month) GCLM+/+ and GCLM-/- mice. Each value represents the mean + SEM of (n = 3) mice.

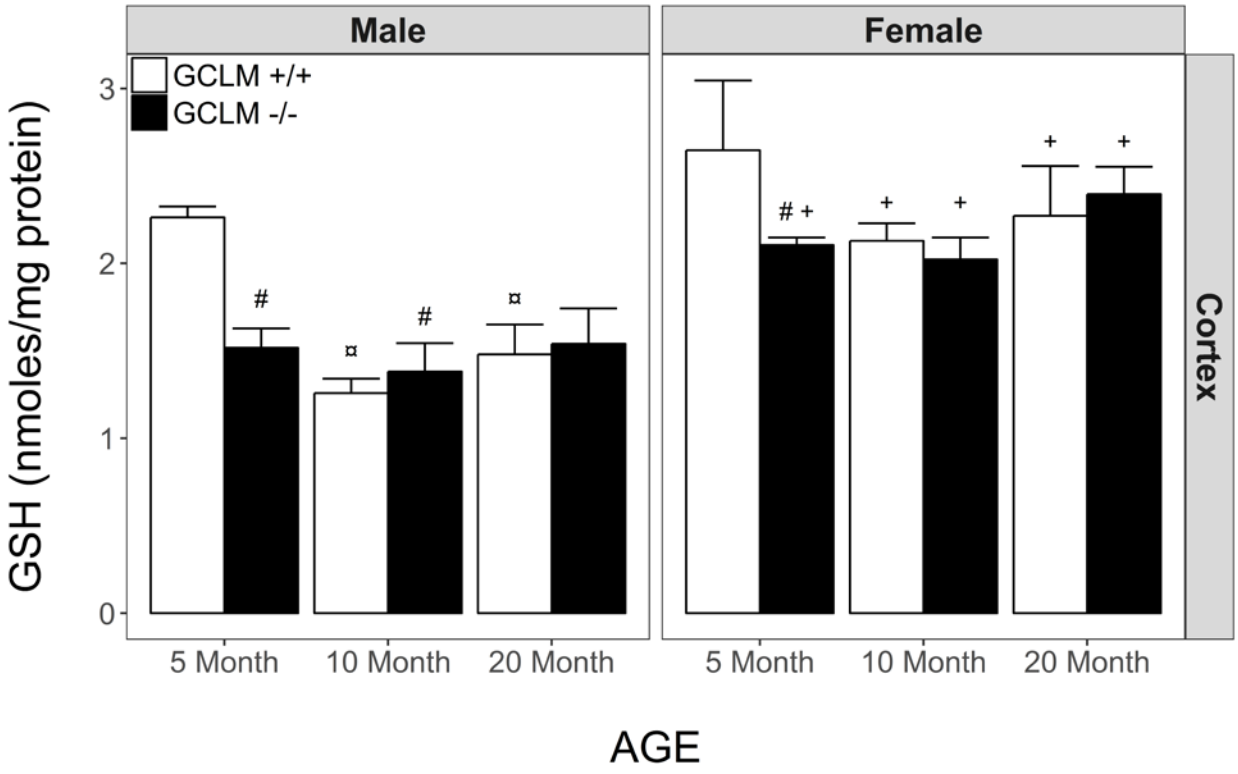

Figure 42. Effects of sex, age and genotype on cortex GSH in young (5 month), adult (10 month), and old (20 month) GCLM+/+ and GCLM-/- mice. Each value represents the mean + SEM of (n = 3) mice. ¤ $p < 0.05$ compared to genotype and sex-matched young; # $p < 0.05$ compared to age and sex-matched GCLM+/+ mice; + $p < 0.05$ compared to age and genotype-matched males.

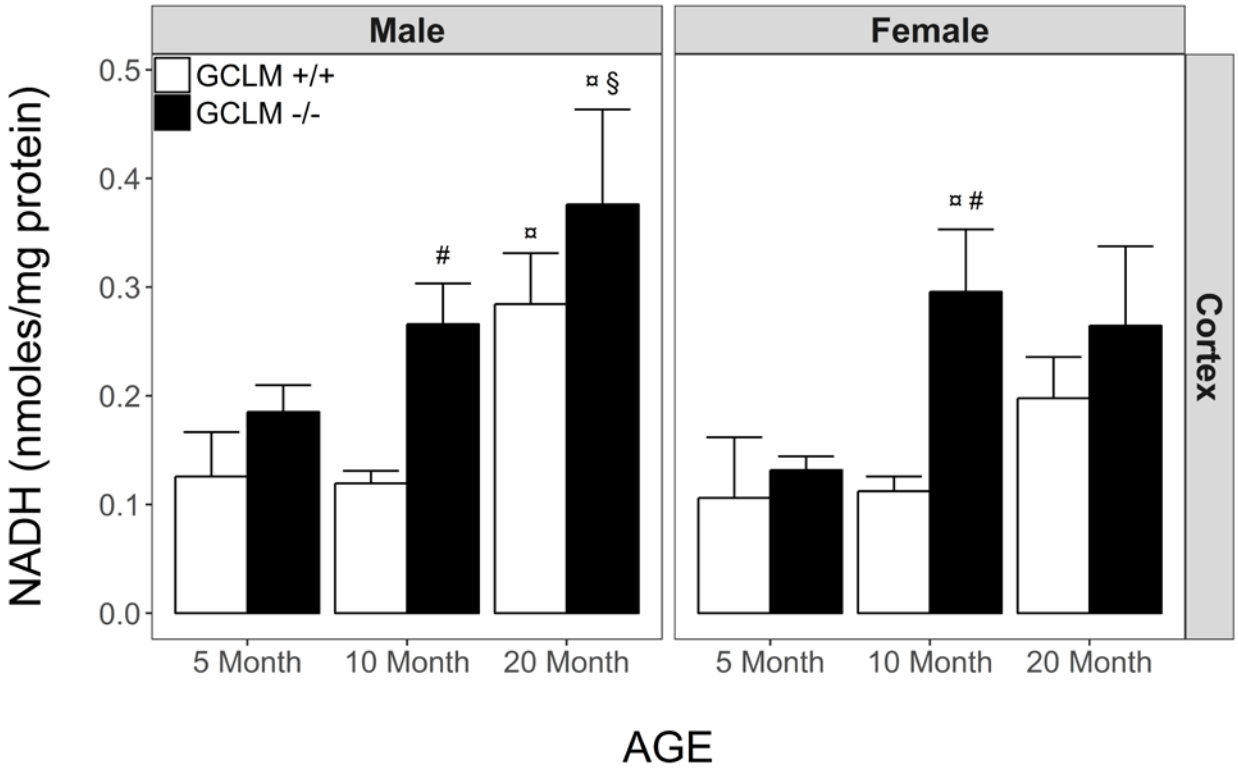

Figure 43. Effects of sex, age and genotype on cortex NADH in young (5 month), adult (10 month), and old (20 month) GCLM+/+ and GCLM-/- mice. Each value represents the mean + SEM of (n = 3) mice. ¤ $p < 0.05$ compared to genotype and sex-matched young; § $p < 0.05$ compared to genotype and sex-matched 10 adult; # $p < 0.05$ compared to age and sex-matched GCLM+/+ mice.

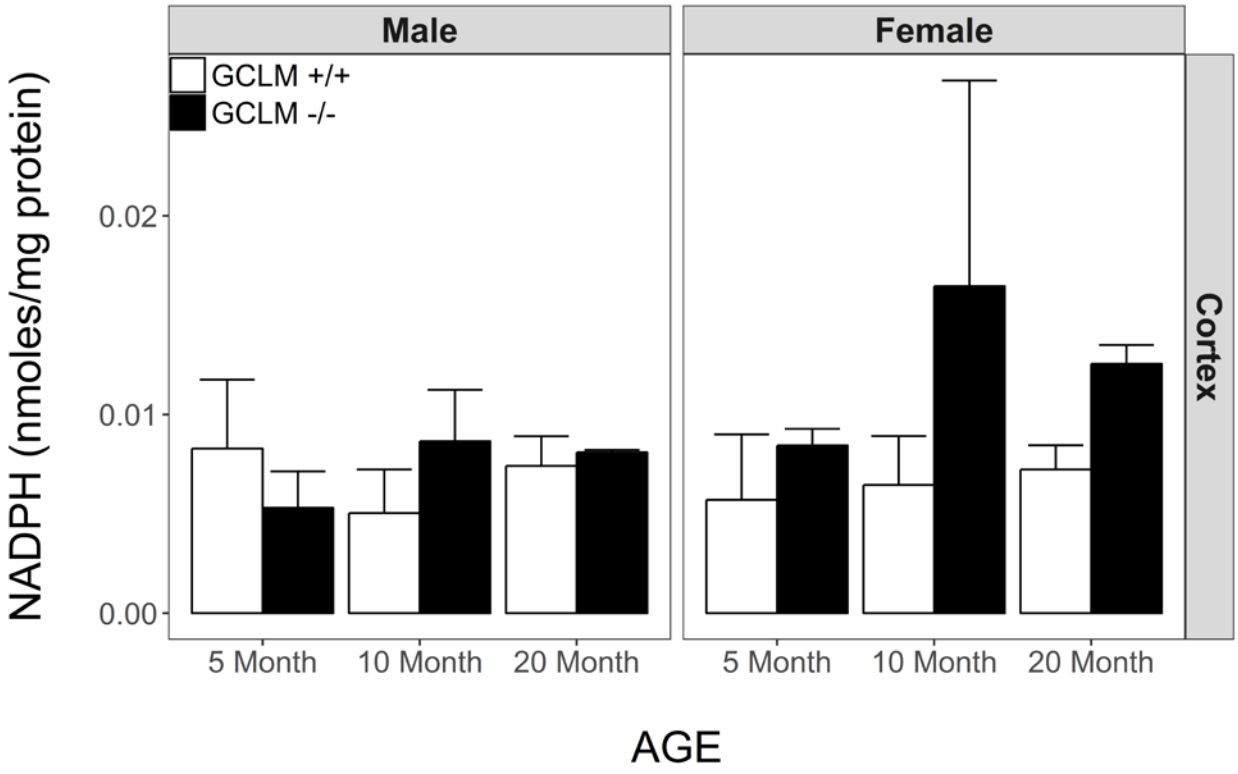

Figure 44. Effects of sex, age and genotype on cortex NADPH in young (5 month), adult (10 month), and old (20 month) GCLM+/+ and GCLM-/- mice. Each value represents the mean + SEM of (n = 3) mice.

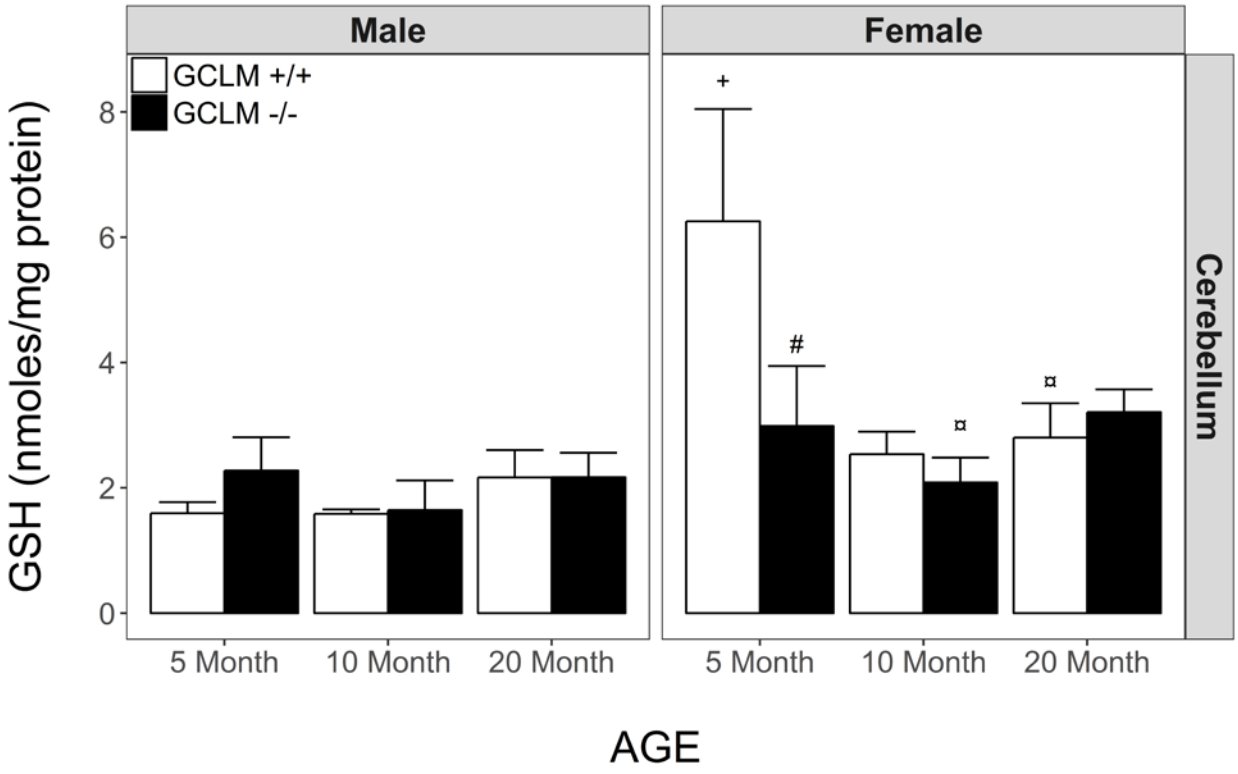

Figure 45. Effects of sex, age and genotype on cerebellum GSH in young (5 month), adult (10 month), and old (20 month) GCLM+/+ and GCLM-/- mice. Each value represents the mean + SEM of (n = 3) mice. ¤ $p < 0.05$ compared to genotype and sex-matched young; # $p < 0.05$ compared to age and sex-matched GCLM+/+ mice; + $p < 0.05$ compared to age and genotype-matched males.

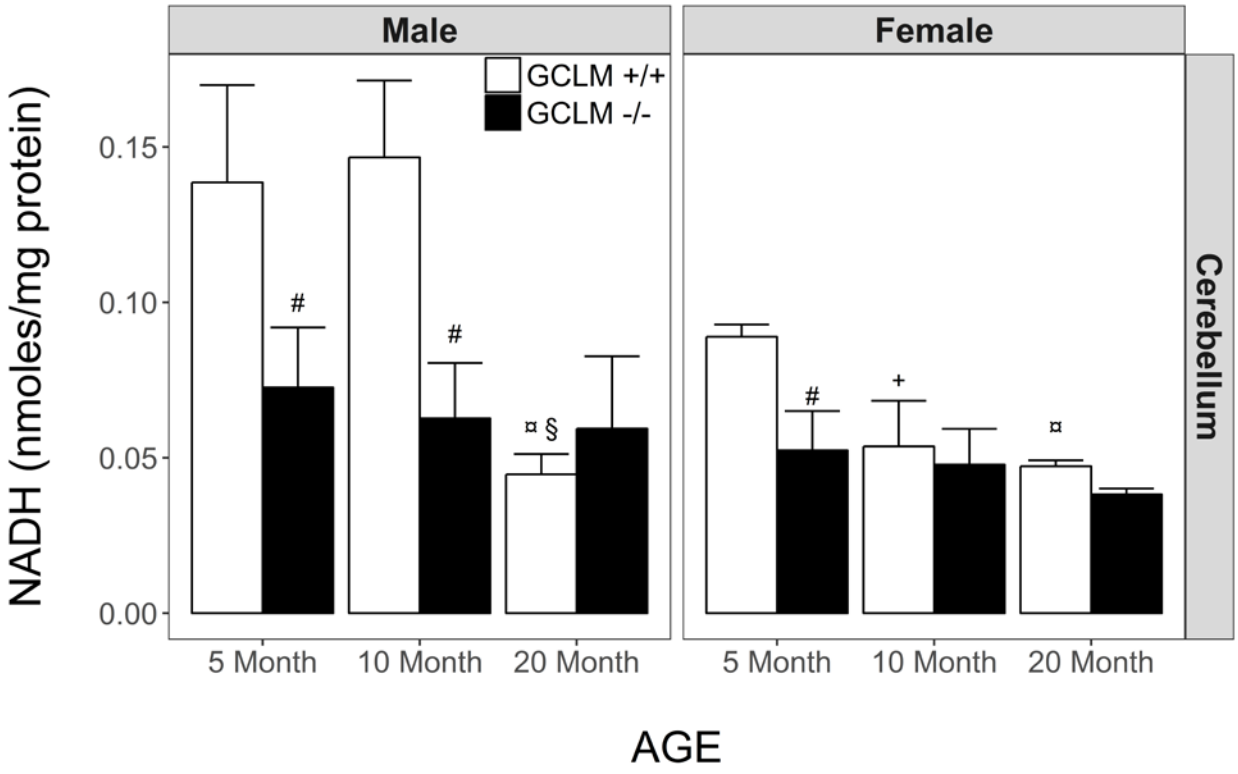

Figure 46. Effects of sex, age and genotype on cerebellum NADH in young (5 month), adult (10 month), and old (20 month) GCLM+/+ and GCLM-/- mice. Each value represents the mean + SEM of (n = 3) mice. ¤ $p < 0.05$ compared to genotype and sex-matched young; § $p < 0.05$ compared to genotype and sex-matched 10 adult; # $p < 0.05$ compared to age and sex-matched GCLM+/+ mice; + $p < 0.05$ compared to age and genotype-matched males.

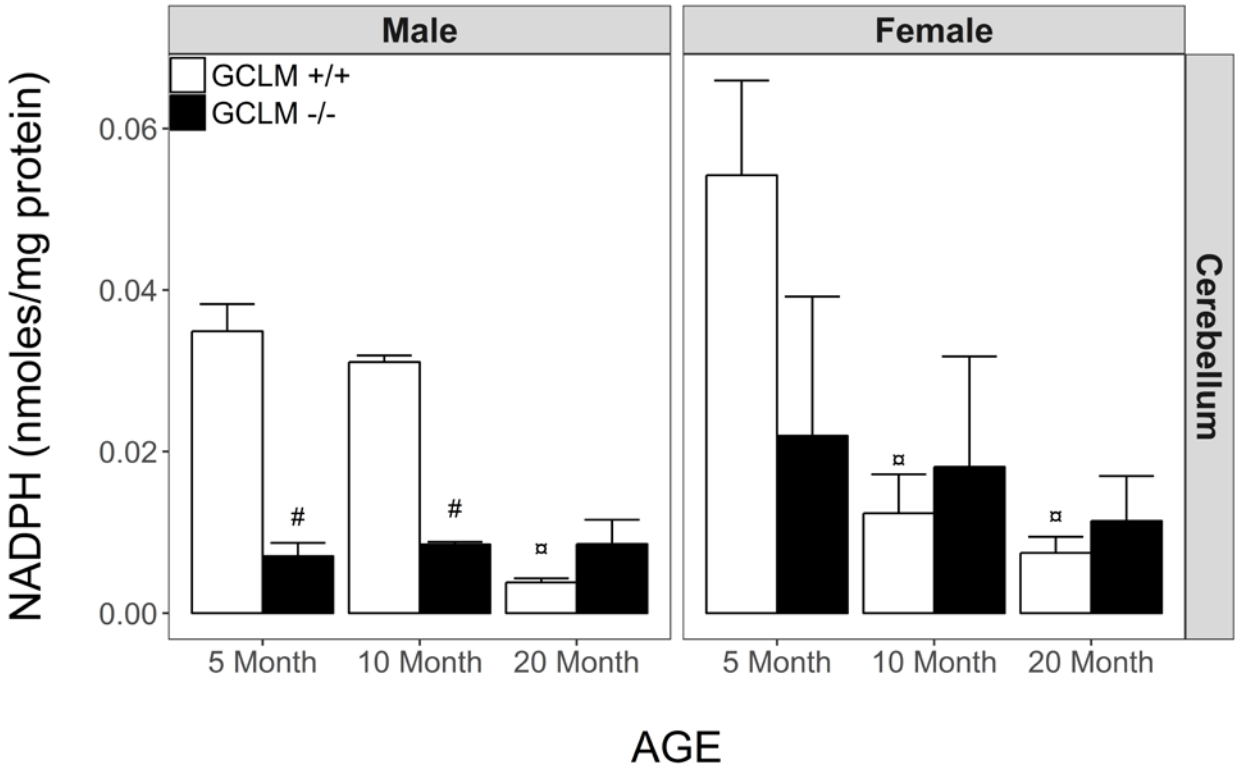

Figure 47. Effects of sex, age and genotype on cerebellum NADPH in young (5 month), adult (10 month), and old (20 month) GCLM+/+ and GCLM-/- mice. Each value represents the mean + SEM of (n = 3) mice. ¤ $p < 0.05$ compared to genotype and sex-matched young; # $p < 0.05$ compared to age and sex-matched GCLM+/+ mice.

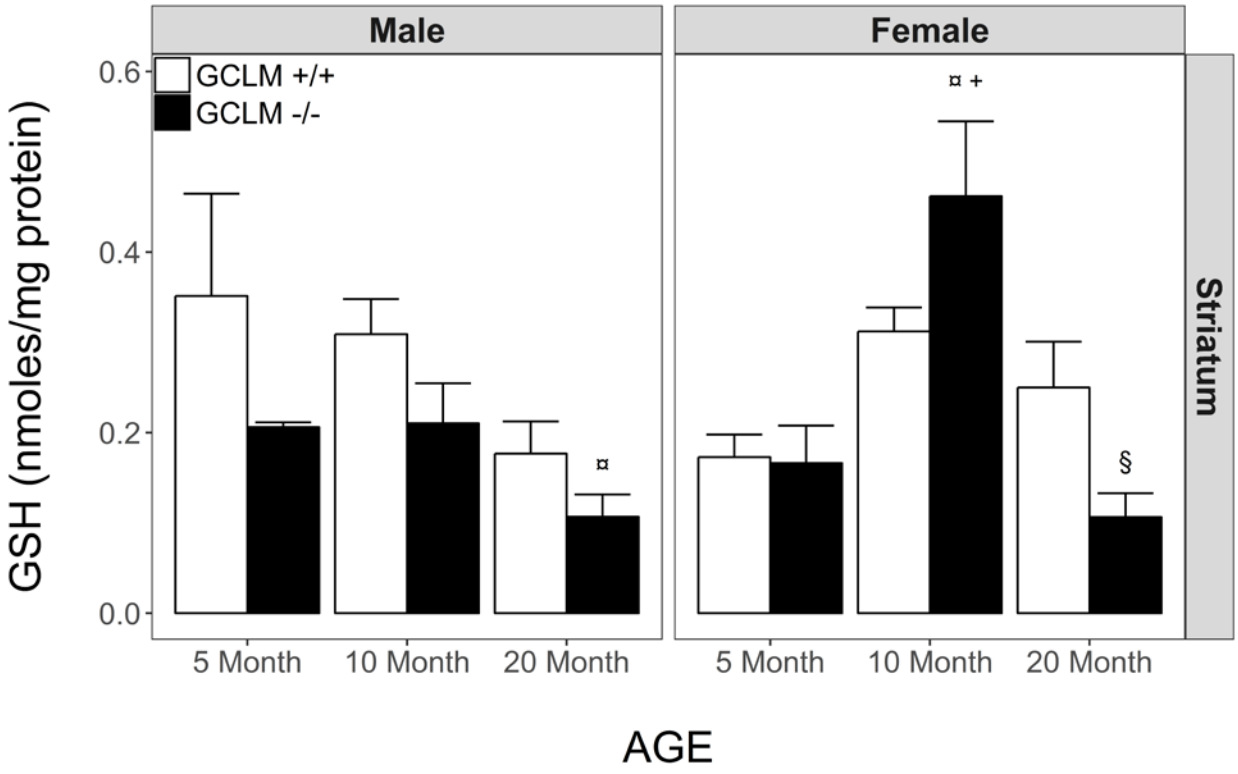

Figure 48. Effects of sex, age and genotype on striatum GSH in young (5 month), adult (10 month), and old (20 month) GCLM+/+ and GCLM-/- mice. Each value represents the mean + SEM of (n = 3) mice. ¤ $p < 0.05$ compared to genotype and sex-matched young; § $p < 0.05$ compared to genotype and sex-matched 10 adult.

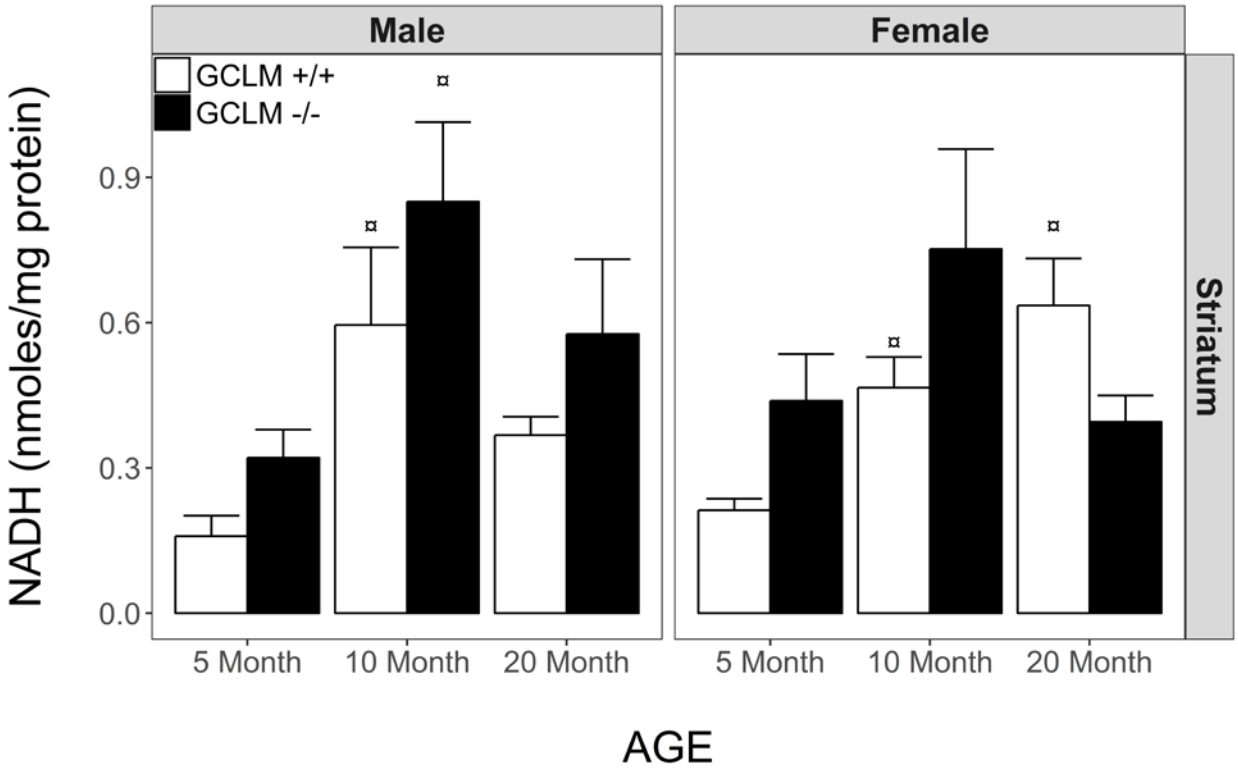

Figure 49. Effects of sex, age and genotype on striatum NADH in young (5 month), adult (10 month), and old (20 month) GCLM+/+ and GCLM-/- mice. Each value represents the mean + SEM of (n = 3) mice. ¤ $p < 0.05$ compared to genotype and sex-matched young.

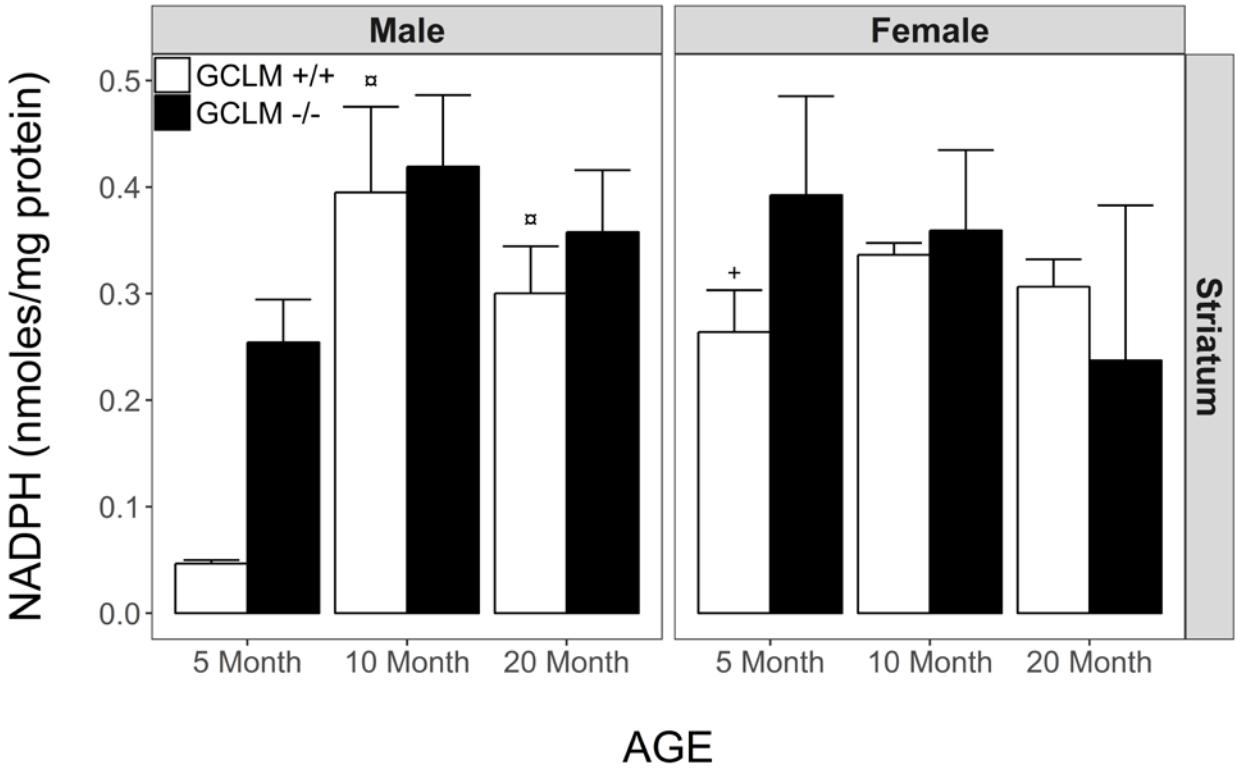

Figure 50. Effects of sex, age and genotype on striatum NADPH in young (5 month), adult (10 month), and old (20 month) GCLM+/+ and GCLM-/- mice. Each value represents the mean + SEM of (n = 3) mice. ¤ $p < 0.05$ compared to genotype and sex-matched young; + $p < 0.05$ compared to age and genotype-matched males.

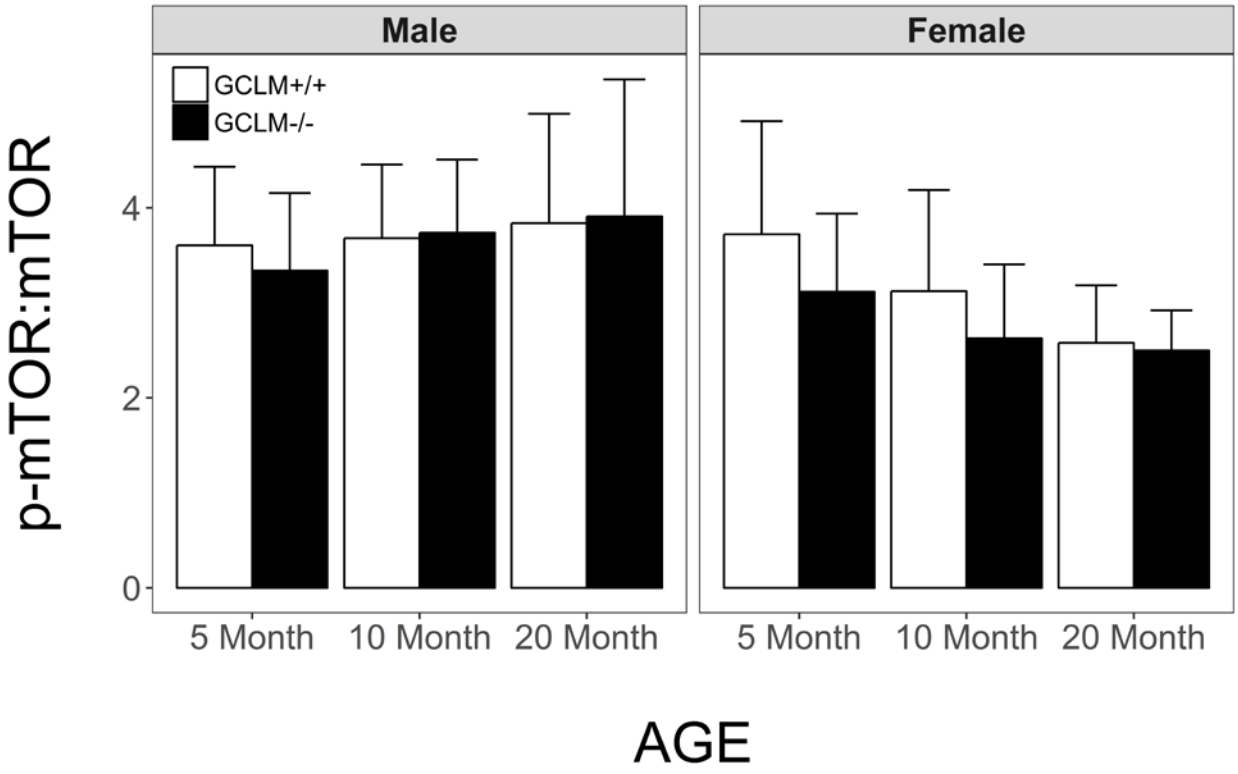

Figure 51. Effects of sex, age and genotype on skeletal muscle mTOR activation in young (5 month), adult (10 month), and old (20 month) GCLM+/+ and GCLM-/- mice. Each value represents the mean + SEM of (n = 6) mice.

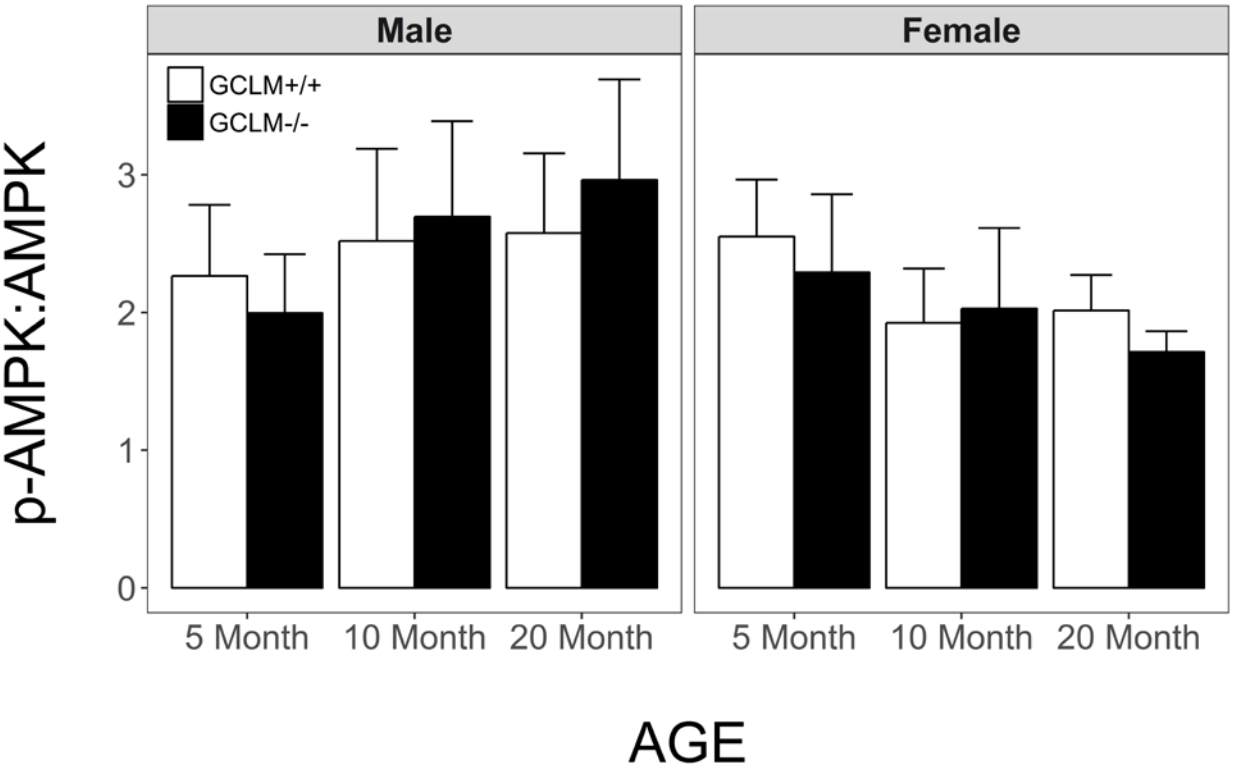

Figure 52. Effects of sex, age and genotype on skeletal muscle AMPK activation in young (5 month), adult (10 month), and old (20 month) GCLM+/+ and GCLM-/- mice. Each value represents the mean + SEM of (n = 6) mice.

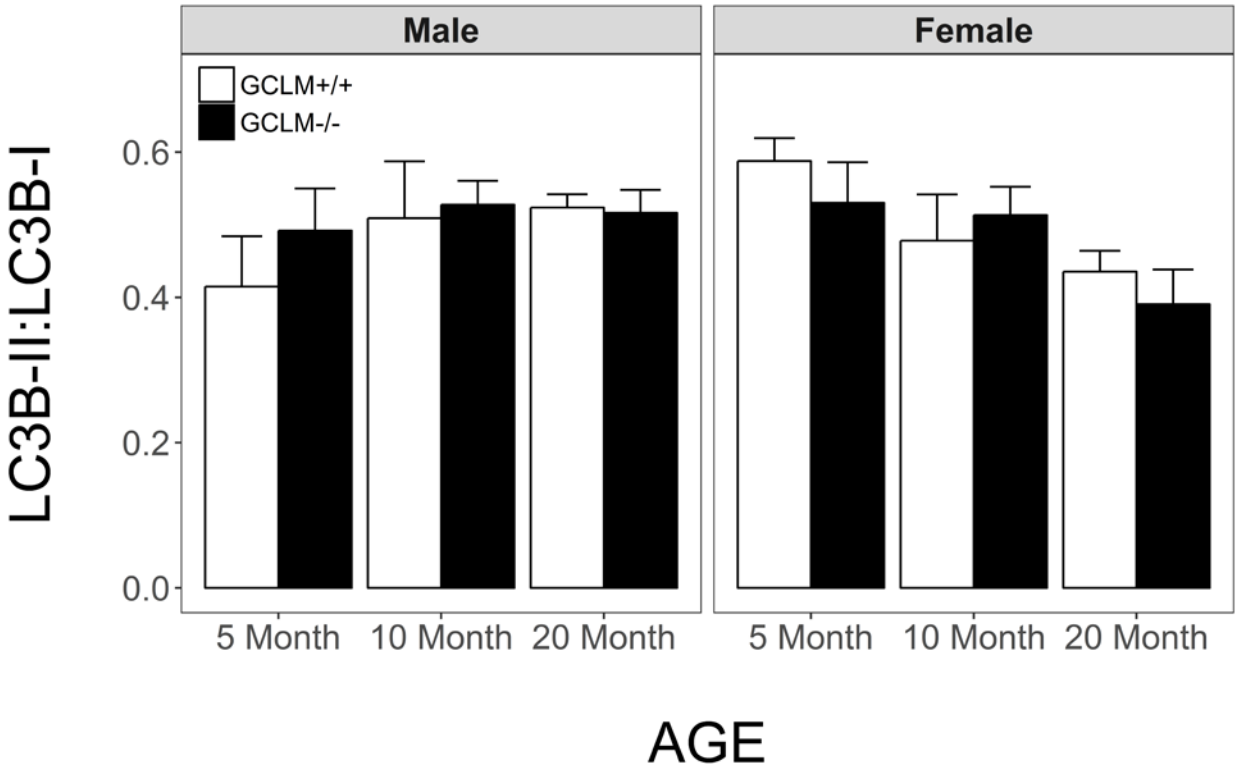

Figure 53. Effects of sex, age and genotype on skeletal muscle autophagy in young (5 month), adult (10 month), and old (20 month) GCLM+/+ and GCLM-/- mice. Each value represents the mean + SEM of (n = 6) mice.

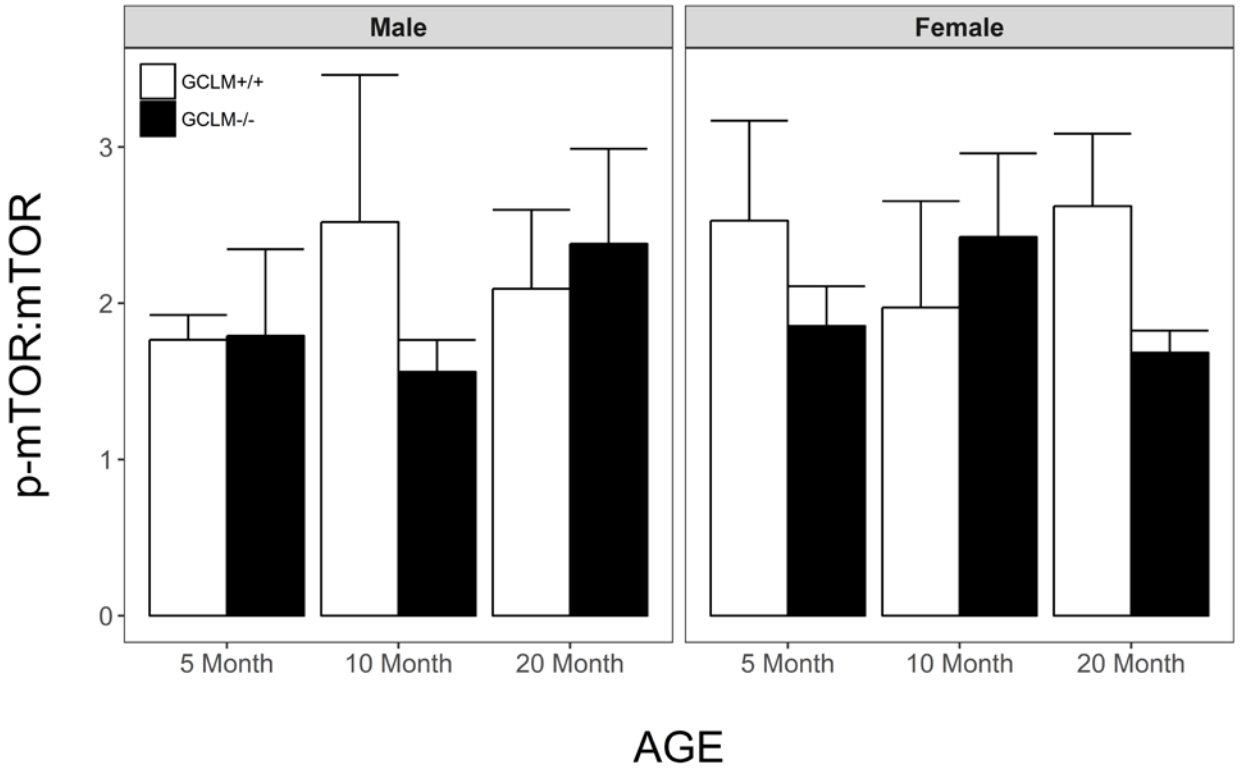

Figure 54. Effects of sex, age and genotype on cortex mTOR activation in young (5 month), adult (10 month), and old (20 month) GCLM+/+ and GCLM-/- mice. Each value represents the mean + SEM of (n = 6) mice.

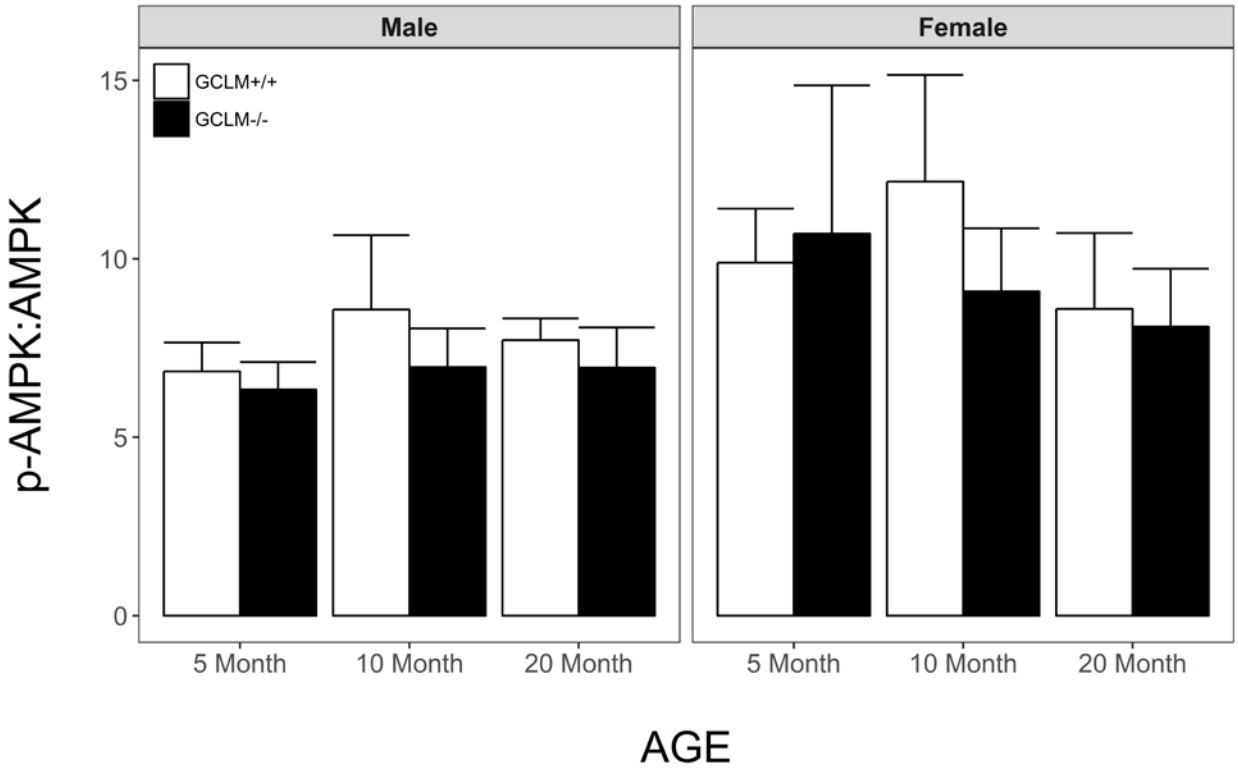

Figure 55. Effects of sex, age and genotype on cortex AMPK activation in young (5 month), adult (10 month), and old (20 month) GCLM+/+ and GCLM-/- mice. Each value represents the mean + SEM of (n = 6) mice.

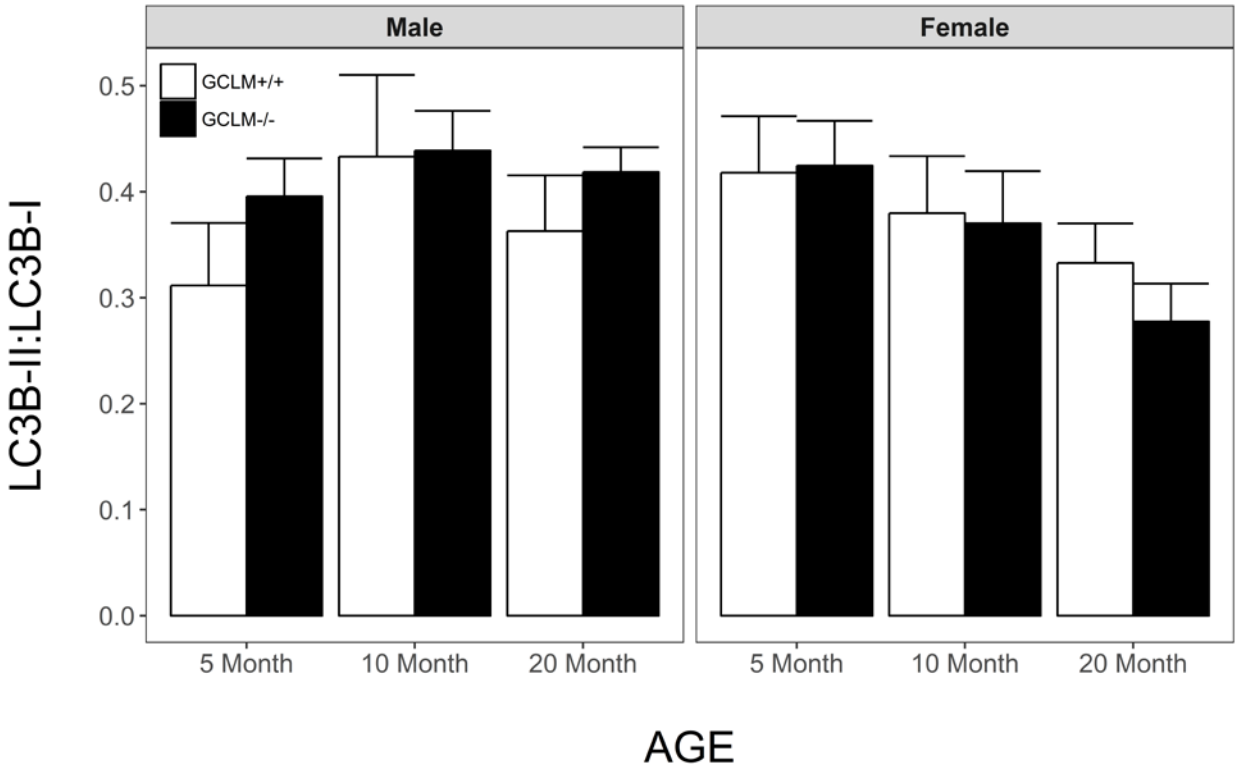

Figure 56. Effects of sex, age and genotype on cortex autophagy in young (5 month), adult (10 month), and old (20 month) GCLM+/+ and GCLM-/- mice. Each value represents the mean + SEM of (n = 6) mice.

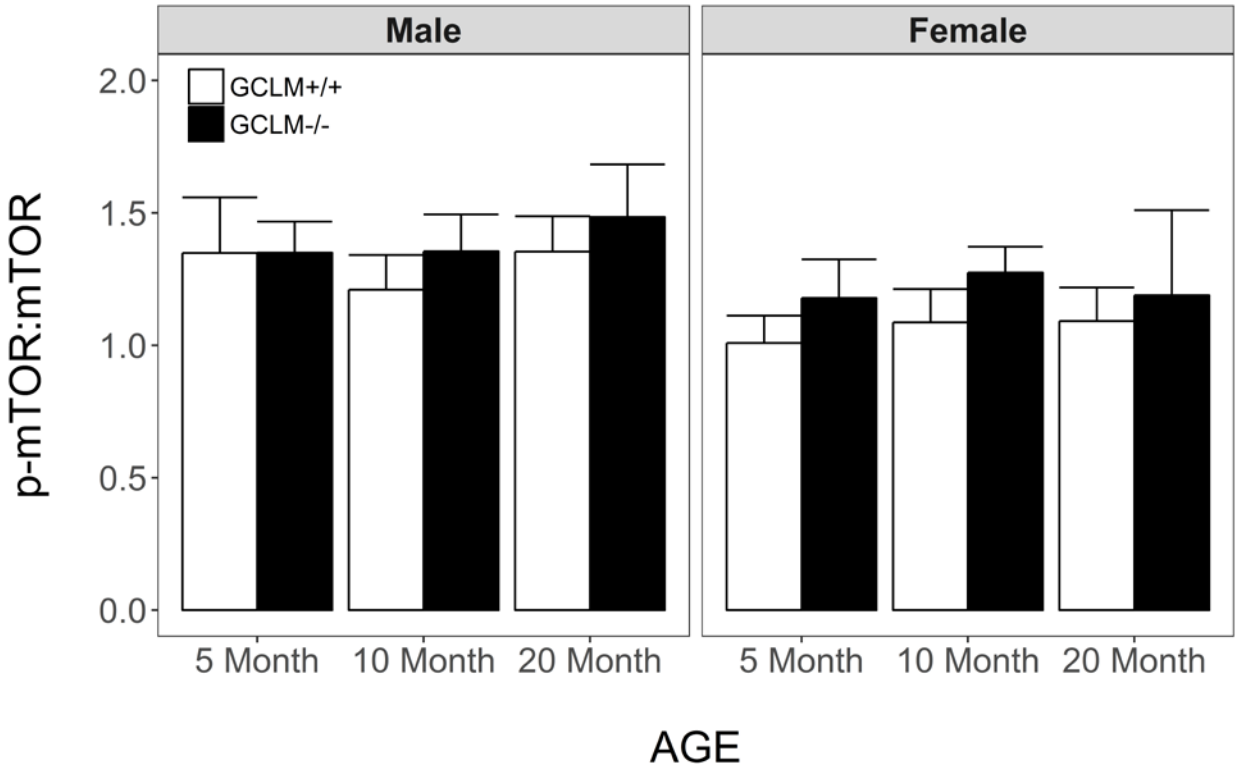

Figure 57. Effects of sex, age and genotype on cerebellum mTOR activation in young (5 month), adult (10 month), and old (20 month) GCLM+/+ and GCLM-/- mice. Each value represents the mean + SEM of (n = 6) mice.

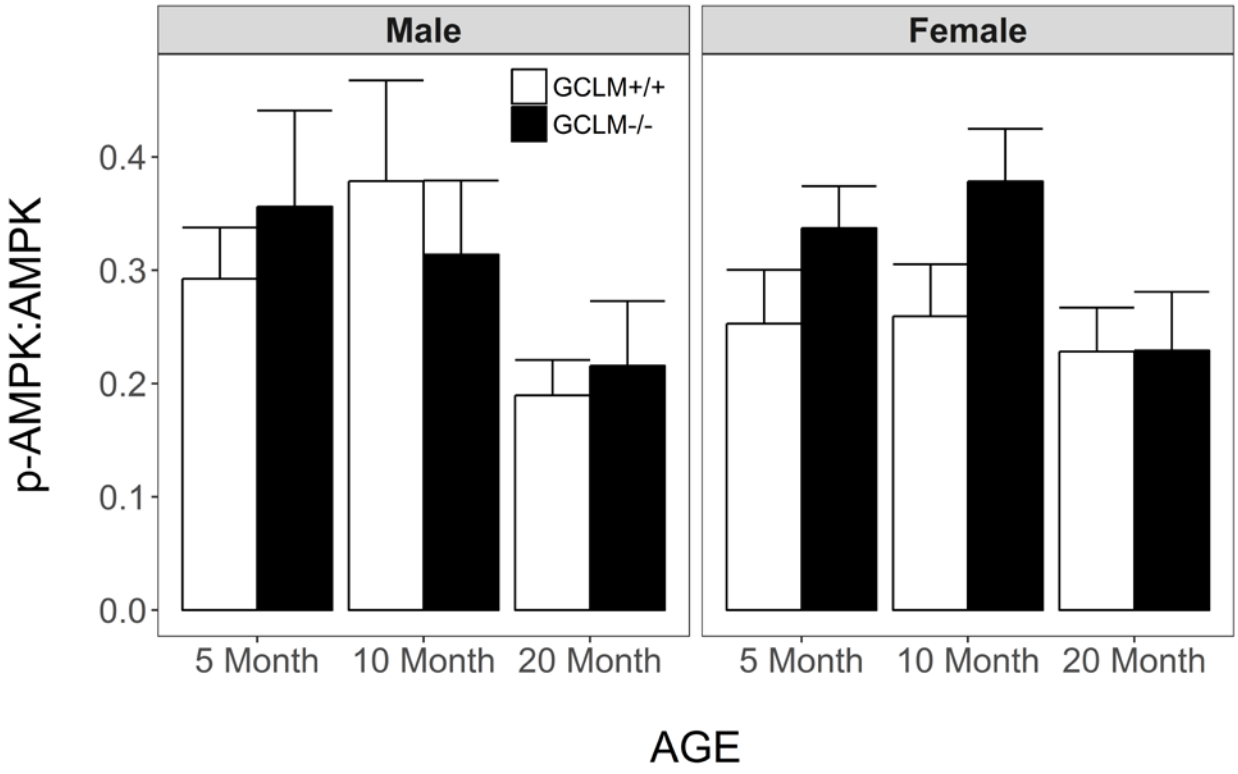

Figure 58. Effects of sex, age and genotype on cerebellum AMPK activation in young (5 month), adult (10 month), and old (20 month) GCLM+/+ and GCLM-/- mice. Each value represents the mean + SEM of (n = 6) mice.

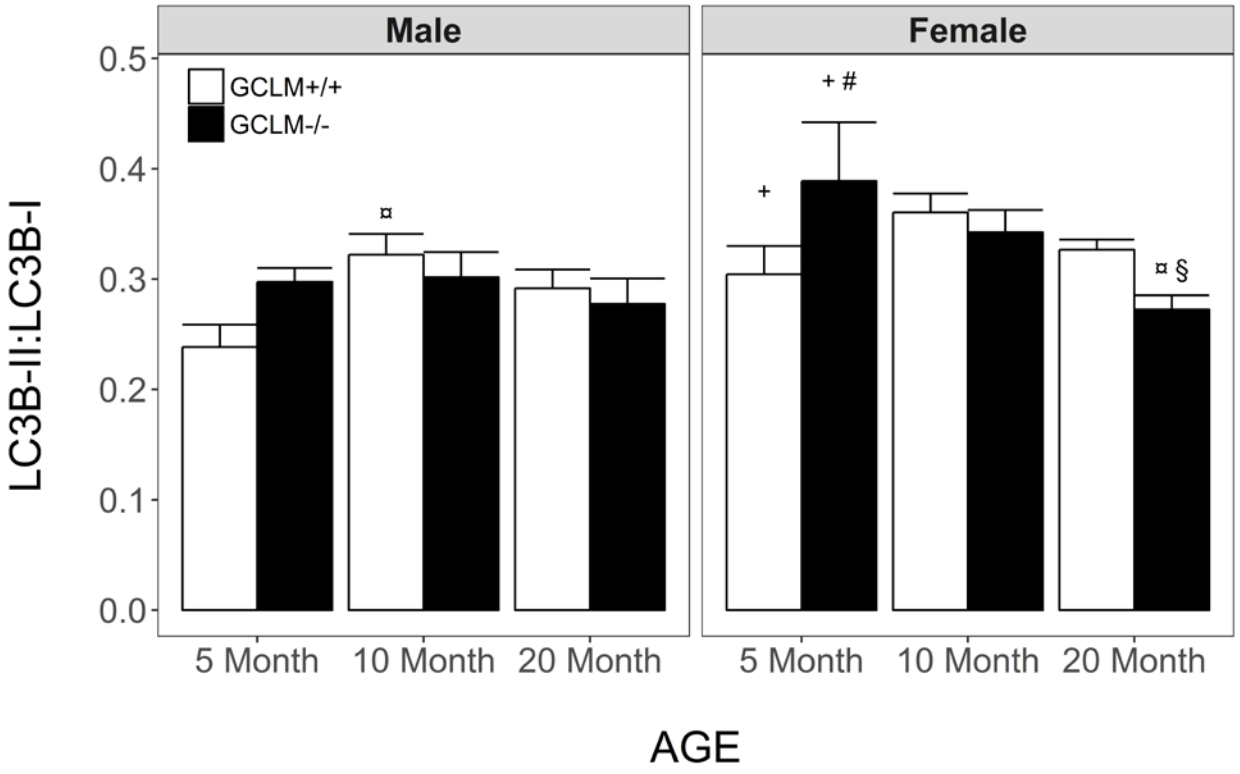

Figure 59. Effects of sex, age and genotype on cerebellum autophagy in young (5 month), adult (10 month), and old (20 month) GCLM+/+ and GCLM-/- mice. Each value represents the mean + SEM of (n = 6) mice. ¤ $p < 0.05$ compared to genotype and sex-matched young; § $p < 0.05$ compared to genotype and sex-matched 10 adult; # $p < 0.05$ compared to age and sex-matched GCLM+/+ mice; + $p < 0.05$ compared to age and genotype-matched males.

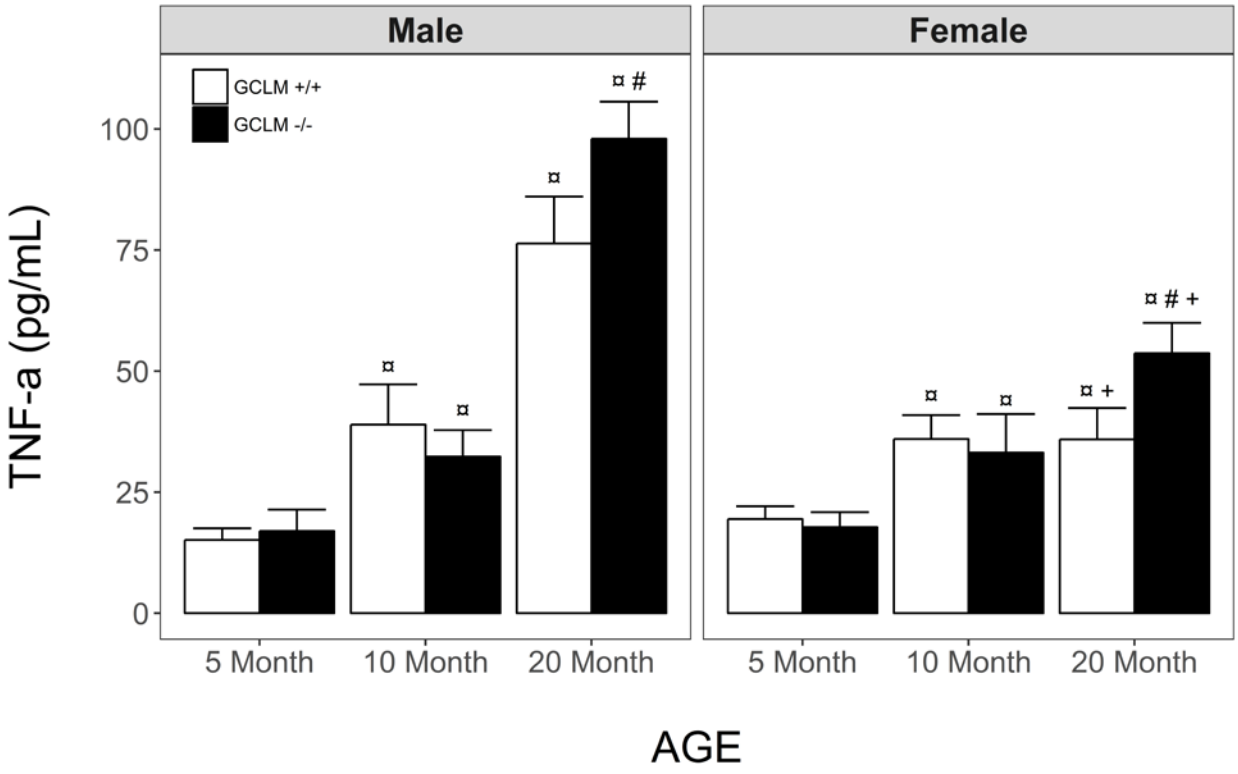

Figure 60. Effects of sex, age and genotype on plasma TNF-a in young (5 month), adult (10 month), and old (20 month) GCLM+/+ and GCLM-/- mice. Each value represents the mean + SEM of (n = 6) mice. ¤ $p < 0.05$ compared to genotype and sex-matched young; # $p < 0.05$ compared to age and sex-matched GCLM+/+ mice; + $p < 0.05$ compared to age and genotype-matched males.

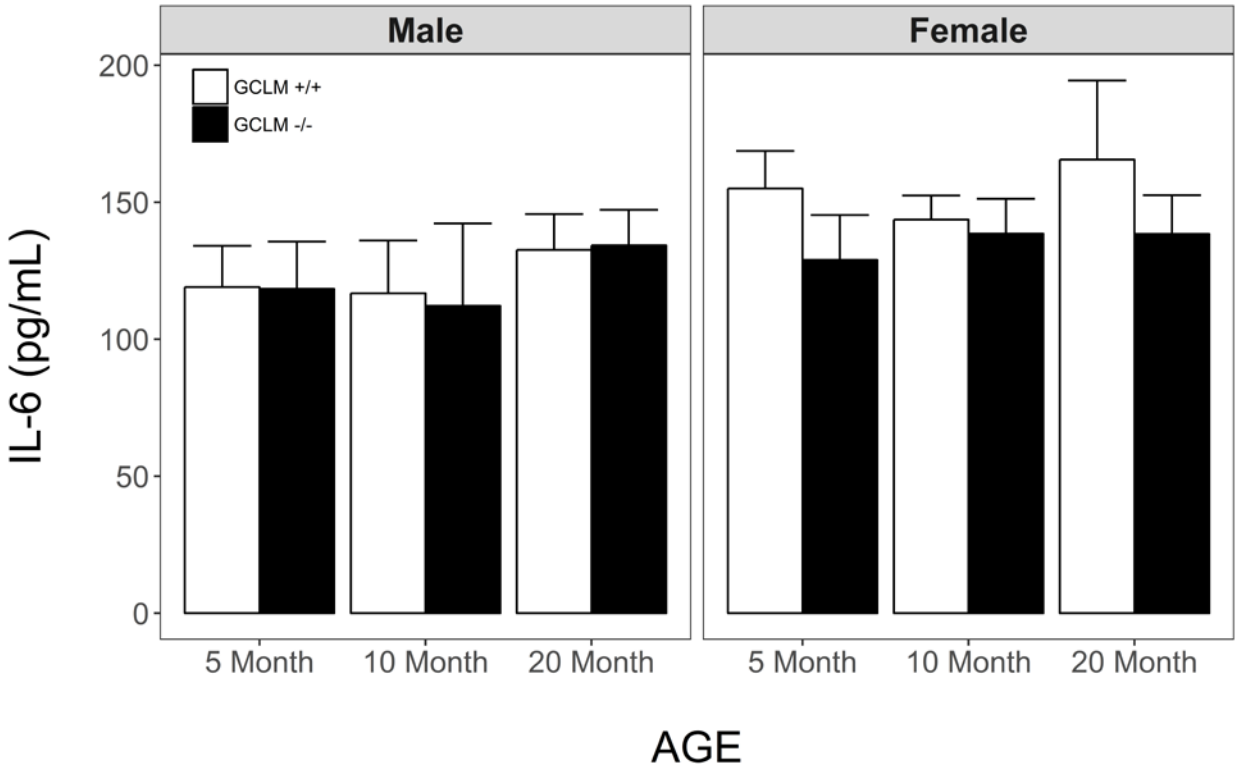

Figure 61. Effects of sex, age and genotype on plasma IL-6 in young (5 month), adult (10 month), and old (20 month) GCLM+/+ and GCLM-/- mice. Each value represents the mean + SEM of (n = 6) mice.

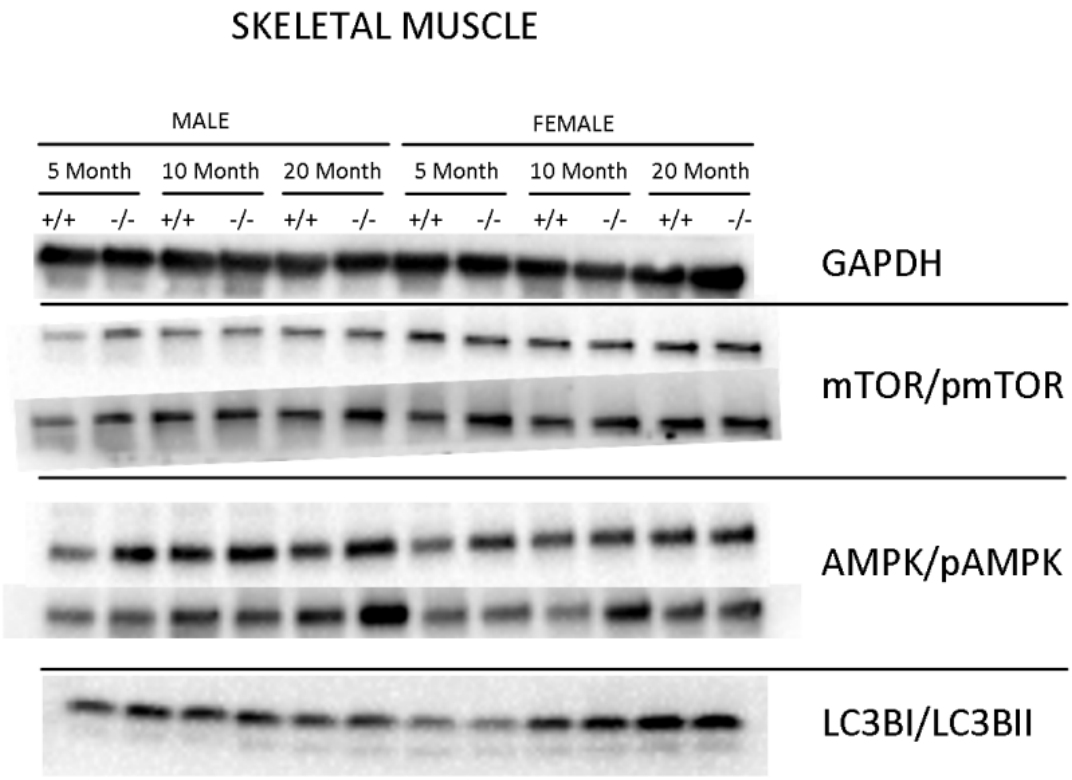

Figure 62. Representative western blots for skeletal muscle in young (5 month), adult (10 month), and old (20 month) GCLM+/+ and GCLM-/- mice.

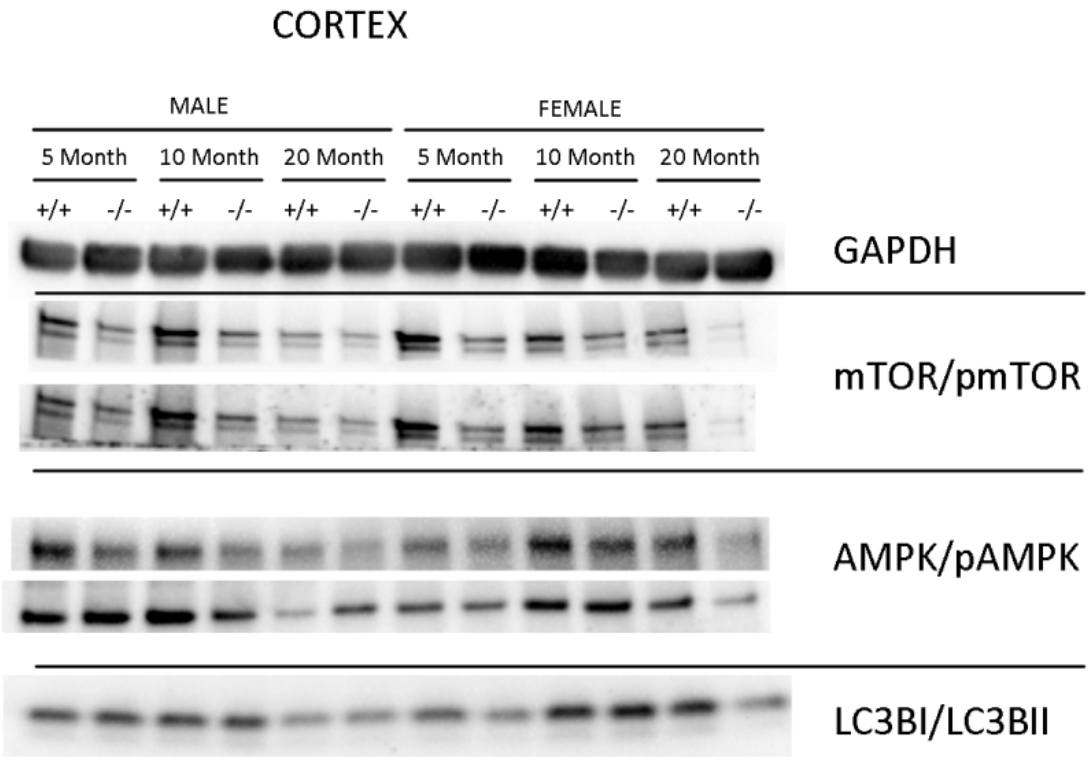

Figure 63. Representative western blots for cortex in young (5 month), adult (10 month), and old (20 month) GCLM+/+ and GCLM-/- mice.

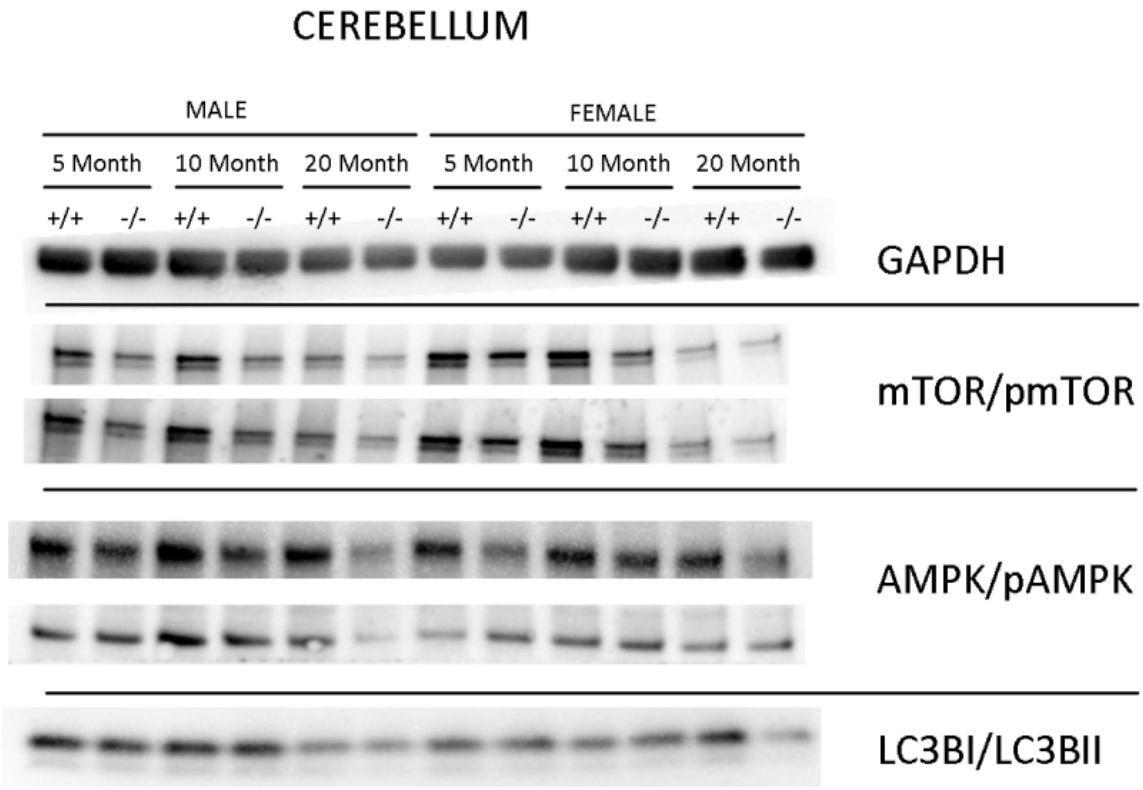

Figure 64. Representative western blots for cerebellum in young (5 month), adult (10 month), and old (20 month) GCLM+/+ and GCLM-/- mice.

CHAPTER IV

DISCUSSION

Aging is associated with a gradual decline in total function eventually leading to mortality of the individual. These functional declines manifest due to deficits in peripheral tissues such as the heart and skeletal muscle as well as brain deficits in key regions such as the cortex, cerebellum, striatum, and hippocampus. Although key changes are observable in these brain regions and peripheral tissues, the underlying causal mechanisms “upstream” of these changes is still under active investigation. Previous literature had suggested that increased oxidative stress concurrent with increased oxidative damage was the underlying mechanism behind these age-related deficits, but a substantial amount of current literature suggests this is not the case. More recent data suggests a role of redox stress, rather than simply oxidative stress, as altering cell signaling and function leading to systemic functional decline. Preliminary data of chronic redox dysregulation in drosophila and acute redox dysregulation in mice suggests that organisms will have shorter lifespans and impaired function with redox dysregulation, but this theory had not been tested in rodent models across their lifespan. Furthermore, the redox stress theory postulates that alterations in redox status throughout the lifespan lead to redox signaling dysregulation and loss of function at the cellular level, ultimately leading to system-level dysfunction, declines in overall function, and increased risk of mortality. The purpose of this study was therefore to examine the effects of redox dysregulation through impairing glutathione

production, and was expected to result in an early-aging phenotype both by shortening lifespan, an earlier onset of functional deficits, and dysregulation in redox state.

The main findings of this study were that (1) GCLM-/- males and females were lighter and had longer lifespans than the GCLM+/+, (2) GCLM-/- mice had generally improved motor function at 5 months and delayed motor function decline at 10 month, independent of body weight changes, (3) GCLM-/- mice had no major deficits in cognition, but did have decreased anxiety-related behaviors along with minor deficits in amygdala-dependent memory, (4) GCLM-/- resulted in redox state deficits across the lifespan in peripheral tissues but only sporadically in the brain (5) sexual dimorphism in motor function age-related decline for both GCLM+/+ and GCLM-/-, , (6) and age increased inflammation for males and females, but to a lesser extent in females.

The two largest phenotypic changes in GCLM-/- mice were an increase in the median and maximal lifespans concurrent with decreased body weight. Other studies in young GCLM-/- mice have reported the same body weight changes, which begin to manifest primarily by 3-4 months of age [1-3]. Importantly, these changes appear to be due primarily to changes in fat tissue, as there was approximately 60% less fat tissue with no significant difference in lean body tissue in the GCLM-/- mice compared to GCLM+/+ mice [1]. Furthermore, these researchers observed a resistance to high-fat diet induced weight gain, where GCLM+/+ mice doubled their percent body fat and GCLM-/- mice had no change in body fat or lean body mass when fed a high-fat diet. This result was confirmed in an alternative study and found that GCLM-/- mice were resistant to high-fat diet induced steatohepatitis, and had no weight gain [4]. Furthermore, GCLM-/- mice had higher oxygen consumption on a normal diet, along with increased H_2O_2 production on a normal or high-fat diet [1]. Altering GSH regeneration by knocking out

glutathione peroxidase, a key enzyme utilizing GSH to detoxify H_2O_2, in mice also leads to increased insulin sensitivity and resistance to high-fat diet induced obesity [5]. These studies highlighted a potential role for impaired redox state and increased H_2O_2 levels to positively modulate metabolic pathways and decreased fat accumulation. Given that metabolic alterations might also explain the increased longevity observed in GCLM-/- mice in a similar fashion as classical caloric restriction (CR) experiments, we sought to explore various redox-sensitive proteins related to both metabolism and increased longevity. Two key protein kinase pathways involved in caloric restriction are AMPK and mTOR, where CR elicits many beneficial effects by increasing AMPK activation and concurrently decreasing mTOR activation, as well as modulating autophagy of damaged cells[6]. While in the present study we did not observe consistent changes in mTOR, AMPK, or autophagy in any tissues at our chosen ages of 5, 10, and 20 months, many other studies have seen changes in these key players of metabolic signaling under similar conditions.

The observed body weight changes in the present study could occur through redox-sensitive signaling alterations in metabolic proteins. Interestingly, decreased expression of superoxide dismutase (SOD), which actually leads to a minor increase in oxidative stress, can increase lifespan in worms, as a potential form of adaptive homeostasis [7, 8]. Additionally, in worms, higher levels of dietary glucose decrease lifespan, while limited dietary glucose led to enhanced mitochondrial respiration, increased oxidative stress, and extended lifespan. However, these benefits are lost when the worm analogue of adenosine monophosphate-activated protein kinase (AMPK), a key protein in energy metabolism, is disrupted, highlighting the importance of this critical nutrient and stress sensor [9]. Another study in worms revealed that the oxidative stressor paraquat (PQ) at low levels increased lifespan [8], and PQ at the same concentration

activates AMPK [10]. In these cases, increased ROS led to a beneficial effect, and is potentially mediated via redox-dependent activation of AMPK. Additionally, the deletion of the target of rapamyacin (TOR) protein kinase, a negative regulator of AMPK, in yeast extends lifespan, although cellular ROS is interestingly decreased even without the SOD gene [11]. Finally, AMPK was found to be activated in GCLM-/- mice, concurrent with increased nuclear factor-erythroid 2–related factor 2 (NRF-2) genes a master regulator of various antioxidant genes, highlighting a connection between redox stress, AMPK activation, and a primary protective pathway [3]. AMPK activation has many potential benefits, including increase fatty acid oxidation with a concurrent decrease in lipid accumulation, increased antioxidant defense through activation of NRF2, increased mitochondrial biogenesis through PGC1-a, and increased autophagy [3, 12].

Similarly, buthionine sulfoximine (BSO), a drug that impairs GCLM function, treatment led to higher PGC-1a expression, the master regulator of mitochondrial biogenesis. This specifically highlights the role of GSH and GCL in redox-regulated signaling cascades [13]. BSO treatment in 3 month old mice undergoing 8 weeks of high fat diet treatment actually also resulted in a loss of fat mass and overall body weight, and limited the accumulation of body weight or fat, similarly to the GCLM-/- mice [14]. Glucose and insulin sensitivity were maintained in BSO-treated mice on high fat diet, while GSH levels in circulation and in the liver were lower in BSO-treated mice [14]. Thus there is a similar result in mouse energy metabolism and redox state changes whether GSH is disrupted acutely or long-term with GCLM-/-. Given the importance of GSH in maintaining defense and signaling with H_2O_2, we further examined how H_2O_2 can affect these redox-sensitive proteins.

Both in vitro hypoxia and low levels of H_2O_2 (100 uM) induce phosphorylation of acetyl-CoA carboxylase (ACC) which is limited by knockout of liver kinase B1 (LKB1) and completely prevented in AMPK knockout mice. Thus the signaling cascade appears to occur as a result of H_2O_2-induced redox stress, requires LKB1, and activates the downstream effectors AMPK to activate ACC [15]. Although H_2O_2 can increase the AMP/ATP ratio, the activation of AMPK and ACC can occur independently of shifts in energy status. Importantly, micromolar levels of H_2O_2 can affect AMPK and the mammalian target of rapamycin (mTOR) signaling, while ROS can lead to the phosphorylation of protein kinases such as LKB1 and calcium/calmodulin dependent protein kinase 2 (CaMKK2) to activate AMPK, leading to increased AMPK signaling without direct modification of AMPK [16]. H_2O_2 treatment also leads to activation of the master regulator of mitochondrial biogenesis PPARG coactivator 1 alpha (PGC-1a) induction in vitro, and PGC1a is necessary for upregulation of antioxidant defense enzymes such as SOD, glutathione peroxidase (GPx), or catalase (CAT) [17]. Thus while we did not measure various antioxidant enzymes expression, they may have been upregulated in as a compensatory mechanism.

AMPK and mTOR are currently key players within aging research, and modulation of the activation of AMPK and inactivation of mTOR through various interventions has had substantial impacts on organismal aging. Cells treated with H_2O_2 had rapid (< 60 min) phosphorylation and activation of Ataxia Telangiectasia Mutated (ATM) kinase leading to phosphorylation and activation of AMPK and a subsequent decreased phosphorylation of mTOR effectors S6 Kinase (S6K) and 4E-binding protein-1 (4EBP1) which modulate cell growth. These changes in phosphorylation state lead to increased autophagy and phosphorylation of acetyl-CoA carboxylase (ACC), a protein involved in fat metabolism, activating this pathway similarly to

caloric restriction. Alternatively, cells lacking ATM had decreased suppression of mTOR, cells lacking Tuberous Sclerosis Complex 2 (Tsc2), a downstream inhibitor of S6K, also had limited activation of AMPK, and limited suppression of mTOR activity [18]. It therefore appears that oxidative stress activates ATM leading to autophosphorylation, and begins the activation of this pathway to phosphorylate and activate LKB1 to activate and phosphorylate AMPK, and finally to activate and phosphorylate TSC2 which inhibits mTOR, leading to decreased downstream cell-growth signaling but increased autophagy. Thus, independent of DNA damage, oxidative stressors appear to lead to ATM activation to eventually increase autophagy. In yeast, deletion of TOR1 leads to extended lifespan and increased respiration, independent of SOD2 defense against oxidative insults in these animals [16].

Acute GSH depletion via BSO treatment in vivo and in vitro leads to thermogenesis and thermogenic gene upregulation such as uncoupling proteins, increased oxygen consumption, but treatment with GSH blocks this signaling. Decreasing GSH in rodent adipose tissue partially converts white adipose tissue into brown adipose tissue, also leading to an overall loss of body weight at least partially due to a loss of adipose tissue [19]. GCLM-/- mice have an increased defense against alcohol-induced steatosis, with activation of AMPK potentially via an LKB1 mediated pathway, and parallel activation of ACC which regulates fat metabolism [3]. These mice had higher levels of oxidative damage as measured with protein carbonyls, but were still more protected than GCLM+/+ animals against an alcohol insult [3]. These studies highlight the dual nature of redox signaling where a certain level of redox stress can lead to positive adaptations with or without some level of oxidative damage.

Glutathione dysregulation appears to beneficially affect motor function in young and adult GCLM-/- mice, independent of changes in body weight. This is relatively unexpected as

oxidative stress and damage have been connected with motor function decline in aging rodents [20]. Interestingly, in the present study skeletal muscle GSH was decreased only in female GCLM-/- mice, while male GCLM-/- mice had GSH levels higher than the GCLM+/+ males. Additionally, GSH levels across the lifespan in the cerebellum, cortex, and striatum of adult and aged mice were only minorly affected by the removal of GCLM, and were similar between GCLM-/- and GCLM+/+ mice. In the present study, peripheral tissue GSH concentrations appear to be more affected by the removal of GCLM, as liver levels were decreased by ~80%, although other studies with the same GCLM-/- mice have found decreased GSH levels in various brain regions including the cerebellum [21, 22]. We did observe deficits in GSH mainly at 5 months for the striatum, cortex, and cerebellum ranging from 20-50%, but the deficits were not consistent across the lifespan and by 10 months there was minimal difference between GCLM+/+ and GCLM-/- brain GSH levels. Previous studies have focused on young GCLM-/- mice (3-5 months), and it is possible that the GCLM-/- dependent alterations in GSH are in fact age-dependent, as seen in our study where deficits in redox state are most apparent at 5 months. The increased performance of GCLM-/- mice on balance, coordination, and motor learning might be due to positive redox adaptations within the key brain regions or in the periphery as the relatively minor shifts in redox state could increase antioxidant defense and elicit other beneficial adaptations related to cell growth, differentiation, and metabolism. This concept is reinforced by studies examining the beneficial effects of short bouts of hypoxia on motor function through the growth of motor neurons in the periphery [23]. As intermittent hypoxia induces mild redox stress [23], there may be a common pathway between the present benefits seen in GCLM-/- mice and mice with induced redox stress via hypoxia. AMPK can be indirectly activated via H_2O_2, possibly through an ATP-dependent mechanism, but under hypoxic conditions AMPK can

activated without changes in ATP [15]. Thus, local changes in AMPK signaling for improved metabolism may explain benefits in motor function or motor neuron health.

While cognition as a whole was not affected by the GCLM-/- genotype, anxiety-related behaviors and fear-based memory were decreased across the lifespan in GCLM-/- mice. Some studies have reported an importance of GSH in particular for regulating these behaviors, where decreased GSH regeneration was associated with decreased anxiety related behavior [24]. Other groups have utilized the same GCLM-/- mice model as used in the present study and reported redox-dysregulation negatively affected social behavior and decreased anxiety-related behavior, suggesting a role for redox signaling and/or GSH in anxiety behavior [25]. GCLM-/- mice were also found to have deficits in pre-pulse inhibition, a phenomenon associated with psychological diseases such as schizophrenia and anxiety-disorders [2]. These results were independent of cognitive deficits in GCLM-/- mice, similarly to the present study. Other studies have confirmed changes in brain chemistry in developing GCLM-/- mice, including changes in the anterior cortex similar to clinical data seen in schizophrenia patients [26]. Young GCLM-/- mice displayed decreased anxiety in the zero maze and hyperlocomotion in response to psychostimulants [27]. Importantly, in all of these studies, GCLM-/- mice had observed deficits in neurological function independent of changes in hippocampal-dependent memory, including tests with the Morris water maze or object recognition. This is likely explained by redox-dependent changes in specific portions of the hippocampus, as the ventral but not dorsal horn of the hippocampus was most affected in GCLM-/- mice. The ventral horn of the hippocampus was functionally disrupted, leading to psychiatric-related and emotional/stress behavioral phenotypes but sparing any deficits in spatial recall [28]. Connecting these neurochemistry deficits in pre-clinical models such as mice to clinical data in humans, GCLM deficiency has been associated

with schizophrenia, suggesting a link between impaired GSH metabolism and altered anxiety-related function in both rodents and humans [29, 30]. Further study will be necessary to confirm these neurochemical results in older animals, although young, adult, and old GCLM-/- mice display the similar phenotype of decreased-anxiety in the present study.

Another consistent result we observed was an increase in inflammation with age in both GCLM+/+ and GLCM-/- mice, but with sexual dimorphism and genetic differences in overall inflammation. We observed age-related increases in only TNF-α, while IL-6 had no real sex-, age- or genotype-dependent effects. These results agree with human data, which reported age-related increases in TNF-α coupled with decreased antioxidant defense, however, basal IL-6 was not affected with age but production under hypoxic stress was increased with age [31]. Additionally, in humans, TNF-α production is associated with metabolic disturbances such as age-dependent hyperglycemia and hyperinsulinemia [32]. In mice, TNF-α levels are also increased with age, and interventions related to metabolism such as CR can decrease TNF-α levels [33]. Inflammation is also connected to GSH for normal brain function, as brains from autistic humans have increased inflammation and lower GSH, along with higher oxidative damage and overall disruption of normal brain function [34]. Interestingly, young GCLM-/- mice are resistant to hepatic inflammatory fibrosis from a high sugar diet compared to GCLM+/+ mice and overall had lower inflammation, lower oxidative damage, and no steatosis [4]. Young GCLM-/- mice exposed to an ozone-induced lung injury had higher resistance and less induction of inflammation to this stressor due to prior compensatory antioxidant defenses from chronic GSH deficiency [35]. Additionally, depletion of GSH in human T-cells impairs activation of NF-kB (nuclear factor kappa-light-chain-enhancer of activated B cells), a key inflammatory mediator, suggesting a strong relationship between GSH and inflammation regulation [36].

These results are confirmed in human liver cells, where GSH-depletion limits TNF-α induced activation of NF-kB [37], and GSH-depletion in endothelial cells inhibits NF-kB activation [38]. Thus, there appears to be a key modulatory effect of GSH levels on NF-kB activation and inflammation in vitro, and decreasing GSH levels in vivo in the present study also appears to limit inflammation in young and adult mice, but exacerbates inflammation in old GCLM-/- mice. Interestingly, these results also align very well with the motor benefits in GCLM-/- mice, where young and adult female GCLM-/- mice had better motor performance than GCLM+/+ mice, along with decreased inflammation but worsened motor performance at old age along with increased inflammation. In conclusion, we can likely contribute part of this sex- and age-dependent shift in motor function with GCLM-/- mice to systemic changes in peripheral inflammation.

While the increased lifespan was unexpected in the current study, maintaining animals under optimal conditions may have affected our results. Importantly, GCLM-/- are highly sensitized to direct oxidative stress insults, however they do have some increased protection against high fat diet induced metabolic dysfunction [1], ethanol-induced damage [3], and some inflammation [35]. Mice already have oxidative damage in the brain by 3 months, and peripheral tissues are sensitized to oxidative insults [39]. Mice are sensitized to direct oxidative insults, but even indirect treatments such as cigarette smoke induced inflammation occurred dramatically faster [40]. Other drug insults impaired sex tissues in both males and females, but did not affect normal function in younger animals [41]. Early life stressors in GCLM-/- mice affect the anterior cingulate cortex region of the hippocampus much more than any other are of the hippocampus, along with parvalbumin interneurons disruption [42]. These early life stressors had long-term effects, but were partially reversed with treatment with N-Acetylcysteine which has some redox

regulation capability. While living under optimal laboratory conditions, our animals therefore do appear to have increased longevity, but further studies will be necessary to both confirm our lifespan results and to examine the effects of various inflammatory or oxidative stressors on longevity and overall resilience. Given that the animals inherently have decreased resilience, it will be interesting to see how they adapt to external stressors.

The conclusion of the present study provides evidence directly against both the oxidative stress and the redox stress hypothesis of aging, and while alterations in redox state or decreasing antioxidant defense [43] may underlie or affect aging, the current evidence does not support this concept. Major deficits in systemic GSH synthesis had no negative effects on classical healthspan measures such as balance, coordination, walking speed, memory, task-switching, or on lifespan, and in fact had some beneficial effects on both healthspan and lifespan (Table 1). Additionally, while glutathione is the dominant redox couple in terms of raw substrate, it is one piece in a series of antioxidant enzymatic and redox couples. NADPH/NADP serves as the primary regenerator of GSH/GSSG, and other studies removing glutathione reductase, the enzyme responsible for this regeneration reaction, results in embryonic lethality [44]. Overexpression of glucose-6-phosphate-dehydrogenase (G6PD), the rate-limiting enzyme for NADPH synthesis, extends healthspan and decreases oxidative damage in mice [45]. Additionally, mice deficient in G6PD have decreased NADPH and GSH, increased oxidative damage, and metabolic disturbances similar to a diabetic phenotype [46], whereas GCLM-/- mice are resistant against high-fat diet induced diabetes and in general have improved metabolic profiles [1, 3]. Thus, while GSH clearly has modulatory activity with regards to metabolism, various routes of GSH or NADPH modulation have contradictory results and GSH levels alone do not appear to be the key modulator of the aging process. NADH, while not directly

regenerating GSH, is upstream of NADPH and is inherently connected to both energy metabolism through the electron transport chain and the pentose-phosphate pathway. The contradictory phenotypes of NADPH vs GSH deficiency are not fully explainable at this time, and further research is needed to fully understand the mechanisms of redox-dependent signaling related to metabolism, oxidative stress, and longevity. Future research into the mechanisms of redox stress and beneficial adaptations may reveal important mechanisms for slowing human aging and improving the lives of our elderly as the present study revealed an extension of lifespan and healthspan with changes in redox state.

Table 1. Summary of functional, biochemical, and lifespan outcomes comparing GCLM-/- males or females to age- and sex-matched GCLM+/+ mice.

	YOUNG		ADULT		OLD	
Outcome	Male	Female	Male	Female	Male	Female
Weight	⇓	⇓	⇓	⇓	⇓	⇓
Anxiety	⇓	⇔	⇔	⇓	⇓	⇓
Motor	⇑	⇑	⇑	⇑	⇔	⇓
Cognition	⇔	⇔	⇔	⇔	⇔	⇔
Peripheral GSH	⇓	⇓	⇓	⇓	⇓	⇓
Central GSH	⇓	⇓	⇔	⇔	⇔	⇔
TNF-a	⇔	⇔	⇔	⇔	⇑	⇑
p-mTOR	⇔	⇔	⇔	⇔	⇔	⇔
p-AMPK	⇔	⇔	⇔	⇔	⇔	⇔
LC3B	⇔	⇔	⇔	⇔	⇔	⇔
Lifespan	–	–	–	–	⇑	⇑

References

1. Kendig, E.L., et al., *Lipid metabolism and body composition in Gclm(-/-) mice.* Toxicol Appl Pharmacol, 2011. **257**(3): p. 338-48.
2. Cole, T.B., et al., *Behavioral Characterization of GCLM-Knockout Mice, a Model for Enhanced Susceptibility to Oxidative Stress.* J Toxicol, 2011. **2011**: p. 157687.
3. Chen, Y., et al., *Chronic Glutathione Depletion Confers Protection against Alcohol-induced Steatosis: Implication for Redox Activation of AMP-activated Protein Kinase Pathway.* Sci Rep, 2016. **6**: p. 29743.
4. Haque, J.A., et al., *Attenuated progression of diet-induced steatohepatitis in glutathione-deficient mice.* Lab Invest, 2010. **90**(12): p. 1704-17.
5. Schneider, K.S. and J.Y. Chan, *Emerging role of Nrf2 in adipocytes and adipose biology.* Adv Nutr, 2013. **4**(1): p. 62-6.
6. Blagosklonny, M.V., *Calorie restriction: decelerating mTOR-driven aging from cells to organisms (including humans).* Cell Cycle, 2010. **9**(4): p. 683-8.
7. Yang, W., J. Li, and S. Hekimi, *A Measurable increase in oxidative damage due to reduction in superoxide detoxification fails to shorten the life span of long-lived mitochondrial mutants of Caenorhabditis elegans.* Genetics, 2007. **177**(4): p. 2063-74.
8. Van Raamsdonk, J.M. and S. Hekimi, *Superoxide dismutase is dispensable for normal animal lifespan.* Proc Natl Acad Sci U S A, 2012. **109**(15): p. 5785-90.
9. Schulz, T.J., et al., *Glucose restriction extends Caenorhabditis elegans life span by inducing mitochondrial respiration and increasing oxidative stress.* Cell Metab, 2007. **6**(4): p. 280-93.

10. Meng, J., et al., *The decay of Redox-stress Response Capacity is a substantive characteristic of aging: Revising the redox theory of aging.* Redox Biol, 2017. **11**: p. 365-374.

11. Bonawitz, N.D., et al., *Reduced TOR signaling extends chronological life span via increased respiration and upregulation of mitochondrial gene expression.* Cell Metab, 2007. **5**(4): p. 265-77.

12. Cardaci, S., G. Filomeni, and M.R. Ciriolo, *Redox implications of AMPK-mediated signal transduction beyond energetic clues.* J Cell Sci, 2012. **125**(Pt 9): p. 2115-25.

13. Aquilano, K., et al., *p53 orchestrates the PGC-1alpha-mediated antioxidant response upon mild redox and metabolic imbalance.* Antioxid Redox Signal, 2013. **18**(4): p. 386-99.

14. Elshorbagy, A.K., et al., *Exploring the Lean Phenotype of Glutathione-Depleted Mice: Thiol, Amino Acid and Fatty Acid Profiles.* PLoS One, 2016. **11**(10): p. e0163214.

15. Emerling, B.M., et al., *Hypoxic activation of AMPK is dependent on mitochondrial ROS but independent of an increase in AMP/ATP ratio.* Free Radic Biol Med, 2009. **46**(10): p. 1386-91.

16. Woods, A., et al., *LKB1 is the upstream kinase in the AMP-activated protein kinase cascade.* Curr Biol, 2003. **13**(22): p. 2004-8.

17. St-Pierre, J., et al., *Suppression of reactive oxygen species and neurodegeneration by the PGC-1 transcriptional coactivators.* Cell, 2006. **127**(2): p. 397-408.

18. Alexander, A., et al., *ATM signals to TSC2 in the cytoplasm to regulate mTORC1 in response to ROS.* Proc Natl Acad Sci U S A, 2010. **107**(9): p. 4153-8.

19. Lettieri Barbato, D., et al., *Glutathione Decrement Drives Thermogenic Program In Adipose Cells.* Sci Rep, 2015. **5**: p. 13091.

20. Forster, M.J., et al., *Age-related losses of cognitive function and motor skills in mice are associated with oxidative protein damage in the brain.* Proc Natl Acad Sci U S A, 1996. **93**(10): p. 4765-9.

21. Giordano, G., T.J. Kavanagh, and L.G. Costa, *Neurotoxicity of a polybrominated diphenyl ether mixture (DE-71) in mouse neurons and astrocytes is modulated by intracellular glutathione levels.* Toxicol Appl Pharmacol, 2008. **232**(2): p. 161-8.

22. Giordano, G., et al., *Glutathione levels modulate domoic acid induced apoptosis in mouse cerebellar granule cells.* Toxicol Sci, 2007. **100**(2): p. 433-44.

23. Dale, E.A., F. Ben Mabrouk, and G.S. Mitchell, *Unexpected benefits of intermittent hypoxia: enhanced respiratory and nonrespiratory motor function.* Physiology (Bethesda), 2014. **29**(1): p. 39-48.

24. Hovatta, I., et al., *Glyoxalase 1 and glutathione reductase 1 regulate anxiety in mice.* Nature, 2005. **438**(7068): p. 662-6.

25. Kulak, A., M. Cuenod, and K.Q. Do, *Behavioral phenotyping of glutathione-deficient mice: relevance to schizophrenia and bipolar disorder.* Behav Brain Res, 2012. **226**(2): p. 563-70.

26. das Neves Duarte, J.M., et al., *N-acetylcysteine normalizes neurochemical changes in the glutathione-deficient schizophrenia mouse model during development.* Biol Psychiatry, 2012. **71**(11): p. 1006-14.

27. Chen, Y., et al., *Effect of chronic glutathione deficiency on the behavioral phenotype of Gclm-/- knockout mice.* Neurotoxicol Teratol, 2012. **34**(4): p. 450-7.

28. Steullet, P., et al., *Redox dysregulation affects the ventral but not dorsal hippocampus: impairment of parvalbumin neurons, gamma oscillations, and related behaviors.* J Neurosci, 2010. **30**(7): p. 2547-58.

29. Tosic, M., et al., *Schizophrenia and oxidative stress: glutamate cysteine ligase modifier as a susceptibility gene.* Am J Hum Genet, 2006. **79**(3): p. 586-92.

30. Gysin, R., et al., *Impaired glutathione synthesis in schizophrenia: convergent genetic and functional evidence.* Proc Natl Acad Sci U S A, 2007. **104**(42): p. 16621-6.

31. de Gonzalo-Calvo, D., et al., *Differential inflammatory responses in aging and disease: TNF-alpha and IL-6 as possible biomarkers.* Free Radic Biol Med, 2010. **49**(5): p. 733-7.

32. Kirwan, J.P., et al., *Human aging is associated with altered TNF-alpha production during hyperglycemia and hyperinsulinemia.* Am J Physiol Endocrinol Metab, 2001. **281**(6): p. E1137-43.

33. Spaulding, C.C., R.L. Walford, and R.B. Effros, *Calorie restriction inhibits the age-related dysregulation of the cytokines TNF-alpha and IL-6 in C3B10RF1 mice.* Mech Ageing Dev, 1997. **93**(1-3): p. 87-94.

34. Rose, S., et al., *Evidence of oxidative damage and inflammation associated with low glutathione redox status in the autism brain.* Transl Psychiatry, 2012. **2**: p. e134.

35. Johansson, E., et al., *Glutathione deficient C57BL/6J mice are not sensitized to ozone-induced lung injury.* Biochem Biophys Res Commun, 2010. **396**(2): p. 407-12.

36. Mihm, S., D. Galter, and W. Droge, *Modulation of transcription factor NF kappa B activity by intracellular glutathione levels and by variations of the extracellular cysteine supply.* FASEB J, 1995. **9**(2): p. 246-52.

37. Lou, H. and N. Kaplowitz, *Glutathione depletion down-regulates tumor necrosis factor alpha-induced NF-kappaB activity via IkappaB kinase-dependent and -independent mechanisms.* J Biol Chem, 2007. **282**(40): p. 29470-81.

38. Liao, B.C., et al., *The glutaredoxin/glutathione system modulates NF-kappaB activity by glutathionylation of p65 in cinnamaldehyde-treated endothelial cells.* Toxicol Sci, 2010. **116**(1): p. 151-63.

39. Yang, Y., et al., *Initial characterization of the glutamate-cysteine ligase modifier subunit Gclm(-/-) knockout mouse. Novel model system for a severely compromised oxidative stress response.* J Biol Chem, 2002. **277**(51): p. 49446-52.

40. Gould, N.S., et al., *Glutathione Depletion Accelerates Cigarette Smoke-Induced Inflammation and Airspace Enlargement.* Toxicol Sci, 2015. **147**(2): p. 466-74.

41. Nakamura, B.N., et al., *Increased sensitivity to testicular toxicity of transplacental benzo[a]pyrene exposure in male glutamate cysteine ligase modifier subunit knockout (Gclm-/-) mice.* Toxicol Sci, 2012. **126**(1): p. 227-41.

42. Cabungcal, J.H., et al., *Early-life insults impair parvalbumin interneurons via oxidative stress: reversal by N-acetylcysteine.* Biol Psychiatry, 2013. **73**(6): p. 574-82.

43. Harman, D., *Free radical theory of aging: an update: increasing the functional life span.* Ann N Y Acad Sci, 2006. **1067**: p. 10-21.

44. Brutsch, S.H., et al., *Expression of inactive glutathione peroxidase 4 leads to embryonic lethality, and inactivation of the Alox15 gene does not rescue such knock-in mice.* Antioxid Redox Signal, 2015. **22**(4): p. 281-93.

45. Nobrega-Pereira, S., et al., *G6PD protects from oxidative damage and improves healthspan in mice.* Nat Commun, 2016. **7**: p. 10894.

46. Xu, Y., et al., *Glucose-6-phosphate dehydrogenase-deficient mice have increased renal oxidative stress and increased albuminuria.* FASEB J, 2010. **24**(2): p. 609-16.

Gait analyses in mice: effects of age and glutathione deficiency

J. Thomas Mock, Sherilynn G. Knight, Philip H. Vann, Jessica M. Wong, Delaney L. Davis, Michael J. Forster, Nathalie Sumien

Department of Pharmacology & Neuroscience, Center for Neuroscience Discovery, Institute for Healthy Aging, University of North Texas Health Science Center at Fort Worth, Fort Worth, TX, 76107 USA.

Running title: effects of age and glutathione deficiency on mouse gait

Address correspondence to: Nathalie Sumien, Dpt of Pharmacology & Neuroscience, Center for Neuroscience Discovery, Institute for Healthy Aging, UNT Health Science Center, 3500 Camp Bowie, Fort Worth, TX 76107, Tel: 817/735-2092; Fax: 817/735-0408;

email: nathalie.sumien@unthsc.edu

Abstract

Minor changes (~0.1 m/s) in human gait speed are predictive of various measures of decline and can be used to identify at-risk individuals prior to further decline. These associations are possible due to an abundance of human clinical research. However, age-related gait changes are not well defined in rodents, even though rodents are used as the primary pre-clinical model for many disease states as well as aging research. Our study investigated the usefulness of a novel automated system, the CatWalk™ XT, to measure age-related differences in gait. Furthermore, age-related functional declines have been associated with decreases in the reduced to oxidized glutathione ratio leading to a pro-oxidizing cellular shift. Therefore the secondary aim of this study was to determine whether chronic glutathione deficiency led to exacerbated age-associated impairments. Groups of male and female wild-type ($gclm^{+/+}$) and knock-out ($gclm^{-/-}$) mice aged 4, 10 and 17 months were tested on the CatWalk and gait measurements recorded. Similar age-related declines in all measures of gait were observed in both males and females, and chronic glutathione depletion was associated with some delays in age-related declines, which were more exacerbated in males. In conclusion, the CatWalk is a useful tool to assess gait changes with age, and further studies will be required to identify the potential compensating mechanisms underlying the effects observed with the chronic glutathione depletion.

Keywords: Aging, glutathione deficiency, gait, speed, catwalk

INTRODUCTION

Aging is associated with a decline in overall motor function across various species, including rodents and humans [1-4]. Interestingly, human gait speed can be utilized to stratify risk of decline in cognitive function, mobility, loss of independence, increased fall risk, institutionalization, as well as overall mortality risk [5]. This association of gait speed with many dimensions of aging has been found consistently in humans, where minor changes (~0.1 m/s) in gait speed were predictive of various measures of decline and can be used to identify at-risk individuals prior to further decline [6]. While human gait research is abundant, age-related gait changes in rodents are not well defined even though they are used as the primary pre-clinical model for many disease states and aging research [7].

Although rodent gait changes as a result of aging are not as well characterized as changes in human gait, research on other aspects of motor function in rodents has shown age-related decreases in spontaneous movement speed [2, 3, 8], physical activity [9, 10], as well as balance and motor coordination [2]. Importantly, both human and mouse functional motor decline follow similar patterns, where motor function decline occurs earlier in life than other more debilitating outcomes which highlights the importance of motor function as both a clinical and preclinical measure [9, 11]. Indirect measures of gait speed through open field [12] or balance beam testing [13] hinted at age-related slowing of gait speed, but with methodological limitations as gait analysis was not the primary measure and no other gait variables were recorded. Direct studies of rodent gait via treadmill analysis at a set speed have shown age-related changes, however studies in mice and humans have demonstrated that treadmill and free gait parameters are not equivalent [14, 15]. Furthermore, most gait analyses in rodents have focused on changes across the first 12 months of life, which equates to adult growth along with aging. This presents an opportunity to

determine quantitative relationships between gait changes and age across the lifespan of free-running rodents. A relatively novel way to measure gait is to use the CatWalk™ XT, an automated system using a sophisticated software allowing rodents to walk in a low-stress environment allowing gait analyses in a low-stress environment. Thus far, the CatWalk has primarily been validated in modeled disease states including traumatic brain injury, stroke, spinal cord injury, Parkinson's disease, osteoarthritis, and ataxia [16-20]. However, to date there have been no studies on the effect of age in mice on the qualitative and quantitative gait outcomes using this apparatus.

Additionally, while the central cause of aging is still under investigation, the redox stress theory of aging postulates that while a moderate level of reactive oxygen species (ROS) is biologically useful for cell signaling, an overabundance of ROS can lead to accumulation of oxidative damage and a pro-oxidizing shift in reduction-oxidation (redox) state preceding cellular dysfunction [21, 22]. This pro-oxidant shift in aging is primarily measured via changes in the ratio of reduced to oxidized glutathione (GSH:GSSG), where aging leads to a decline in the GSH:GSSG ratio indicating less redox potential [23]. Although several redox couples interact with GSH to maintain overall cellular redox state, the glutathione redox couple (GSH:GSSG) is the most abundant, and as such modulation of redox status can be achieved by altering levels of GSH [24]. Synthesis of GSH occurs in two subsequent enzymatic reactions, formation of y-glutamylcysteine (y-GC) from glutamate and cysteine via glutamate cysteine ligase followed by conversion of y-GC to GSH via GSH synthetase [25]. The synthesis of GSH is rate-limited by the glutamate cysteine ligase (gcl) enzyme, a heterodimer consisting of a catalytic (gclc) and modifier (gclm) subunit [25]. While gclc contains all catalytic capacity, gclm increases the V_{max} and the affinity for glutamate, and decreases feedback inhibition from GSH

[26]. While homozygous knockout of gclc is embryonic lethal, global knockout of the gcl modifier subunit ($gclm^{-/-}$) in mice leads to a 70-90% decrease in GSH levels across various tissues, including liver, brain, kidney, and lung [27]. Adult $gclm^{-/-}$ mice present with chronically decreased levels of GSH, are more susceptible to oxidative insults [28], and have a more pro-oxidative redox cellular environment [27]. These changes in $gclm^{-/-}$ mice could lead to an early aging phenotype if a more oxidative redox state is in fact a determinant factor in aging. Accordingly, the objectives of this study were to validate the Catwalk™ XT in assessment of age-related gait changes and determine if chronic glutathione depletion exacerbated these gait variations. To achieve the goals, male and female $gclm^{-/-}$ and $gclm^{+/+}$ mice were tested on the Catwalk at 3 different target ages (4, 10 and 17 months). The operational hypothesis was that gait measures would decline with advanced age and that impairments would occur earlier in glutathione depleted mice.

MATERIALS AND METHODS

Animals

Procedures were approved by the Institutional Animal Care and Use Committee at the University of North Texas Health Science Center at Fort Worth, and adhered to NIH guidelines. The mice heterozygous for gclm were generated on a C57BL/6J (B6.129) background, acquired from Dr. Terence Kavanaugh, rederived and backcrossed at least 7 generations into C57BL/6 mice by Jackson Laboratories. Once in the UNT Health Science Center vivarium, triads of $gclm^{+/-}$ were mated to obtain wild-type ($gclm^{+/+}$) and knock-out ($gclm^{-/-}$) littermates. From the in-house breeding colony, male and female mice were housed and aged in groups of 2-4, separated according to sex and genotype, in standard polycarbonate cages (28 x 17 x 12.5 cm) with

corncob bedding and *ad libitum* access to water and standard rodent chow (LabDiet® R&M 5LG6 5S84; catalog number: 1813505 from TestDiet, Richmond, IN), and were maintained at ambient temperature (23 ± 1° C), under a 12-h light/dark cycle starting at 0600. At the target ages of 4, 10, and 17 months for this study, squads of mice from the aging colony were used for gait analyses (**Table 1**) in a cross-sectional design.

Table 1. Number of animals per group according to genotype and age

	Males			**Females**			**Total**		
Age (months)	**4**	**10**	**17**	**4**	**10**	**17**	**4**	**10**	**17**
Gclm$^{+/+}$	15	15	15	13	15	9	28	30	24
Gclm$^{-/-}$	15	15	8	14	12	12	29	27	20

Quantitative gait analyses

Gait measures were determined using the CatWalk™ XT system (Noldus Information Technology, The Netherlands). The CatWalk is an apparatus used for semi-automated objective rodent gait analysis via video recording. Importantly, this system allows for the animals to voluntarily move at preferred speeds in a similar fashion to clinical gait testing in humans. The device consists of (i) a 130 cm long hardened glass platform with an adjustable alleyway to limit movements to straight lines, (ii) a red overhead light, (iii) a green LED light attached to the glass platform, and (iv) a high speed color camera mounted below the platform. The green LED light attached to the apparatus emits light into the glass plate, and this light is only refracted wherever rodent paws contact the glass, allowing the high speed digital camera to capture precise rodent paw placement in real time. The overhead red light creates contrast for recording of the body

outline. The visual data is digitized and transferred to an attached computer where the CatWalk™ XT software can be used for semi-automated labeling and analysis of static and dynamic gait kinematics via distance, time, and intensity differences between paw prints. Gait data can then be exported for data storage and subsequent analyses.

The alley was adjusted to be 8 cm wide, and the walkway for data recoding was defined at 8 cm x 32 cm which allowed 4 full step cycles in the center of the alley. Visual scaling was calibrated prior to each use. On testing days, animals are transferred from their home cages into a polycarbonate carrier and brought into the pitch black room to acclimate for 10 minutes prior to testing. A single animal was placed onto the platform and allowed to cross the defined walkway up to 20 times. Each crossing of the platform is called a run and non-compliant runs were defined as more than 60% speed variation within a run or longer than 5 seconds. From the pool of compliant runs, only runs with less than 10% speed variation between runs were used for further analyses. The mice were not given a formal training to the apparatus, and if they stopped mid-run and/or required auditory stimulation to move, that run was not included in the final analyses as it did not reach our a-priori set criterion for compliant runs. We selected five variables that are similar in humans and relevant to human aging (**Table 2**), including gait speed, base of support, stride length, swing speed, and step cycle duration. All measures besides gait speed were analyzed separately for front and hind paws.

Table 2. Gait variable definitions

Gait speed	Rate of body movement in cm/s
Base of support	Width between the two front or two hind paws in cm
Stride Length	Distance between subsequent placements of the same paw

	for the two front or two hind paws in cm
Swing Speed	Rate of movement of a paw during the swing phase for the two front or two hind paws in cm/s
Step Cycle Duration	Time to go through both the stand and swing phases for the two front or two hind paws in s

Statistical Analyses

A three-way analyses of covariance (ANCOVA) was run with Sex, Genotype and Age as between-group factors and Body Weight as the covariate to ensure that body weights were not responsible for driving the main effects. Body weights and the various gait measures were compared using three-way analyses of variance (ANOVA) with Sex, Genotype and Age as between-group factors. Following significance of either a main effect or interaction, individual comparisons between different Sex, Genotype, or Age were performed using a single degree-of-freedom F test involving the error term from the overall ANOVA. The individual relationships between various gait measures with gait speed were determined via Pearson's or logarithmic correlations. The α level was set at 0.05 for all analyses. The software used for the analyses was Systat 13 (Systat Software Inc., San Jose, CA, USA).

RESULTS

Body Weight

The effects of sex, age and genotype on the body weights are presented in **Figure 1**. Overall, the males weighed more than the females regardless of genotype (13%, 17% and 5% difference in

young, adult, and old respectively). The gclm$^{-/-}$ weighed less than the gclm$^{+/+}$ regardless of age (11-17% difference). The weight difference was more pronounced between 4 and 10 months in males, and between 10 and 17 months in females. A three-way ANOVA yielded a significant interaction between Sex, Age and Genotype supporting these observations ($p = 0.015$).

Gait Speed

The effects of sex, age and genotype on the gait speed are presented in **Figure 2**. There was no major difference in speed between males and females at any age. While the gait speed in both the gclm$^{+/+}$ and gclm$^{-/-}$ mice declined with age (gclm$^{+/+}$: 41% in males, 33% in females; gclm$^{-/-}$: 32% in males, 48% in females), the rate of decline was different between the two genotypes. In the gclm$^{+/+}$ mice, the majority of the age-related decline in speed occurred between 4 and 10 months (35% for males, 28% for females), whereas in the gclm$^{-/-}$ mice the decline was more gradual between 4 and 10 months and between 10 and 17 months. However, while males and females gclm$^{-/-}$ declined similarly between 4 and 10 months (~21%), the decrease in speed between 10 and 17 months was more than double in the females (35%) than in the males (14%). A three-way ANOVA revealed significant main effects of Age ($p < 0.001$) and Genotype ($p = 0.032$), but there was no main effect of Sex or interactions between Sex, Age and Genotype (all $ps > 0.162$).

Base of Support

The effects of sex, age and genotype on the front and hind paw base of support are presented in **Figure 3**. In males, the front and hind paws base of support widened by 10% in gclm$^{+/+}$, which occurred mostly between 4 and 10 months. The hind paws base of support for the gclm$^{-/-}$ was

widened by 11% by 10 months along with a narrowing of 6% for the front paws base of support. Additionally, the base of support was narrower by 9% in the $gclm^{-/-}$ at 10 and 17 months for the front paws and by 8% at 4 months for the hind paws. In $gclm^{+/+}$ females, there was a widening of the base of support for the front paws by 10% which occurred between 10 and 17 months, while the 11% widening of the base of support for the hind paws occurred between 4 and 10 months, followed by a small narrowing of 5% between 10 and 17 months. The widening of the front paws base of support for the $gclm^{-/-}$ was similar to that of the $gclm^{+/+}$, while there was a gradual widening of the hind paws base of support for the $gclm^{-/-}$. The hind paws base of support was about 6% narrower in the $gclm^{-/-}$ than the $gclm^{+/+}$ at 4 and 10 months. For the front paws base of support, a three-way ANOVA revealed a significant main effect of Age ($p = 0.01$), but there was no main effect of Genotype ($p = 0.084$) or any interaction between Sex, Age and Genotype (all $ps >= 0.224$). For the hind paws base of support, a three-way ANOVA revealed significant main effects of Age ($p < 0.001$) and Genotype ($p = 0.011$) and interaction of Age x Genotype ($p = 0.028$).

Stride Length

The effects of sex, age and genotype on the front and hind paw stride length are presented in **Figure 4**. In males, the front and hind paws stride length in both $gclm^{+/+}$ and $gclm^{-/-}$ mice decreased by 14% at 10 months, and further decreased by another 7-12% at 17 months. There was no difference between the $gclm^{+/+}$ and $gclm^{-/-}$ mice. In females, the $gclm^{+/+}$ mice exhibited a gradual decrease in stride length reaching 10% for both front and hind paws. While the shortening of the stride was similar in both genotypes between 4 and 10 months, it was 4 times higher between 10 and 17 months in the $gclm^{-/-}$ compared to the $gclm^{+/+}$. At 17 months, the

female gclm$^{-/-}$ exhibited stride length for either paws 15% shorter than that of the age-matched gclm$^{+/+}$. For the front paws, a three-way ANOVA revealed a significant main effect of Age (p < 0.001) but there was no main effect of Genotype (p = 0.125) or Sex (p = 0.201) or any interactions between Sex, Age and Genotype (all ps > 0.265). For the hind paws, a three-way ANOVA revealed significant main effects of Age (p < 0.001) and Genotype (p = 0.02), but there was no main effect of Sex (p = 0.112)or interaction of Sex, Age and Genotype (all ps > 0.237).

Swing Speed

The effects of sex, age and genotype on the front and hind paw swing speed are presented in **Figure 5**. In males, the swing speed for both hind and front paws declined by ~36% in glcm$^{+/+}$ and by 26% in gclm$^{-/-}$. While the decline was gradual in the gclm$^{+/+}$, most of the decrease occurred between 10 and 17 months in the gclm$^{-/-}$. The swim speed of the gclm$^{-/-}$ was higher than that of the gclm$^{+/+}$ at 10 (front paws: 32%; hind paws: 22%) and 17 months (~22% for both front and hind paws), though it was only statistically significant at 10 months. In females, the swing speed for both hind and front paws declined by ~25% in glcm$^{+/+}$ and by ~34% in gclm$^{-/-}$. Contrary to the males, the decline was gradual in the gclm$^{-/-}$ while most of the decrease occurred between 4 and 10 months in the gclm$^{+/+}$. For both front and hind paws, three-way ANOVAs revealed significant main effects of Age (all ps < 0.001) and Genotype (all $ps \leq 0.035$), however there was no main effect of Sex (all ps > 0.305) or interaction of Sex, Age and Genotype (All $ps \geq 0.064$).

Step Cycle Duration

The effects of sex, age and genotype on the front and hind paw step cycle duration are presented in **Figure 6**. In males, step cycle duration for both front and hind paws increased with age in the $gclm^{+/+}$ by ~ 45% while it remained largely unaffected in the $gclm^{-/-}$. The step cycle duration of the $gclm^{-/-}$ was similar to that of the $gclm^{+/+}$ at 4 months, but was 20% and 34% lower at 10 and 17 months, respectively. In females, both genotypes exhibited an increase in step cycle duration for both front and hind paws by 36-40%. The observed deficit was fairly gradual in the $gclm^{-/-}$ but occurred mostly between 4 and 10 months in the $gclm^{+/+}$. At 10 months, the $gclm^{-/-}$ had a step cycle duration 18% shorter than that of the $gclm^{+/+}$. Three-way ANOVAs for front and hind paws step cycle duration revealed significant main effects of Age (all $ps < 0.001$) and Genotype (all $ps < 0.001$), but there was no interaction of Sex, Age and Genotype (all $ps \geq 0.19$) even though Sex x Genotype approached significance ($p = 0.064$ (front paws), $p = 0.088$ (hind paws)).

Relationship of gait kinematics to gait speed

The relationships of gait speed with front and hind base of support, stride length, step cycle duration, and swing speed are presented in **Figure 7** (since there were no differences between males and females, these analyses use the combined dataset). Front paw and hind paw stride length and swing speed increased as a function of gait speed. Pearson's correlation revealed significant relationships with gait speed for front paw ($r = 0.86$, $p < 0.01$) and hind paw stride length ($r = 0.83$, $p < 0.01$), as well as for front paw ($r = 0.95$, $p < 0.01$) and hind paw ($r = 0.95$, $p < 0.01$) swing speed. Front paw and hind paw base of support decreased as a function of gait speed. Pearson's correlations revealed significant linear relationships of both front paw ($r = -0.31$, $p < 0.01$) and hind paw ($r = -0.35$, $p < 0.01$) base of support with gait speed. Front paw and hind paw step cycle duration decreased as a curvilinear function of gait speed. Polynomial

regression revealed significant curvilinear relationships of both front paw ($r^2 = 0.88$, $p < 0.01$) and hind paw ($r^2 = 0.87$, $p < 0.01$) step cycle duration with gait speed.

DISCUSSION

The main findings of this study were that (1) aging is associated with a slowing of gait speed, swing speed, and step cycle duration, a widening of base of support, and a shortening of the stride length, (2) glutathione deficiency delayed some of these age-related declines, with the delays being more pronounced in males, and (3) a strong relationship between all the gait variables and gait speed exists.

While CatWalk measured gait changes have been used to determine or predict function in rodent disease models such as spinal cord and brain injury, Parkinson's disease, Huntington's disease, amyotrophic lateral sclerosis, and arthritic damage [16-20], there remains a lack of research on quantitative gait changes as a result of aging alone. The CatWalk is a novel tool in preclinical aging research, allowing for robust quantitative measurement of rodent gait and analysis of changes across the lifespan. Most studies of aged mice have utilized measures of gait such as gait speed and function in the open field [12] or treadmill-based systems that require animals to move at set speeds [29]. While these techniques have been previously published, each has its own limitations, such as manual scoring of weight distribution, gait coordination, or stepping in the open field which leads to substantial inter and intra-observer variability, set speed of the treadmill which artificially mandates a gait speed rather than allowing the animals to move

at their preferred gait speed, and ink smearing for painted foot print analysis which makes quantification difficult [16], and all lack gait kinematics analyses.

While treadmill-based gait analyses objectively quantify the same variables as the CatWalk, gait results are not equivalent between free movement and treadmill-based systems as there are known differences in gait mechanics used for the respective apparatus [14, 15]. Furthermore, Wooley *et al*. have demonstrated that the primary factor affecting gait results on the treadmill in mice is body size [4]. They later performed a predictive regression analysis based on body size (weight) for animals aged 1 - 12 months, however at 18 months animals did not fit into this trend, showing changes opposite the expected outcomes due to a decrease in body size. These results indicate that changes observed at 18 months are likely not dependent on body size changes and rather hint at age-specific gait changes [29]. Therefore at a set speed, which is the procedure for treadmill-based measurements, larger mice will have changes in various gait measures as they physically have longer legs and wider bodies. To determine whether body weight was a contributing factor to the age-related changes in gait in our study, we ran an ANCOVA on each measure with body weight as the covariate and all age effects remained indicating that body weight was not a confounding factor in our analyses of gait (all *p*s > 0.01 for age effect). Overall, the CatWalk method allows for freely-moving animals to move at their preferred speed, objectively measures many gait variables within individual runs, allows for instantaneous data analysis through digitization, thereby improving preclinical measurements of gait.

Age-related deficits in movement speed, stride length, base of support, step cycle duration and swing speed were observed at both 10 and 17 months. The gradual slowing and alteration in kinematic gait variables in the aged mice is similar to that observed with aging in

humans, primarily a decline in gait speed, shortening of stride length, and a wider base of support [30]. These strategies that the elderly use are to reduce fall risk by limiting vertical center of mass displacement and increasing dynamic stability, leading to an overall less destabilizing gait pattern [31-34]. Static and dynamic balance is dependent upon the vestibular, visual and somatosensory systems as well as overall strength, and these systems have been shown to decline with age in both humans [35-37] and rodents [2, 38-41]. As a result of these changes with age, both rodents and humans employ similar adaptive strategies in gait speed and kinematics. The similarities in age-related declines in balance and gait adaptation between the two species strengthen the adequacy of the use of rodents for pre-clinical assessments of gait during aging.

In addition to the novel use of the CatWalk™ XT to examine age-related gait changes in mice, we wanted to examine potential effects of redox impairment on gait measurements. Of note, $gclm^{-/-}$ mice exhibited age-related decline across most variables, but the age-related impairments seemed to be delayed compared to the $gclm^{+/+}$ mice. However, the results of the ANCOVA determined that body weight was a confounding factor in the genotype differences we observed, as including weight as a covariate did not yield any significant main effects of Genotype. It is noteworthy that in the $gclm^{-/-}$ mice step cycle duration was largely unaffected by age and swing speed declines were delayed after 10 months. While our data confirmed previous studies done in 3-5 months old mice that reported no declines in motor function of $gclm^{-/-}$ mice [42, 43], literature evidence of effects in the old mice is non-existent. Previous studies have demonstrated that increased oxidative damage in the cerebellum with age was correlated with a worsening of motor function and balance [44]. Furthermore, acute GSH deficiency leads to impaired motor function and balance in young rodents, worsens motor neuron decline in disease

models, and disrupts redox signaling in young and old rodents [45-47]. Based on the literature and our hypothesis, we expected that chronic GSH deficiency across the lifespan would lead to an accelerated pattern of functional declines, including gait measures, however, our results do not support our original hypothesis as the $gclm^{-/-}$ exhibited age-related declines similar to $gclm^{+/+}$. It is possible that the endogenous antioxidant defense or beneficial redox signaling pathways have compensated for the large deficiency in GSH and concurrent shift in redox state, and further research is warranted to pursue this hypothesis.

Sex has been implicated as a variable of interest due to potential sexual dimorphism in gait mechanics [4, 29]. Our results do not support sex differences in gait, as none of our variables had main effects or interactions with sex (all p values > 0.112), which remained even once body weights were used as a covariate. Several other studies that examined both sexes have also reported no sex differences in CatWalk-tested mice [48] or ink-tested freely-moving mice [49]. Other studies have simply combined sexes without explicit statistical justification [50]. Alternatively, sex differences in some gait measures were observed in studies using treadmill-based systems [4, 29], and could be related to differences in body size at a set speed. Additionally, sex-dependent responses in motor and gait decline in transgenic mouse models of ALS have been observed [29, 51], suggesting a differential response to both redox state and disease. There are few studies examining age-related functional decline that report the use of both sexes, but those that do have combined sexes or noted a lack of sexual dimorphism in these aged but otherwise healthy animals [52, 53], although one group examining overall frailty rather than motor function reported sex differences in their very old cohort (28 months) [54]. Including both sexes when collecting mouse data across many aspects of functional testing is generally

lacking, and warrants further research to determine if both sexes age differentially in motor function and gait.

Previous studies have determined that more than 90% of the 162 gait variables measured via the CatWalk are dependent on speed [55], which we confirmed for our variables through correlation and regression testing (**Figure 7**). In the context of a disease model at a set age, it is important to not confound test results that are dependent on the disease state with changes simply due to speed variance between animals. In our case, we were primarily interested in the age-related slowing of gait, and as such we did not seek to control for speed between animals [55]. By allowing speed variation we were able to capture the natural age-related slowing across the lifespan, which would otherwise be lost in a treadmill-based system. Importantly, the gait signature in relation to speed is similar between mice and humans, and hind paw gait measures have been used to compare gait dysfunction between mice and humans [56]. Additionally, the normal and maximal walking speeds both decline with age in humans [57], and this gait speed decline has previously been correlated with a shorter life expectancy [6].

CONCLUSION

The associative nature of gait speed with overall health that is found in aging humans could be found to a similar extent in rodents, allowing for an additional functional outcome measure in preclinical aging studies or similar predictions of mortality, disability, or disease used in humans to be used in future mice models. Our study determined that the CatWalk is a useful tool in aging research, allowing for robust quantitative measurement of rodent gait, and analysis of changes across the lifespan. Overall, mice appear to undergo similar changes to humans, namely a "slowing" of gait with concurrent changes in gait measures. Interestingly, chronic glutathione

deficiency had no detrimental effects but rather partially and mildly delayed some age-related deficits. These results warrant further examination to determine if alternative redox compensation is occurring, but the current data appears to not support the redox stress theory of aging.

ACKNOWLEDGEMENTS

We would like to thank Dr. Kavanaugh for the gclm$^{+/-}$ mice that we used to begin our breeding colony. This work was supported by the National Institutes of Health/National Institute on Aging (P01 AG027956; P01 AG022550; T32 AG020494)**.**

REFERENCES

[1] Rosso AL, Studenski SA, Chen WG, Aizenstein HJ, Alexander NB, Bennett DA, et al. (2013). Aging, the central nervous system, and mobility. J Gerontol A Biol Sci Med Sci, 68: 1379-1386

[2] Sumien N, Sims MN, Taylor HJ, Forster MJ (2006). Profiling psychomotor and cognitive aging in four-way cross mice. Age (Dordr), 28: 265-282

[3] Hebert MA, Gerhardt GA (1998). Normal and drug-induced locomotor behavior in aging: comparison to evoked DA release and tissue content in fischer 344 rats. Brain Res, 797: 42-54

[4] Wooley CM, Xing S, Burgess RW, Cox GA, Seburn KL (2009). Age, experience and genetic background influence treadmill walking in mice. Physiol Behav, 96: 350-361

[5] Abellan van Kan G, Rolland Y, Andrieu S, Bauer J, Beauchet O, Bonnefoy M, et al. (2009). Gait speed at usual pace as a predictor of adverse outcomes in community-dwelling older people an International Academy on Nutrition and Aging (IANA) Task Force. The journal of nutrition, health & aging, 13: 881-889

[6] Studenski S, Perera S, Patel K, Rosano C, Faulkner K, Inzitari M, et al. (2011). Gait speed and survival in older adults. JAMA : the journal of the American Medical Association, 305: 50-58

[7] Denayer T, Stöhr T, Van Roy M (2014). Animal models in translational medicine: Validation and prediction. New Horizons in Translational Medicine, 2: 5-11

[8] Skalicky M, Bubna-Littitz H, Viidik A (1996). Influence of physical exercise on aging rats: I. Life-long exercise preserves patterns of spontaneous activity. Mech Ageing Dev, 87: 127-139

[9] Ingram DK (2000). Age-related decline in physical activity: generalization to nonhumans. Medicine and science in sports and exercise, 32: 1623-1629

[10] Hamrick MW, Ding KH, Pennington C, Chao YJ, Wu YD, Howard B, et al. (2006). Age-related loss of muscle mass and bone strength in mice is associated with a decline in physical activity and serum leptin. Bone, 39: 845-853

[11] Hamrick MW, Ding K-H, Pennington C, Chao YJ, Wu Y-D, Howard B, et al. (2006). Age-related loss of muscle mass and bone strength in mice is associated with a decline in physical activity and serum leptin. Bone, 39: 845-853

[12] Justice JN, Carter CS, Beck HJ, Gioscia-Ryan RA, McQueen M, Enoka RM, et al. (2014). Battery of behavioral tests in mice that models age-associated changes in human motor function. Age (Dordr), 36: 583-592

[13] Fahlstrom A, Yu Q, Ulfhake B (2011). Behavioral changes in aging female C57BL/6 mice. Neurobiology of aging, 32: 1868-1880

[14] Herbin M, Hackert R, Gasc JP, Renous S (2007). Gait parameters of treadmill versus overground locomotion in mouse. Behavioural brain research, 181: 173-179

[15] Elliott BC, Blanksby BA (1976). A cinematographic analysis of overground and treadmill running by males and females. Med Sci Sports, 8: 84-87

[16] Hamers FP, Koopmans GC, Joosten EA (2006). CatWalk-assisted gait analysis in the assessment of spinal cord injury. J Neurotrauma, 23: 537-548

[17] Neumann M, Wang Y, Kim S, Hong SM, Jeng L, Bilgen M, et al. (2009). Assessing gait impairment following experimental traumatic brain injury in mice. Journal of neuroscience methods, 176: 34-44

[18] Vandeputte C, Taymans JM, Casteels C, Coun F, Ni Y, Van Laere K, et al. (2010). Automated quantitative gait analysis in animal models of movement disorders. BMC Neurosci, 11: 92

[19] Gerber YN, Sabourin JC, Rabano M, Vivanco M, Perrin FE (2012). Early functional deficit and microglial disturbances in a mouse model of amyotrophic lateral sclerosis. PloS one, 7: e36000

[20] Parvathy SS, Masocha W (2013). Gait analysis of C57BL/6 mice with complete Freund's adjuvant-induced arthritis using the CatWalk system. BMC musculoskeletal disorders, 14: 14

[21] Sohal RS, Orr WC (2012). The redox stress hypothesis of aging. Free Radic Biol Med, 52: 539-555

[22] Muller FL, Lustgarten MS, Jang Y, Richardson A, Van Remmen H (2007). Trends in oxidative aging theories. Free Radic Biol Med, 43: 477-503

[23] Rebrin I, Sohal RS (2008). Pro-oxidant shift in glutathione redox state during aging. Advanced drug delivery reviews, 60: 1545-1552

[24] Schafer FQ, Buettner GR (2001). Redox environment of the cell as viewed through the redox state of the glutathione disulfide/glutathione couple. Free Radic Biol Med, 30: 1191-1212

[25] Lu SC (2013). Glutathione synthesis. Biochimica et biophysica acta, 1830: 3143-3153

[26] Franklin CC, Backos DS, Mohar I, White CC, Forman HJ, Kavanagh TJ (2009). Structure, function, and post-translational regulation of the catalytic and modifier subunits of glutamate cysteine ligase. Mol Aspects Med, 30: 86-98

[27] McConnachie LA, Mohar I, Hudson FN, Ware CB, Ladiges WC, Fernandez C, et al. (2007). Glutamate cysteine ligase modifier subunit deficiency and gender as determinants of acetaminophen-induced hepatotoxicity in mice. Toxicol Sci, 99: 628-636

[28] Yang Y, Dieter MZ, Chen Y, Shertzer HG, Nebert DW, Dalton TP (2002). Initial characterization of the glutamate-cysteine ligase modifier subunit Gclm(-/-) knockout mouse. Novel model system for a severely compromised oxidative stress response. J Biol Chem, 277: 49446-49452

[29] Wooley CM, Sher RB, Kale A, Frankel WN, Cox GA, Seburn KL (2005). Gait analysis detects early changes in transgenic SOD1(G93A) mice. Muscle & nerve, 32: 43-50

[30] Samson MM, Crowe A, de Vreede PL, Dessens JAG, Duursma SA, Verhaar HJJ (2001). Differences in gait parameters at a preferred walking speed in healthy subjects due to age, height and body weight. Aging clinical and experimental research, 13: 16-21

[31] Maki BE (1997). Gait changes in older adults: predictors of falls or indicators of fear. Journal of the American Geriatrics Society, 45: 313-320

[32] Orendurff MS, Segal AD, Klute GK, Berge JS, Rohr ES, Kadel NJ (2004). The effect of walking speed on center of mass displacement. Journal of rehabilitation research and development, 41: 829-834

[33] England SA, Granata KP (2007). The influence of gait speed on local dynamic stability of walking. Gait & posture, 25: 172-178

[34] Winter DA, Patla AE, Frank JS, Walt SE (1990). Biomechanical walking pattern changes in the fit and healthy elderly. Phys Ther, 70: 340-347

[35] Manchester D, Woollacott M, Zederbauer-Hylton N, Marin O (1989). Visual, vestibular and somatosensory contributions to balance control in the older adult. Journal of gerontology, 44: M118-127

[36] Cabeza R, Anderson ND, Locantore JK, McIntosh AR (2002). Aging gracefully: compensatory brain activity in high-performing older adults. NeuroImage, 17: 1394-1402

[37] Fukagawa NK, Wolfson L, Judge J, Whipple R, King M (1995). Strength Is a Major Factor in Balance, Gait, and the Occurrence of Falls. The Journals of Gerontology: Series A, 50A: 64-67

[38] Sturnieks DL, St George R, Lord SR (2008). Balance disorders in the elderly. Neurophysiol Clin, 38: 467-478

[39] Shiga A, Nakagawa T, Nakayama M, Endo T, Iguchi F, Kim TS, et al. (2005). Aging effects on vestibulo-ocular responses in C57BL/6 mice: comparison with alteration in auditory function. Audiology & neuro-otology, 10: 97-104

[40] Shaffer SW, Harrison AL (2007). Aging of the somatosensory system: a translational perspective. Phys Ther, 87: 193-207

[41] Gutierrez-Castellanos N, Winkelman BH, Tolosa-Rodriguez L, De Gruijl JR, De Zeeuw CI (2013). Impact of aging on long-term ocular reflex adaptation. Neurobiology of aging, 34: 2784-2792

[42] Cole TB, Giordano G, Co AL, Mohar I, Kavanagh TJ, Costa LG (2011). Behavioral Characterization of GCLM-Knockout Mice, a Model for Enhanced Susceptibility to Oxidative Stress. Journal of toxicology, 2011: 157687

[43] Chen Y, Curran CP, Nebert DW, Patel KV, Williams MT, Vorhees CV (2012). Effect of chronic glutathione deficiency on the behavioral phenotype of Gclm-/- knockout mice. Neurotoxicology and teratology, 34: 450-457

[44] Forster MJ, Dubey A, Dawson KM, Stutts WA, Lal H, Sohal RS (1996). Age-related losses of cognitive function and motor skills in mice are associated with oxidative protein damage in the brain. Proc Natl Acad Sci U S A, 93: 4765-4769

[45] Diaz-Hung ML, Blanco L, Pavon N, Leon R, Estupinan B, Orta E, et al. (2014). Sensory-motor performance after acute glutathione depletion by L-buthionine sulfoximine injection into substantia nigra pars compacta. Behavioural brain research, 271: 286-293

[46] Chi L, Ke Y, Luo C, Gozal D, Liu R (2007). Depletion of reduced glutathione enhances motor neuron degeneration in vitro and in vivo. Neuroscience, 144: 991-1003

[47] Morrison JP, Coleman MC, Aunan ES, Walsh SA, Spitz DR, Kregel KC (2005). Aging reduces responsiveness to BSO- and heat stress-induced perturbations of glutathione and antioxidant enzymes. American journal of physiology. Regulatory, integrative and comparative physiology, 289: R1035-1041

[48] Clarke KA, Still J (1999). Gait analysis in the mouse. Physiol Behav, 66: 723-729

[49] Glynn D, Drew CJ, Reim K, Brose N, Morton AJ (2005). Profound ataxia in complexin I knockout mice masks a complex phenotype that includes exploratory and habituation deficits. Human molecular genetics, 14: 2369-2385

[50] Serradj N, Jamon M (2009). The adaptation of limb kinematics to increasing walking speeds in freely moving mice 129/Sv and C57BL/6. Behavioural brain research, 201: 59-65

[51] Veldink JH, Bar PR, Joosten EA, Otten M, Wokke JH, van den Berg LH (2003). Sexual differences in onset of disease and response to exercise in a transgenic model of ALS. Neuromuscul Disord, 13: 737-743

[52] Zhang Y, Bokov A, Gelfond J, Soto V, Ikeno Y, Hubbard G, et al. (2014). Rapamycin extends life and health in C57BL/6 mice. J Gerontol A Biol Sci Med Sci, 69: 119-130

[53] Parks RJ, Fares E, Macdonald JK, Ernst MC, Sinal CJ, Rockwood K, et al. (2012). A procedure for creating a frailty index based on deficit accumulation in aging mice. J Gerontol A Biol Sci Med Sci, 67: 217-227

[54] Whitehead JC, Hildebrand BA, Sun M, Rockwood MR, Rose RA, Rockwood K, et al. (2014). A clinical frailty index in aging mice: comparisons with frailty index data in humans. J Gerontol A Biol Sci Med Sci, 69: 621-632

[55] Batka RJ, Brown TJ, McMillan KP, Meadows RM, Jones KJ, Haulcomb MM (2014). The need for speed in rodent locomotion analyses. Anat Rec (Hoboken), 297: 1839-1864

[56] Broom L, Ellison BA, Worley A, Wagenaar L, Sorberg E, Ashton C, et al. (2017). A translational approach to capture gait signatures of neurological disorders in mice and humans. Scientific reports, 7: 3225

[57] Bohannon RW (1997). Comfortable and maximum walking speed of adults aged 20-79 years: reference values and determinants. Age and ageing, 26: 15-19

Figure Legends

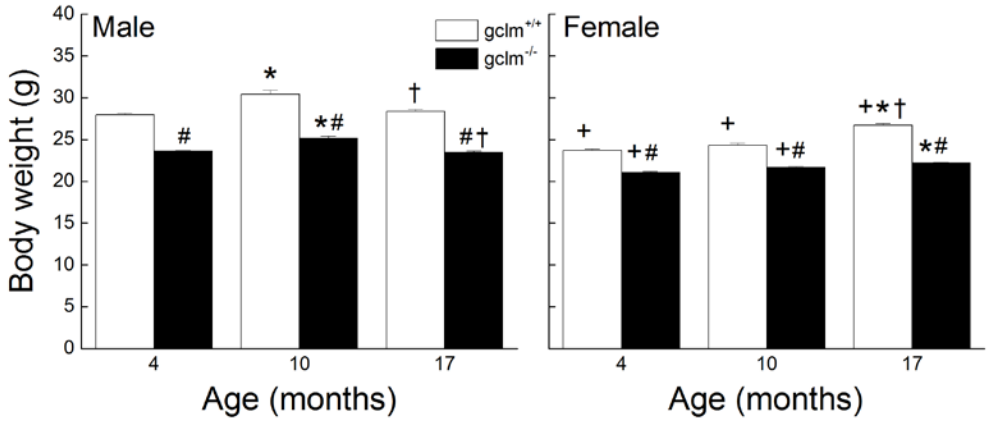

Figure 1. Effects of age, sex and genotype on body weights (g) in young (4 month), adult (10 month), and old (17 month) $gclm^{+/+}$ and $gclm^{-/-}$ mice. Each value represents the mean + SEM. $^{+}$ $p<0.05$ compared to age and genotype-matched males; $^{*}p < 0.05$ compared to genotype-matched young; †$p<0.05$ adult compared to genotype-matched old; $^{\#}p < 0.05$ compared to age-matched $gclm^{+/+}$.

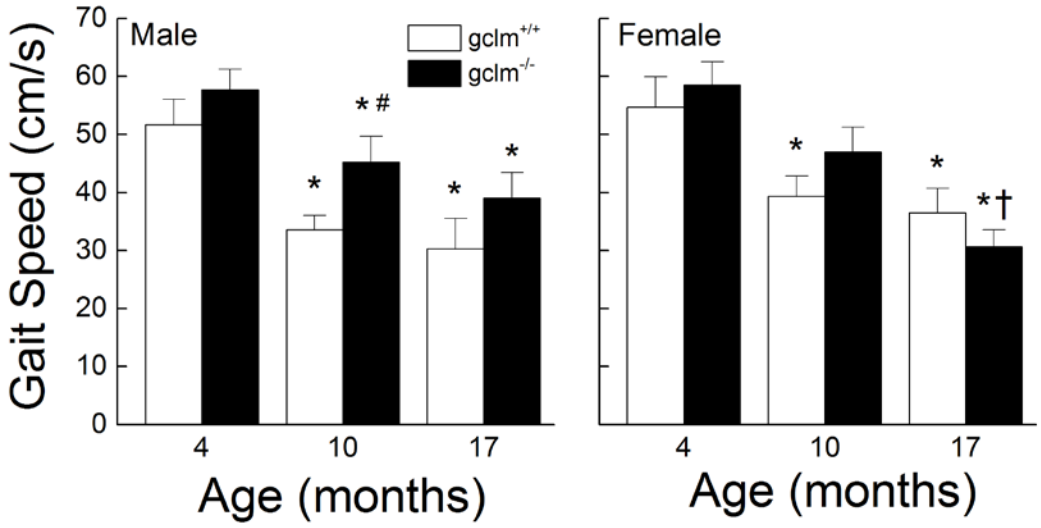

Figure 2. Effects of sex, age and genotype on gait speed (cm/s) in young (4 month), adult (10 month), and old (17 month) $gclm^{+/+}$ and $gclm^{-/-}$ mice. Each value represents the mean + SEM. $^{*}p < 0.05$ compared to genotype-matched young; †$p<0.05$ adult compared to genotype-matched old; $^{\#}p < 0.05$ compared to age-matched $gclm^{+/+}$.

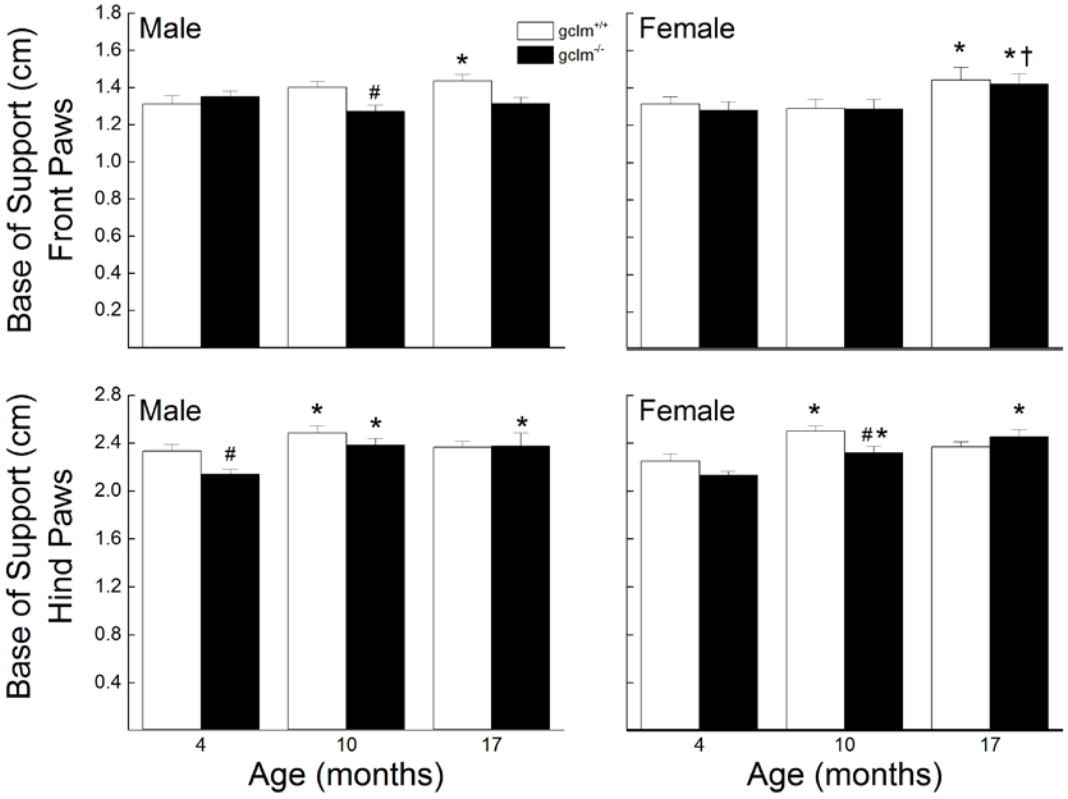

Figure 3. Effects of sex, age and genotype on width of the front and hind paw base of support (cm) in young (4 month), adult (10 month), and old (17 month) $gclm^{+/+}$ and $gclm^{-/-}$ mice. Each value represents the mean + SEM. $^{*}p < 0.05$ compared to genotype-matched young; †$p<0.05$ adult compared to genotype-matched old; $^{\#}p < 0.05$ compared to age-matched $gclm^{+/+}$.

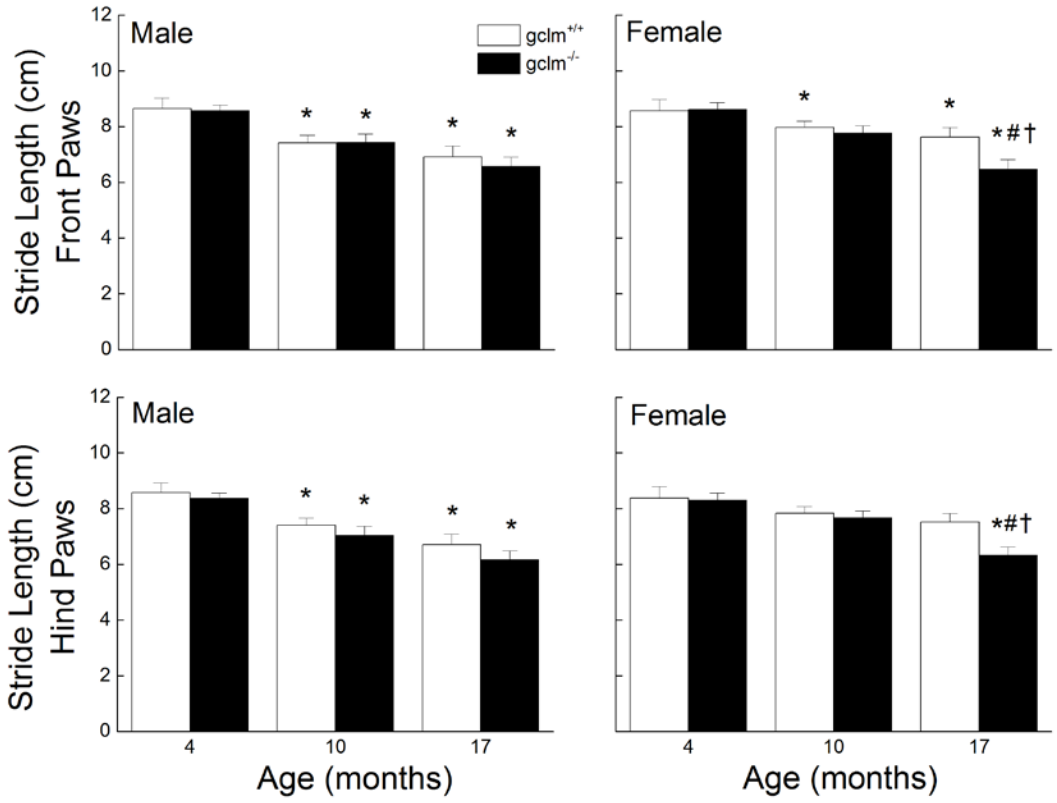

Figure 4. Effects of sex, age and genotype on the front and hind paw stride length (cm) in young (4 month), adult (10 month), and old (17 month) $gclm^{+/+}$ and $gclm^{-/-}$ mice. Each value represents the mean + SEM. $^{*}p < 0.05$ compared to genotype-matched young; †$p<0.05$ adult compared to genotype-matched old; $^{\#}p < 0.05$ compared to age-matched $gclm^{+/+}$.

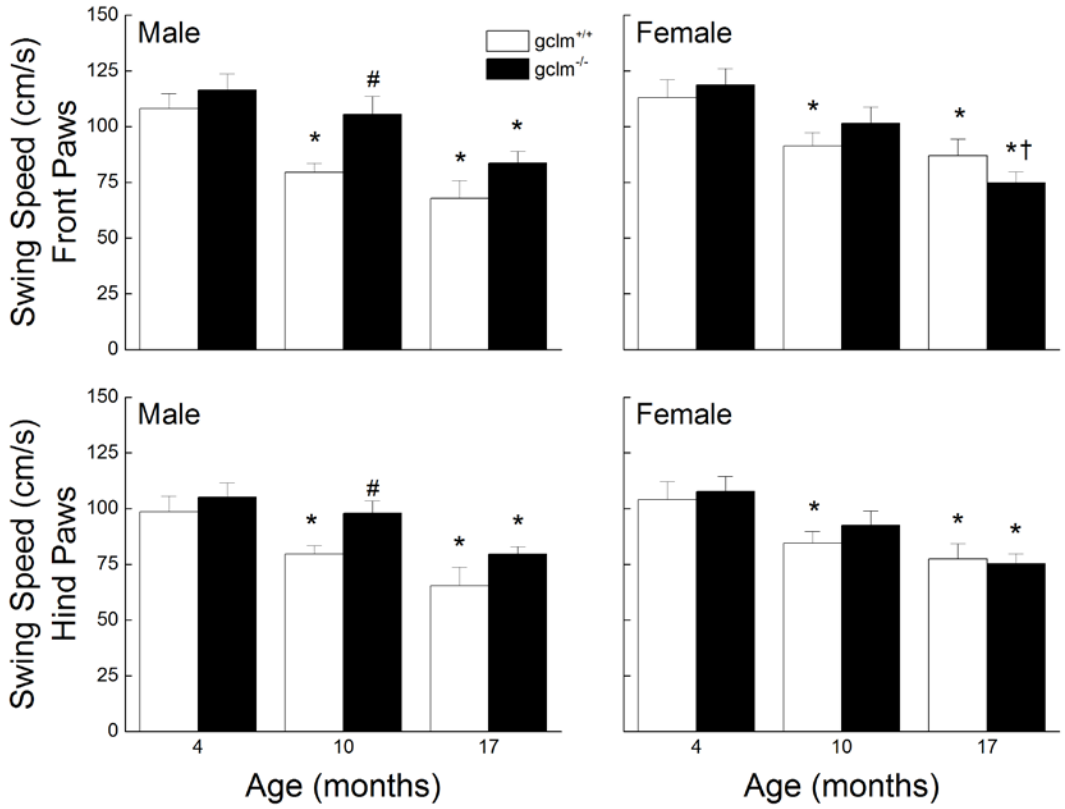

Figure 5. Effects of sex, age and genotype on the front and hind paw swing speed (cm/s) in young (4 month), adult (10 month), and old (17 month) $gclm^{+/+}$ and $gclm^{-/-}$ mice. Each value represents the mean + SEM. $^{*}p < 0.05$ compared to genotype-matched young; †$p<0.05$ adult compared to genotype-matched old; $^{\#}p < 0.05$ compared to age-matched $gclm^{+/+}$.

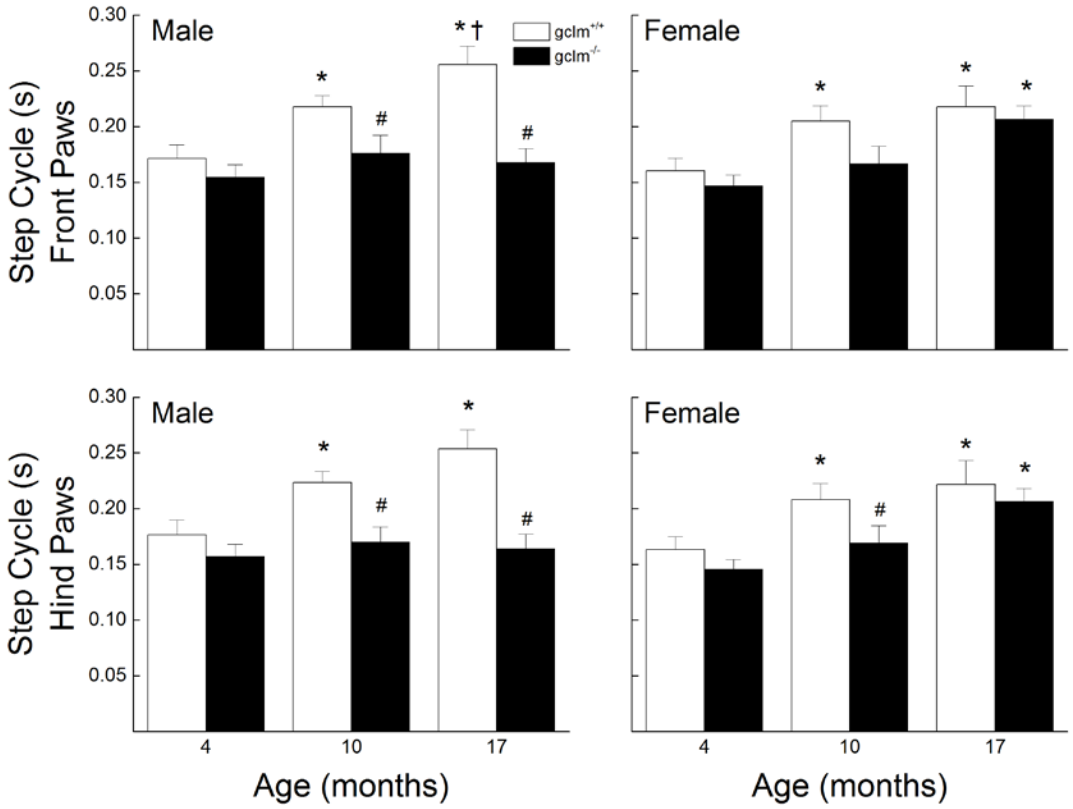

Figure 6. Effects of sex, age and genotype on the front and hind paw step cycle duration (s) in young (4 month), adult (10 month), and old (17 month) $gclm^{+/+}$ and $gclm^{-/-}$ mice. Each value represents the mean + SEM. $^{*}p < 0.05$ compared to genotype-matched young; †$p<0.05$ adult compared to genotype-matched old; $^{\#}p < 0.05$ compared to age-matched $gclm^{+/+}$.

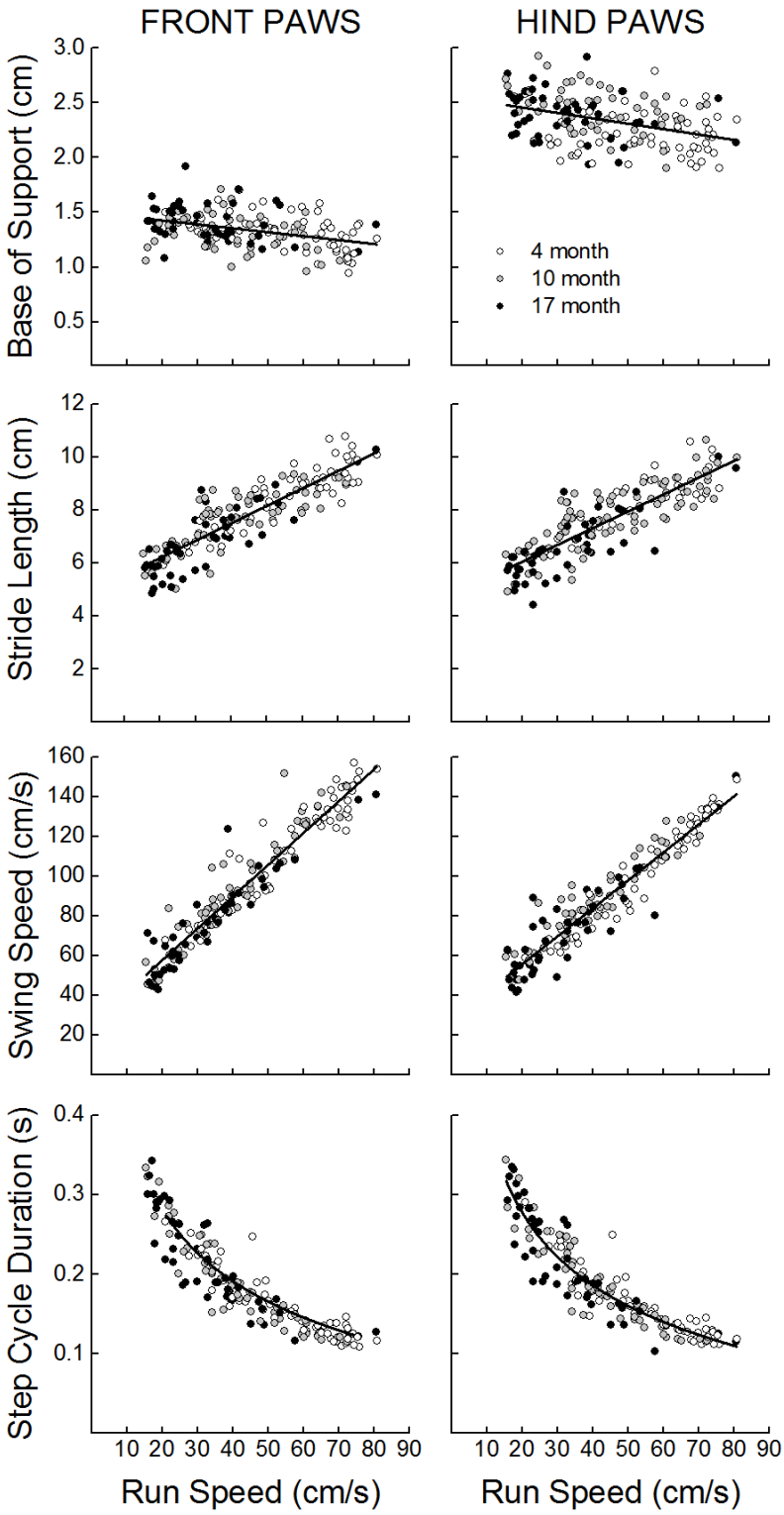

Figure 7. Relationship of speed with base of support, stride length, step cycle duration, and swing speed in the front and hind paws of young (4 month), adult (10 month), and old (17 month) gclm$^{+/+}$ and gclm$^{-/-}$ male and female mice. Each value represents a single animal.